uOttawa

L'Université canadienne
Canada's university

FACULTÉ DES ÉTUDES SUPÉRIEURES ET POSTOCTORALES

uOttawa

L'Université canadienne
Canada's university

FACULTY OF GRADUATE AND POSDOCTORAL STUDIES

Wei Zhang
AUTEUR DE LA THÈSE / AUTHOR OF THESIS

Ph.D. (Electrical Engineering)
GRADE / DEGREE

School of Information Technology and Engineering
FACULTÉ, ÉCOLE, DÉPARTEMENT / FACULTY, SCHOOL, DEPARTMENT

Soft-input Soft-output Multiuser Detection for Coded Wireless Multiuser Systems

TITRE DE LA THÈSE / TITLE OF THESIS

Abbas Yongacoglu
DIRECTEUR (DIRECTRICE) DE LA THÈSE / THESIS SUPERVISOR

Claude D'Amours
CO-DIRECTEUR (CO-DIRECTRICE) DE LA THÈSE / THESIS CO-SUPERVISOR

EXAMINATEURS (EXAMINATRICES) DE LA THÈSE / THESIS EXAMINERS

Sofiene Affes

Jean-Yves Chouinard

Yongyi Mao

Ian Marsland

Gary W. Slater
LE DOYEN DE LA FACULTÉ DES ÉTUDES SUPÉRIEURES ET POSTDOCTORALES /
DEAN OF THE FACULTY OF GRADUATE AND POSTDOCORAL STUDIES

Soft-Input Soft-Output Multiuser Detection for Coded Wireless Multiuser Systems

by

Wei Zhang, B.A.Sc., M.A.Sc.

A thesis submitted to the
Faculty of Graduate and Postdoctoral Studies
of the University of Ottawa in partial fulfillment
of the requirements for the degree of

Doctor of Philosophy

Ottawa-Carleton Institute for Electrical and Computer Engineering
School of Information Technology and Engineering
Faculty of Engineering
University of Ottawa

Ottawa, Ontario, Canada

May 2005

Your file Votre référence
ISBN: 0-494-11040-6
Our file Notre référence
ISBN: 0-494-11040-6

To my husband and son Chenyu

Abstract

Multiuser detection permits the joint detection of signals from multiple sources. An optimal multiuser detector for coded multiuser systems is usually practically infeasible due to the associated complexity. An iterative receiver consisting of a soft-input soft-output (SISO) multiuser detector and a bank of SISO single user decoders can provide a system performance which approaches to that of the single user system after many iterations. On the other hand, it has a feasible computational complexity.

We first propose and analyze three types of SISO multiuser detectors, which are mainly based on the underlying ideas of the traditional (non-SISO) multiuser detectors. These are: decorrelators, linear minimum mean square error (MMSE) detectors and parallel decision feedback detectors. In contrast to these traditional detectors, our SISO multiuser detectors make good use of soft inputs provided by SISO single user decoders and in turn, provide soft outputs to them. The resulting system performance converges quickly, while keeping the computational complexity of the SISO detectors proportional to the number of users cubed. This is a significant complexity reduction in comparison to the optimal detector which has a complexity exponentially proportional to the number of users.

Secondly, we consider adaptive SISO multiuser detection. As it is well known, the optimum and many suboptimum SISO multiuser detectors require a lot of a priori information of the multiuser system, such as all users' transmitted waveforms, relative delays as well as the channel impulse response. In this thesis, we apply adaptive algorithms in the SISO multiuser detector in order to avoid the need for this a priori information. We propose two adaptive SISO parallel decision feedback detectors based on the normalized least mean square (NLMS) and recursive least squares (RLS) algorithms for both synchronous and asynchronous direct-sequence code-division multiple-access (DS-CDMA)

systems. Compared with traditional non-SISO adaptive detectors, our SISO adaptive detectors effectively exploit the a priori information of coded symbols to further improve their convergence performance. This a priori information is obtained from a bank of single user decoders. Monte-Carlo simulation results are presented and compared. Moreover, we extend adaptive SISO parallel decision feedback detection to asynchronous DS-CDMA systems over slow frequency non-selective Rayleigh fading channels.

Acknowledgements

First of all, I would like to thank my supervisor, Professor Abbas Yongaçoğlu for his inspiration and invaluable support throughout this research work, and my second supervisor, Associate Professor Claude D'Amours, for his enthusiasm, patience and detailed comments. I am deeply grateful for their funding and our fruitful discussions which always gave me creative ideas and constructive comments.

I also like to express my sincere gratitude and deep appreciation to

Dr. Jean-Yves Chouinard (Université Laval)

Dr. Ian Marsland (Carleton University)

for their review of both the candidacy paper and this thesis;

Dr. Sofiene Affes (INRS-ÉMT, Montréal)

Dr. Yongyi Mao (University of Ottawa)

for their review of this thesis;

Dr. Michael Moher (Space-Time DSP Inc.)

for his review of the candidacy paper. They gave me a lot of helpful suggestions and comments.

All of my colleagues in our research group in the communication and signal processing (CASP) lab, have contributed to a highly appreciated work environment. Particularly, I would like to thank Güneş Karabulut, Tolga Kurt, Tuncer Baykas and Ozgur Ekici for their valuable advice and friendly help.

I would like to give my loving thanks to my husband, Dong Liu and baby son, David Chenyu Liu, for their encouragement and understanding without which I would never finish this work. I also like to give special thanks to my parents, and parents-in-law for

their always believing in me and helping me.

There are many other people whose names have not been mentioned. I would like to thank all of them.

The financial support of the University of Ottawa is highly appreciated.

Contents

List of Acronyms

Acronym	Explanation	Page # (where acronym is first used)
ADD	Addition	88
APP	A Posteriori Probability	23
AWGN	Additive White Gaussian Noise	29
BER	Bit Error Rate	12
BCJR	the initials of four authors (L. Bahl, J. Cocke, F. Jelinek and J. Raviv) of reference paper [Bah74], which is further referred to the algorithm proposed in that paper	32
BPSK	Binary Phase-Shift Keying	8
CC	Convolutional Code	59
CDMA	Code-Division Multiple-Access	8
DS-CDMA	Direct-Sequence Code-Division Multiple-Access	3
EM	Expectation-Maximization	160
FDMA	Frequency-Division Multiple-Access	8
FEC	Forward Error Correction	44
IDMA	Interleaver-Division Multiple-Access	61
ISI	Intersymbol Interference	113
LAN	Local Area Network	1
LLR	Log-Likelihood Ratio	23
LMS	Least Mean Square	124

Acronym	Explanation	Page # (where acronym is first used)
MAC	Multiply and Accumulation	88
MAI	Multiple Access Interference	109
MAP	Maximum A Posteriori	6
MCE	Minimum Cross-Entropy	45
MLSD	Maximum Likelihood Sequence Detector	6
MMSE	Minimum Mean Square Error	3
M-QAM	M-ary Quadrature Amplitude Modulation	55
MUL	Multiplication	88
NLMS	Normalized Least Mean Square	114
PCC	Parallel Concatenated Code	25
PCCC	Parallel Concatenated Convolutional Code	25
PDFD	Parallel Decision Feedback Detector	115
RLS	Recursive Least Squares	114
RSC	Recursive Systematic Convolutional	25
SCC	Serially Concatenated Code	29
SCCC	Serially Concatenated Convolutional Code	59
SIC	Soft Interference Canceller	71
SISO	Soft-Input Soft-Output	2
SNR	Signal-to-Noise Ratio	13
SOVA	Soft Output Viterbi Algorithm	32
WLS	Weighted Least Squares	113

List of Notations

Throughout this thesis, we use the following notations. Matrices and vectors are denoted as boldface upper case and lower case, respectively. If $\mathbf{x}$ is a vector, x_i indicates the ith element of $\mathbf{x}$. If $\mathbf{M}$ is a matrix, $(\mathbf{M})_{ij}$ refers to the element at the ith row and the jth column.

Notation	Meaning	Page # (where notation is first used)
K	number of users	7
T	symbol interval	8
A_k	received amplitude of the kth user's signal	8
$s_k(t)$	normalized waveform assigned to the kth user	8
$n(t)$	white Gaussian noise process	8
σ^2	double-sided power spectral density of the additive white Gaussian noise	8
$\mathbf{S}(z)$	discrete-time channel transfer function of the asynchronous multiuser system	11
η_k	asymptotic multiuser efficiency of user k	13
$\bar{\eta}_k$	near-far resistance of user k	14
Q	length of the information bit frame	24
F	length of the coded bit frame, it is also the length of the channel symbol frame when BPSK modulation is employed	24
$\log(\cdot)$	natural logarithm of $(\cdot)$	24
$L(\cdot, I)$	a priori LLR of $(\cdot)$ at the input of the SISO module	24
$\Lambda^e(\cdot, O)$	extrinsic LLR of $(\cdot)$ at the output of the SISO module	24
$\Lambda(\cdot)$	a posteriori LLR of $(\cdot)$	25
ν	code constraint length	44
$H[s, q]$	cross-entropy of two distributions s and q	46
$\mathcal{M}(\mathbf{x}; \mathbf{y})$	the mutual information between $\mathbf{x}$ and $\mathbf{y}$	47
$d_k(i)$	the ith information bit of user k	55
$b_k(i)$	the ith modulated symbol of user k	55
$(\cdot)^P$	quantity obtained from the previous iteration	57

Notation	Meaning	Page # (where notation is first used)
$(\cdot)^E$	quantity containing extrinsic information	57
$\Lambda_1[b_k(i)]$	a posteriori LLR of $b_k(i)$ provided by the multiuser detector	57
$\lambda_1^P[b_k(i)]$	a priori LLR of $b_k(i)$ provided by the multiuser detector in the previous iteration	59
$\lambda_1^E[b_k(i)]$	the extrinsic LLR of $b_k(i)$ provided by the multiuser detector	57
$\Lambda_2[b_k(i)]$	a posteriori LLR of $b_k(i)$ provided by the kth user's decoder	58
$\lambda_2^P[b_k(i)]$	a priori LLR of $b_k(i)$ provided by the kth user's decoder in the previous iteration	57
$\lambda_2^E[b_k(i)]$	the extrinsic LLR of $b_k(i)$ provided by the kth user's decoder	59
$\hat{b}_k$	soft symbol estimate of b_k	65
$\mathbf{I}$	identity matrix	65
$N_0/2$	double-sided power spectral density of the additive white Gaussian noise $n(t)$, equal to σ^2	71
$\lambda_i(b_k)$	soft input of the SISO detector which is the a priori LLR of coded symbol b_k	71
$\mathbf{R}_u$	equivalent cross-correlation matrix of the waveforms of multiple users at the output of soft interference cancellation	72
$\hat{\mathbf{R}}_u$	approximate cross-correlation matrix of $\mathbf{R}_u$	74
x_k^{DEC}	output value of the SISO decorrelating detector of user k	75
$\lambda_o^{DEC}[b_k]$	soft output of coded symbol b_k of the SISO decorrelating detector	75

Notation	Meaning	Page # (where notation is first used)
ρ	cross correlation of any two users in a K-symmetric multiuser system	78
$\mathbf{m}_k$	linear minimum mean square error filter of user k	89
x_k^{MMSE}	output value of the linear SISO MMSE detector of user k	91
$\lambda_o^{MMSE}[b_k]$	soft output of coded symbol b_k of the linear SISO MMSE detector	91
$\mathbf{m}_{fk}$	feedforward filter of user k in a synchronous multiuser system	106
$\mathbf{m}_{bk}$	feedback filter of user k in a synchronous multiuser system	106
x_k^{PDFD}	output value of the SISO parallel decision feedback detector of user k	107
τ_k	transmission delay of the kth user	116
$f_k(t)$	transmitted signature waveform of the kth user	116
$h_k(t)$	channel impulse response of the kth user	116
$\delta(\cdot)$	Dirac delta function	116
T_c	chip duration	118
N	spreading gain	118
$\tilde{\mu}_f$	step size of the adaptive feedforward filter	124
$\tilde{\mu}_b$	step size of the adaptive feedback filter	124
$e_k(m)$	error signal of the mth symbol of user k in the NLMS algorithm	124

Notation	Meaning	Page # (where notation is first used)
$\xi_k(m+1)$	a priori error signal of the mth symbol of user k in the RLS algorithm	125
$\lambda_k^a(m)$	soft output of the adaptive detector of the m symbol of user k	126
$\mathbf{s}_k$	signature vector of user k	118
$\bar{\boldsymbol{m}}_{fk}$	finite-length feedforward filter of user k in asynchronous systems	141
$\bar{\boldsymbol{m}}_{bk}$	finite-length feedback filter of user k in asynchronous systems	141

List of Figures

List of Tables

Chapter 1

Introduction

Multiuser detection is indispensable for efficient operation of multiuser systems, such as cellular wireless communication systems, satellite communication systems, high-speed data transmission lines, wireless local area networks (LAN), etc, which are subject to multiple access interference. Multiuser detectors consider the so called interfering signals as useful information and exploit the structure of the received superimposed multiuser signal. Employing suitable multiuser detection techniques, we can improve the bandwidth efficiency of the system while still providing a reasonable performance.

With evergrowing signal processing capabilities, in order to improve the system performance, most multiuser systems employ forward error correction codes. For these coded multiuser systems, traditional receivers consist of a multiuser detector followed by a bank of single user decoders. These two parts operate separately and the way in which the multiuser detector generates and transfers its outputs to the following decoders influences the system performance. The information loss due to serial concatenation of these two parts is a main disadvantage of traditional receivers.

The optimum receiver for coded multiuser systems follows maximum likelihood se-

quence detection based on the super trellis of the multiuser system, which combines the trellises of the multiple access channel and single user encoders. Its computational complexity is exponentially proportional to the sum of the constraint lengths of individual encoders. When all single user encoders have the same constraint length, the complexity is exponentially proportional to the product of the number of users and the code constraint length. The resulting complexity is prohibitive for systems with a large number of users and/or for long constraint length codes.

From the concept of turbo codes, which has revolutionized the field of coding theory, the concept of an iterative receiver has emerged which can provide a near single user performance for coded multiuser systems, while being computationally feasible. Similarly to the traditional receiver, two parts (i.e. a multiuser detector and a bank of single user decoders) are included in this receiver. However, instead of operating separately, they cooperate iteratively by transferring extrinsic information (a type of soft information, in comparison with hard symbol decisions) of coded symbols to one another. Therefore, the detector and single user decoders have soft inputs and soft outputs and are called soft-input soft-output (SISO) detector and decoders, respectively. As we increase the number of iterations and increase the signal-to-noise ratio, the system performance approaches to that of the single user system. The SISO multiuser detection is the main topic of this thesis.

1.1 Thesis Outline

This thesis consists of seven chapters including the introduction and conclusion chapters. The focuses of the five intermediate chapters are listed as follows:

- **Chapter 2** briefly introduces multiuser detection fundamentals. First, discrete-time system models of both synchronous and asynchronous multiuser systems are

presented. Then, two important performance measures of multiuser systems, i.e. asymptotic multiuser efficiency and near-far resistance, are introduced. Following this, several traditional multiuser detectors: conventional detectors, optimum detectors, linear and non-linear multiuser detectors, are briefly described and analyzed.

- **Chapter 3** presents the well-known turbo principles, which provide us the underlying idea of the iterative receiver. A general SISO a posteriori probability (APP) module for iterative decoding of concatenated codes is first given. Based on this, we present turbo principles by using serially and parallel concatenated convolutional codes as examples. Furthermore, at the end of this chapter, we provide several algorithms to calculate soft outputs of the SISO APP module.

- **Chapter 4** reviews the current literature about SISO multiuser detection for synchronous multiuser systems. It starts by presenting a theory fundamentally based on minimum cross-entropy for iterative receivers of coded multiuser systems. Additionally, in order to give a clear description, we introduce a general iterative receiver structure which is based on turbo principles. Then, a complete review focusing on SISO multiuser detection is provided.

- **Chapter 5** proposes and analyzes three types of SISO multiuser detectors, such as SISO decorrelators, linear SISO minimum mean square error (MMSE) detectors and SISO parallel decision feedback detectors, which are adapted from the corresponding traditional (non-SISO) ones, respectively. We conclude this chapter by comparing these three types of SISO detectors.

- **Chapter 6** considers adaptive SISO multiuser detectors when the a priori information of direct-sequence code-division multiple-access (DS-CDMA) systems is unknown to the receiver. For example, in some cases, the knowledge of multiple users' signature waveforms, relative delays or the channel impulse response is not

available in the receiver. We propose and analyze adaptive SISO parallel decision feedback detectors for both synchronous and asynchronous DS-CDMA systems. The least mean square and recursive least squares algorithms are used. Finally, we extend our adaptive SISO detectors to DS-CDMA systems over slow frequency non-selective Rayleigh fading channels.

1.2 Thesis Contributions

This thesis focuses on SISO multiuser detection for coded multiuser systems. Chapter 5 and Chapter 6 contain our main contributions which can be summarized as follows:

- The introduction of a novel SISO decorrelating detector for synchronous multiuser systems.
- The adaptation of three types of traditional multiuser detectors, namely decorrelators, linear MMSE detectors and parallel decision feedback detectors, to SISO ones which can cooperate iteratively with a bank of SISO single user decoders.
- Comparison of these three types of SISO multiuser detectors.
- The proposal of an adaptive SISO parallel decision feedback detector for synchronous DS-CDMA systems when multiple users' signature waveforms are unknown to the receiver. A training sequence is required by each user. The adaptive algorithms, normalized least mean square and recursive least squares, are employed.
- An optimum SISO parallel decision feedback detector is derived for an asynchronous DS-CDMA systems where not only multiple users' signature waveforms but also relative delays are not available in the receiver. Furthermore, its adaptive version is proposed.

- Evaluation of bit error rate performance of multiuser systems is performed by Monte-Carlo simulation techniques.

Furthermore, there are many potential applications to which our SISO detectors can be applied. For example, our detectors can be directly extended to more general multi-path channels. They can also be used in the distributed antenna system where multiple antennas introduce interference.

Chapter 2

Multiuser Detection Fundamentals

Traditional multiuser detectors output hard decisions or some types of soft decisions, which can either be final decisions in uncoded systems or be delivered to the following decoders in coded systems. In particular, in a coded multiuser system, the multiuser detector and multiple users' decoders operate separately. A good review for traditional multiuser detectors is provided by [Ver98].

A conventional detector gives hard symbol decisions based on the output of each matched filter. It treats the matched filter output as a single user signal, considering the interfering users' signals as noise. It is the simplest one among all types of multiuser detectors. However, it has a poor bit error probability performance for non-orthogonal multiuser systems and suffers severely from the near-far problem.

Optimum multiuser detection is based on the maximum a posteriori (MAP) probability of each transmitted symbol of each user or the maximum a posteriori probability of each symbol vector consisting of all users' symbols. Under some approximation, it can be implemented by a maximum likelihood sequence detector (MLSD), which has a computational complexity increasing exponentially in the number of users in the system.

Due to the poor performance provided by the conventional detector and the prohibitive complexity of the optimum multiuser detector, suboptimum detectors are investigated. These detectors exhibit good tradeoffs between the system performance and complexity and fall into two main categories: linear detectors and non-linear (decision-driven) detectors. Both decorrelating detectors and minimum mean square error detectors belong to the class of linear detectors, which applies filtering to the output of matched filters to eliminate or suppress multiuser interference. Non-linear multiuser detectors make symbol decisions and then use these decisions in a feedback loop to eliminate multiple user interference. This type of detectors includes successive detectors (serial interference cancellers), multistage detectors (parallel interference cancellers) and decision feedback detectors.

In this chapter, we briefly introduce these multiuser detectors, based on which we exploit the main topic of this thesis, i.e. soft-input soft-output multiuser detectors for coded multiuser systems, in the following chapters. In Section 2.1, both synchronous and asynchronous multiuser system models are given. Two important performance measures of multiuser systems – asymptotic multiuser efficiency and near-far resistance – are introduced in Section 2.2. We present the conventional multiuser detector, optimum multiuser detector, linear multiuser detector and non-linear multiuser detector in the following four sections, respectively.

2.1 System Model

We will consider both synchronous and asynchronous multiuser systems in this chapter. Here we give their system models in [Ver98], based on which we introduce different types of multiuser detectors in the following sections.

For a synchronous K-user multiuser system with binary phase-shift keying (BPSK)

modulation, the received signal $r(t)$ can be expressed as:

$$r(t) = \sum_{k=1}^{K} A_k b_k s_k(t) + n(t), \quad t \in [0, T], \tag{2.1}$$

where T is the symbol interval, A_k is the received amplitude of the kth user's signal, $b_k \in \{-1, +1\}$ is the BPSK modulated symbol of the kth user, $s_k(t)$ is the energy normalized waveform assigned to the kth user and is assumed to be zero outside the interval $[0, T]$, and $n(t)$ is the white Gaussian noise process with double-sided power spectral density σ^2. The waveform $s_k(t)$ can be arbitrary. For example, it can be a narrow band FDMA (frequency-division multiple-access) waveform or a wideband CDMA (code-division multiple-access) waveform. In the receiver, we use a bank of matched filters which are matched to multiple users' waveforms, respectively. The output y_k of the kth matched filter is:

$$y_k = \int_0^T r(t) s_k(t) dt. \tag{2.2}$$

Then the output vector $\mathbf{y}$ of a bank of matched filters can be expressed as:

$$\mathbf{y} = \mathbf{RAb} + \mathbf{n}, \tag{2.3}$$

where $\mathbf{R} = \{\rho_{ij}\}$ is the normalized cross-correlation matrix with diagonal elements equal to 1,

$$\rho_{ij} = \int_0^T s_i(t) s_j(t) dt, \tag{2.4}$$

$$\mathbf{y} = [y_1, \ldots, y_K]^T, \tag{2.5}$$

$$\mathbf{b} = [b_1, \ldots, b_K]^T, \tag{2.6}$$

$$\mathbf{A} = \text{diag}[A_1, \ldots, A_K], \tag{2.7}$$

and $\mathbf{n}$ is a zero-mean Gaussian random vector with covariance matrix equal to:

$$E[\mathbf{n}\mathbf{n}^T] = \sigma^2 \mathbf{R}. \tag{2.8}$$

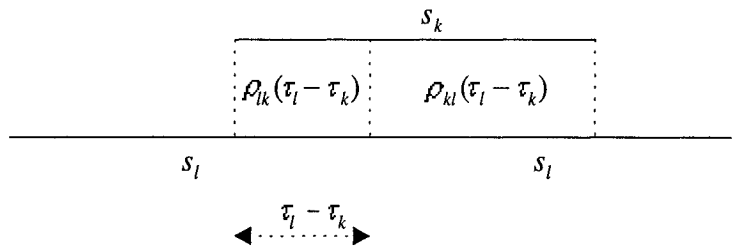

Figure 2.1: Definition of asynchronous crosscorrelations ($k < l$)

The output vector $\mathbf{y}$ provides the sufficient statistics for the following multiuser detector.

In an asynchronous multiuser system, the received signal $r(t)$ can be expressed as:

$$r(t) = \sum_{k=1}^{K} \sum_{i=-M}^{M} A_k b_k[i] s_k(t - iT - \tau_k) + n(t), \tag{2.9}$$

where we assume that each user transmits $(2M+1)$ frames or packets and τ_k is the kth user's delay, $\tau_k \in [0, T)$ for $k = 1, \ldots, K$. For a simple notation and without loss of generality, we assume that

$$\tau_1 \leq \tau_2 \ldots \leq \tau_K. \tag{2.10}$$

For asynchronous systems, two cross-correlations between any two waveforms are defined, which depend on the offset between these signals. If $k < l$, then we denote:

$$\rho_{kl}(\tau_l - \tau_k) = \int_{\tau_l - \tau_k}^{T} s_k(t) s_l(t - \tau_l + \tau_k) dt, \tag{2.11}$$

$$\rho_{lk}(\tau_l - \tau_k) = \int_{0}^{\tau_l - \tau_k} s_k(t) s_l(t + T - \tau_l + \tau_k) dt, \tag{2.12}$$

which are also shown in Fig. 2.1. For simplicity, in the following, we denote:

$$\rho_{kl} = \rho_{kl}(\tau_l - \tau_k), \tag{2.13}$$

$$\rho_{lk} = \rho_{lk}(\tau_l - \tau_k). \tag{2.14}$$

The output of the matched filter for user k is:

$$y_k[i] = \int_{\tau_k+iT}^{\tau_k+iT+T} r(t)s_k(t-iT-\tau_k)dt. \tag{2.15}$$

Then the output vector of a bank of matched filters during the ith symbol duration can be expressed as:

$$\mathbf{y}[i] = \mathbf{R}^T[1]\mathbf{A}\mathbf{b}[i+1] + \mathbf{R}[0]\mathbf{A}\mathbf{b}[i] + \mathbf{R}[1]\mathbf{A}\mathbf{b}[i-1] + \mathbf{n}[i], \tag{2.16}$$

where the matrices $\mathbf{R}[0]$ and $\mathbf{R}[1]$ are defined by:

$$R_{jk}[0] = \begin{cases} 1, & \text{if } j = k; \\ \rho_{jk}, & \text{if } j < k; \\ \rho_{kj}, & \text{if } j > k; \end{cases} \tag{2.17}$$

$$R_{jk}[1] = \begin{cases} 0, & \text{if } j \geq k; \\ \rho_{kj}, & \text{if } j < k; \end{cases} \tag{2.18}$$

and the zero-mean Gaussian vector $\mathbf{n}[i]$ has autocorrelation matrix:

$$E\left[\mathbf{n}[i]\mathbf{n}^T[j]\right] = \begin{cases} \sigma^2\mathbf{R}^T[1], & \text{if } j = i+1; \\ \sigma^2\mathbf{R}[0], & \text{if } j = i; \\ \sigma^2\mathbf{R}[1], & \text{if } j = i-1; \\ \mathbf{0}, & \text{otherwise.} \end{cases} \tag{2.19}$$

Denote a $K(2M+1)$-dimensional vector of all transmitted symbols $\mathbf{b}_M$ as:

$$\mathbf{b}_M = \left[\mathbf{b}^T[-M], \mathbf{b}^T[-M+1], \ldots, \mathbf{b}^T[M]\right]^T. \tag{2.20}$$

The corresponding matched filter output vector $\mathbf{y}_M$ and the noise vector $\mathbf{n}_M$ are:

$$\mathbf{y}_M = \left[\mathbf{y}^T[-M], \mathbf{y}^T[-M+1], \ldots, \mathbf{y}^T[M]\right]^T, \tag{2.21}$$

and

$$\mathbf{n}_M = \left[\mathbf{n}^T[-M], \mathbf{n}^T[-M+1], \ldots, \mathbf{n}^T[M]\right]^T, \tag{2.22}$$

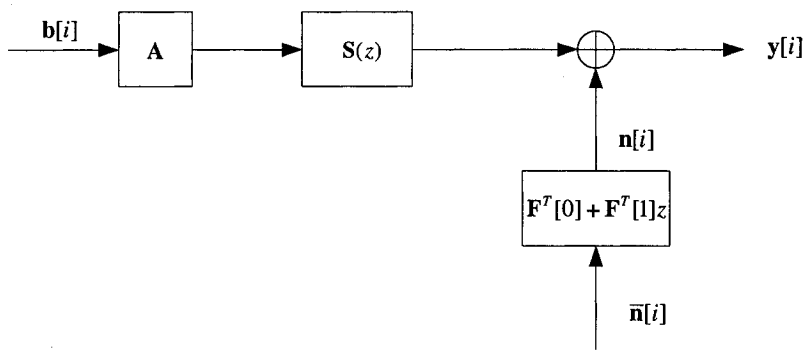

Figure 2.2: The output vector of a bank of matched filters for a K-user asynchronous system

respectively. Let $\mathbf{A}_M$ be the $K(2M+1) \times K(2M+1)$ diagonal matrix whose $k+iK$ diagonal element is equal to A_k. Let $\mathbf{R}_M$ be the $K(2M+1) \times K(2M+1)$ matrix as following:

$$\mathbf{R}_M = \begin{pmatrix} \mathbf{R}[0] & \mathbf{R}^T[1] & \mathbf{0} & \dots & \mathbf{0} & \mathbf{0} \\ \mathbf{R}[1] & \mathbf{R}[0] & \mathbf{R}^T[1] & \dots & \mathbf{0} & \mathbf{0} \\ \mathbf{0} & \mathbf{R}[1] & \mathbf{R}[0] & \dots & \mathbf{0} & \mathbf{0} \\ \dots & \dots & \dots & \dots & \dots & \dots \\ \mathbf{0} & \mathbf{0} & \mathbf{0} & \dots & \mathbf{R}[1] & \mathbf{R}[0] \end{pmatrix}. \tag{2.23}$$

Then the output vector of matched filters $\mathbf{y}_M$ in the whole transmission duration for asynchronous systems can be expressed as:

$$\mathbf{y}_M = \mathbf{R}_M \mathbf{A}_M \mathbf{b}_M + \mathbf{n}_M. \tag{2.24}$$

The vector discrete model in (2.16) can be represented in the z-transform domain as shown in Fig. 2.2, where the discrete-time channel transfer function $\mathbf{S}(z)$ is:

$$\mathbf{S}(z) = \mathbf{R}^T[1]z + \mathbf{R}[0] + \mathbf{R}[1]z^{-1}, \tag{2.25}$$

and $\bar{\mathbf{n}}[i]$ is a Gaussian vector with covariance matrix $\sigma^2\mathbf{I}$. The matrix in (2.25) can be expressed as:

$$\mathbf{S}(z) = \left[\mathbf{F}[0] + \mathbf{F}[1]z\right]^T \left[\mathbf{F}[0] + \mathbf{F}[1]z^{-1}\right], \tag{2.26}$$

where $\mathbf{F}[0]$ is lower triangular and $\mathbf{F}[1]$ is upper triangular with zero diagonal, such that

$$\mathbf{R}[0] = \mathbf{F}^T[0]\mathbf{F}[0] + \mathbf{F}^T[1]\mathbf{F}[1], \tag{2.27}$$

$$\mathbf{R}[1] = \mathbf{F}^T[0]\mathbf{F}[1], \tag{2.28}$$

$$\det\mathbf{F}[0] = \exp\left(\frac{1}{2}\int_0^1 \log(\det\mathbf{S}(e^{j2\pi f}))df\right). \tag{2.29}$$

2.2 Asymptotic Multiuser Efficiency and Near-Far Resistance

In general, the bit error probability performance is the main performance measure of interest in digital communications. However, sometimes it is difficult to obtain a closed expression of the bit error probability. Therefore, usually we resort to simulations to estimate the bit error rate (BER) . In addition, there are several performance measures derived from the bit error probability that are useful in performance analysis. In this section, we introduce two important performance measures for multiuser systems: asymptotic multiuser efficiency [Ver83b], [Ver86] and near-far resistance.

Multiuser efficiency of user k is a measure of the performance degradation of this user due to multiple access interference in the multiuser system compared with that in the single user system. Denote $P_k(\sigma)$ as the bit error probability of user k in a multiuser system with the background Gaussian noise variance σ^2. Then the effective energy of user k, $e_k(\sigma)$, is defined as the energy that user k would require to achieve the same bit

error probability as $P_k(\sigma)$ in a single user system with the equal background Gaussian noise, that is:

$$P_k(\sigma) = Q\left(\frac{\sqrt{e_k(\sigma)}}{\sigma}\right). \tag{2.30}$$

As we know, the error probability of any multiuser detector is lower bounded by the single user error probability, i.e.

$$P_k(\sigma) \geq Q\left(\frac{A_k}{\sigma}\right). \tag{2.31}$$

Therefore, the effective energy is always upper bounded by the actual energy:

$$e_k(\sigma) \leq A_k^2. \tag{2.32}$$

The multiuser efficiency of user k is defined as the ratio between its effective and actual energies, $e_k(\sigma)/A_k^2$. From (2.32), the efficiency is in the interval [0,1] and quantifies the performance loss due to the existence of multiple access interference in the system. Multiuser efficiency depends on the parameters of the multiuser system, such as multiple users' waveforms, received signal-to-noise ratios (SNRs) and the detector employed. The asymptotic multiuser efficiency is defined as:

$$\eta_k = \lim_{\sigma \to 0} \frac{e_k(\sigma)}{A_k^2}. \tag{2.33}$$

In fact, it measures the speed at which $P_k(\sigma)$ goes to 0 when we increase SNRs in the high signal-to-noise ratio region, that is:

$$\begin{aligned} \eta_k &= \sup\left\{0 \leq r \leq 1 : \lim_{\sigma \to 0} P_k(\sigma)/Q\left(\frac{\sqrt{r}A_k}{\sigma}\right) = 0\right\} \\ &= \frac{2}{A_k^2} \lim_{\sigma \to 0} \sigma^2 \log[1/P_k(\sigma)]. \end{aligned} \tag{2.34}$$

Since the asymptotic bit error probability of the single user system is zero, we can immediately conclude that in those situations where the bit error probability of the multiuser system does not vanish as the signal-to-noise ratio increases to infinity, the asymptotic multiuser efficiency is equal to 0. Conversely, if the asymptotic multiuser

efficiency is positive, then the bit error probability of the multiuser system not only goes to zero but also it does so exponentially as a function of the signal-to-noise ratio.

Another common problem in the system with mobile transmitters is the near-far problem. Since the distances between these transmitters and the receiver are not equal, the received signal powers from some transmitters are higher than those from other transmitters. Sometimes, in the receiver the lower power signals will be submerged in the higher power signals and can not be correctly recovered. This is so called near-far problem. The measure to quantify the degree of robustness against the near-far problem is called near-far resistance, which is defined as the asymptotic multiuser efficiency minimized over the received energies of all the other users in [Lup86], [Lup89]. For example, the near-far resistance $\bar{\eta}_k$ of user k is defined as:

$$\bar{\eta}_k = \min_{j \neq k} \min_{A_j > 0} \eta_k, \tag{2.35}$$

where η_k is the asymptotic multiuser efficiency of user k, A_j is the received amplitude of the jth user's signal.

In the following sections, we will introduce different types of multiuser detectors and compare their asymptotic multiuser efficiencies, near-far resistances and computational complexities.

2.3 Conventional Multiuser Detection

The conventional multiuser detector (i.e. single user matched filter) was first proposed in [Nor63] and was used for code-division multiple-access (CDMA) modulation in [Sim94]. It gives hard symbol decisions based on the matched filter outputs,

$$\hat{b}_k[i] = \text{sign}(y_k[i]). \tag{2.36}$$

It considers the multiple access interference to be noise and has the lowest computational complexity. In the K-user synchronous and asynchronous systems, the multiuser efficiencies of user k are:

$$\eta_k^c = \left[\max\left\{0, \left(1 - \sum_{j \neq k} \frac{A_j}{A_k}|\rho_{jk}|\right)\right\}\right]^2 \tag{2.37}$$

and

$$\eta_k^c = \left[\max\left\{0, \left(1 - \sum_{j \neq k} \frac{A_j}{A_k}(|\rho_{jk}| + |\rho_{kj}|)\right)\right\}\right]^2, \tag{2.38}$$

respectively. By minimizing (2.37) or (2.38) over signal amplitudes of interfering users $\{A_j, j \neq k\}$, we obtain the near-far resistance $\bar{\eta}_k^c$ of user k according to the definition in (2.35). We can see that the near-far resistance of the kth user is equal to 0 unless $\rho_{jk} = \rho_{kj} = 0$ for all $j \neq k$, which means that the kth user's waveform must be orthogonal to each of the partially overlapping waveforms of every interferer. Usually this condition cannot be satisfied for all offsets in an asynchronous system. Therefore, the conventional multiuser detector is not near-far resistant, except for the multiuser system with synchronous orthogonal waveforms.

2.4 Optimum Multiuser Detection

The derivation and analysis of the optimum multiuser receiver appeared in the early eighties [Ver83a], [Ver83b]. There are two types of optimum multiuser detectors in the different optimum senses. For synchronous systems, the jointly optimum detector maximizes the joint a posteriori probability:

$$P[\mathbf{b}|r(t), 0 \leq t \leq T], \tag{2.39}$$

which will provide the minimum joint error probability of the vector $\mathbf{b}$. On the other hand, the individually optimum detector maximizes the a posteriori probability of each user's symbol:

$$P[b_k|r(t), 0 \leq t \leq T], \quad 1 \leq k \leq K, \tag{2.40}$$

which provides the minimum bit error rate of b_k. The jointly optimum and individually optimum decisions are not necessarily the same, since usually $\{b_k, 1 \leq k \leq K\}$ are not independent of each other conditioned on the received signal $r(t)$. The solution to jointly optimum detection is the maximum likelihood solution, which has lower computational complexity compared with individually optimum detection. Moreover, the error probability of each symbol achieved by the maximum-likelihood solution is extremely close to the minimum, unless the signal-to-noise ratio is very low. Therefore, in the following we will focus on the jointly optimum detector. The implementation of the minimum bit error rate multiuser receiver can be based on a backward-forward dynamic programming algorithm [Abe70], [Bah74], [Cha66], [Ver87].

Since all possible $\mathbf{b}$ are equiprobable, the jointly optimum decision rule selects a vector $\mathbf{b}$ that maximizes the following likelihood probability:

$$p[r(t), 0 \leq t \leq T|\mathbf{b}] = \exp\left(-\frac{1}{2\sigma^2}\int_0^T \left[r(t) - \sum_{k=1}^{K} A_k b_k s_k(t)\right]^2 dt\right). \tag{2.41}$$

The maximum likelihood solution $\mathbf{b}$ is chosen such that $\sum_{k=1}^{K} A_k b_k s_k(t)$ is the closest to the received signal in the mean square error sense. Equivalently, the maximum likelihood solution in (2.41) maximizes

$$\begin{aligned}\Omega(\mathbf{b}) &= 2\int_0^T \left[\sum_{k=1}^{K} A_k b_k s_k(t)\right] r(t)dt - \int_0^T \left[\sum_{k=1}^{K} A_k b_k s_k(t)\right]^2 dt \\ &= 2\mathbf{b}^T\mathbf{A}\mathbf{y} - \mathbf{b}^T\mathbf{A}\mathbf{R}\mathbf{A}\mathbf{b}.\end{aligned} \tag{2.42}$$

The maximization of (2.42) is a combinatorial optimization problem. It has the computational complexity $\sim O(2^K/K)$ per symbol per user.

As in the synchronous system, the objective for the asynchronous system is to compute the $\mathbf{b}_M$ that maximizes:

$$p\left[r(t), t \in [-MT, MT+2T]|\mathbf{b}_M\right] = \exp\left(-\frac{1}{2\sigma^2}\int_{-MT}^{MT+2T} \left(r(t) - S_t(\mathbf{b}_M)\right)^2 dt\right), \tag{2.43}$$

where

$$S_t(\mathbf{b}_M) = \sum_{k=1}^{K} \sum_{i=-M}^{M} A_k b_k[i] s_k(t - iT - \tau_k). \tag{2.44}$$

Then the maximization of (2.43) is equivalent to selecting $\mathbf{b}_M$ that maximizes:

$$\begin{aligned} \Omega(\mathbf{b}_M) &= 2\int S_t(\mathbf{b}_M) r(t) dt - \int S_t^2(\mathbf{b}_M) dt \\ &= 2\mathbf{b}_M^T \mathbf{A}_M \mathbf{y}_M - \mathbf{b}_M^T \mathbf{A}_M \mathbf{R}_M \mathbf{A}_M \mathbf{b}_M. \end{aligned} \tag{2.45}$$

To search for the symbol vector $\mathbf{b}_M$ which maximizes (2.45), we can use the Viterbi algorithm. The computational complexity is $\sim O(2^K)$ per symbol per user, which is exponentially proportional to the number of users and similar to that for the synchronous case.

The optimum asymptotic multiuser efficiency for synchronous systems is:

$$\eta_k^o = \frac{d_{k,\min}^2}{A_k^2} = \min_{\epsilon \in \{-1,0,1\}^K, \epsilon_k = 1} \frac{1}{A_k^2} \boldsymbol{\epsilon}^T \mathbf{A}\mathbf{R}\mathbf{A}\boldsymbol{\epsilon}, \tag{2.46}$$

where $d_{k,\min}$ is the normalized minimum distance between any two multiuser signals modulated by two K-dimensional sequences: $\mathbf{b}_1^k$ and $\mathbf{b}_2^k$ which differ in the kth component. That is:

$$d_{k,\min}^2 = \min_{\mathbf{b}_1^k, \mathbf{b}_2^k} \frac{1}{4} \int_0^T \left[S(\mathbf{b}_1^k, t) - S(\mathbf{b}_1^k, t) \right]^2 dt, \tag{2.47}$$

where the multiuser signal $S(\mathbf{b}, t)$ is defined as:

$$S(\mathbf{b}, t) = \sum_{k=1}^{K} A_k b_k s_k(t). \tag{2.48}$$

If we assume that the cross-correlation matrix $\mathbf{R}$ is nonsingular, we have the optimum near-far resistance as following:

$$\bar{\eta}_k^o = 1 - \mathbf{a}_k^T \mathbf{R}_k^{-1} \mathbf{a}_k, \tag{2.49}$$

where $(K-1) \times (K-1)$ matrix $\mathbf{R}_k$ results by striking out the kth column and the kth row from $\mathbf{R}$ and $(K-1)$ vector $\mathbf{a}_k$ results from eliminating the kth component from the kth column of $\mathbf{R}$.

2.5 Suboptimum Linear Multiuser Detection

The suboptimum linear multiuser detectors include the decorrelating detector [Ver98] and minimum mean square error detector [Ver98], which we will introduce in this section. The decorrelating detector recovers the transmitted symbols error-free in the absence of noise, and does not require knowledge of the received amplitudes. In the synchronous system, by assuming that the cross-correlation $\mathbf{R}$ is invertible, it first premultiplies the output vector $\mathbf{y}$ of a bank of matched filters by $\mathbf{R}^{-1}$, then gives the hard decisions:

$$\hat{b}_k = \text{sign}\Big((\mathbf{R}^{-1}\mathbf{y})_k\Big). \tag{2.50}$$

For the asynchronous system, the decorrelating detector employs the inverse of the discrete-time channel transfer function $\mathbf{S}^{-1}(z)$ to premultiply the output vector of matched filters [Koh83], [Lup88], [Lup90].

The multiuser efficiency of the decorrelator for the synchronous case is equal to:

$$\eta_k^d = 1 - \mathbf{a}_k^T \mathbf{R}_k^{-1} \mathbf{a}_k, \tag{2.51}$$

which is the same as (2.49). Since this efficiency only depends on the cross-correlation matrix (without depending on either the noise level or the interfering amplitudes), it is equal to the asymptotic multiuser efficiency and to the near-far resistance as well. Therefore, the decorrelating detector achieves the maximum near-far resistance [Ver86].

The linear MMSE detector applies a linear filter on the output of matched filters which minimizes the mean square errors between transmitted symbols and recovered symbols [Mad94], [Xie90]. In the synchronous system, we choose a linear filter $\mathbf{m}_k$ (which is a K-dimensional column vector) for user k, which satisfies the following MMSE criterion:

$$\min_{\mathbf{m}_k} E\Big[(b_k - \mathbf{m}_k^T \mathbf{y})^2\Big]. \tag{2.52}$$

It is equivalent to choosing a $K \times K$ matrix $\mathbf{M}$, whose kth column is equal to $\mathbf{m}_k$, satisfying:

$$\min_{\mathbf{M}} E\left[\|\mathbf{b} - \mathbf{M}^T\mathbf{y}\|^2\right]. \tag{2.53}$$

The solution of (2.53), i.e. the linear MMSE detector, is:

$$\mathbf{M} = \left[\mathbf{R} + \sigma^2\mathbf{A}^{-2}\right]^{-1}. \tag{2.54}$$

In the asynchronous case, the linear MMSE detector has the following transfer function:

$$\left[\mathbf{R}^T[1]z + \mathbf{R}[0] + \sigma^2\mathbf{A}^{-2} + \mathbf{R}[1]z^{-1}\right]^{-1}. \tag{2.55}$$

If all of the received amplitudes are fixed and $\sigma \rightarrow 0$, i.e. signal-to-noise ratios go to infinity, then the linear MMSE filter converges to the decorrelating detector. Therefore, the asymptotic multiuser efficiency and near-far resistance of the linear MMSE detector are the same as those of the decorrelating detector. For the low signal-to-noise ratios, the linear MMSE detector provides a better performance than the decorrelator, since it takes into account both the multiple access interference and the background noise.

2.6 Suboptimum Non-Linear Multiuser Detection

In this section, we introduce three non-linear multiuser detectors: successive detectors (serial interference cancellers) (for more details, please refer to [Den92], [Div98], [Hol95], [Koh91], [Pat93], [Yoo93a], [Yoo93b]), multistage detectors (parallel interference cancellers) ([Koh90], [Var88], [Var90], [Var91], [Faw95], [Yoo93b]), and decision feedback detectors ([Abd92], [Abd94], [Due92], [Due93], [Due95], [Haf96], [Pet94], [Tid95], [Var99], [Woo99], [Wei94], [Wu94], [Xie90], [Yan94]).

In successive detection, each of the interfering waveforms is cancelled from the received signal one at a time. First we sort the received powers of the multiple users in a decreasing

order with the user index, i.e. user 1 has the maximum power and user K has the minimum power. When making a decision about the kth user in the synchronous case, we assume that the decisions of users $1, \ldots, k-1$ are correct and we ignore the presence of users $k+1, \ldots, K$. Therefore,

$$\hat{b}_k = \text{sign}\left(y_k - \sum_{j=1}^{k-1} A_j \rho_{jk} \hat{b}_j\right). \tag{2.56}$$

The order of cancellation influences the performance of the successive detector and is further examined in [Kub92], [Pat93], [Pat94], [Ped96], [Ses98]. This detector can be easily generalized to the asynchronous case.

In multistage detection, in each stage (except for the first stage), all of the interfering signals of each user are cancelled from the received signal based on the decisions of interfering users in the previous stage. In the mth stage,

$$\hat{b}_k(m) = \text{sign}\left(y_k - \sum_{j \neq k} A_j \rho_{jk} \hat{b}_j(m-1)\right). \tag{2.57}$$

In the initial stage, the detector can follow conventional detection, decorrelating detection or linear MMSE detection. Multistage detectors for asynchronous systems need to store tentative decisions in sliding windows for each stage.

A general decision feedback detector in [Woo02] for each user consists of a feedforward filter applied to the received signal and a feedback filter applied to the fedback decisions. The optimum filters are determined by minimizing the mean square error between the transmitted symbol and the recovered symbol. For the synchronous system, the received discrete signal $\mathbf{r}_{N\times 1}$ in each symbol duration can be expressed as:

$$\mathbf{r} = \mathbf{S}\mathbf{b} + \mathbf{n}, \tag{2.58}$$

where

$$\mathbf{S} = [\mathbf{s}_1, \mathbf{s}_2, \ldots, \mathbf{s}_K]_{N\times K} \tag{2.59}$$

and the $N \times 1$ column vector $\mathbf{s}_k$ is the discrete waveform of user k. The noise vector $\mathbf{n}_{N\times 1}$ is a zero-mean Gaussian vector with covariance matrix $\sigma^2\mathbf{I}$. For user k, we denote its feedforward filter and feedback filter by vectors $(\mathbf{m}_{fk})_{N\times 1}$ and $(\mathbf{m}_{bk})_{K\times 1}$, respectively. The output of the decision feedback detector of user k is:

$$z_k = \mathbf{m}_{fk}^T\mathbf{r} + \mathbf{m}_{bk}^T\hat{\mathbf{b}}_D, \tag{2.60}$$

where the $K \times 1$ vector $\hat{\mathbf{b}}_D$ has nonzero elements as the fedback symbol decisions. The optimum filters satisfy the following MMSE criterion:

$$\min_{\mathbf{m}_{fk},\mathbf{m}_{bk}} E\Big[[z_k - b_k]^2\Big] = \min_{\mathbf{m}_{fk},\mathbf{m}_{bk}} E\Big[[\mathbf{m}_{fk}^T\mathbf{r} + \mathbf{m}_{bk}^T\hat{\mathbf{b}}_D - b_k]^2\Big]. \tag{2.61}$$

The solution of (2.61) is:

$$\mathbf{m}_{fk} = (\mathbf{S}_U \cdot \mathbf{S}_U^T + \sigma^2\mathbf{I})^{-1}\mathbf{s}_k, \tag{2.62}$$

$$\mathbf{m}_{bk} = -\mathbf{S}_D^T \cdot \mathbf{m}_{fk}, \tag{2.63}$$

where the columns of $\mathbf{S}_U$ consist of the waveforms of users whose symbols are not fedback and the columns of $\mathbf{S}_D$ are the waveforms of users whose symbols are fedback. The feedforward filter in (2.62) is actually an MMSE filter for users whose symbols are not fedback. Note that the general detector in (2.60) can be a successive decision feedback detector or parallel decision feedback detector depending on the fedback symbols in $\hat{\mathbf{b}}_D$.

2.7 Summary

We reviewed most of traditional multiuser detectors in this chapter. These detectors gave us the background knowledge for soft-input soft-output multiuser detectors, which will be focused on in the later chapters.

Chapter 3

Turbo Principles

The novel turbo code proposed in 1993 [Ber93a] brought a revolution to the channel coding field. The turbo code is a hot research topic since it can provide a bit error performance that is very close to the Shannon limit, while it has a computational complexity which is not significantly higher than that of the decoder for single component codes by iterative decoding. The more important thing is that the underlying principles of iterative turbo decoders (turbo principles) can be extended and applied to many other functions in the receiver, such as multiuser detection, channel equalization and channel estimation, etc, to obtain a good system performance with a feasible complexity.

Based on turbo principles [Chu01], [Hag96], [Skl97], any function block in the receiver can be modeled as a soft-input soft-output module which not only can employ the soft inputs from all other blocks as a priori information of transmitted coded symbols and information bits, but also can output the extrinsic soft information to other blocks. All of these SISO modules cooperate iteratively by transferring extrinsic soft information between them. The receiver performance should improve in successive iterations and converge to a near ideal performance.

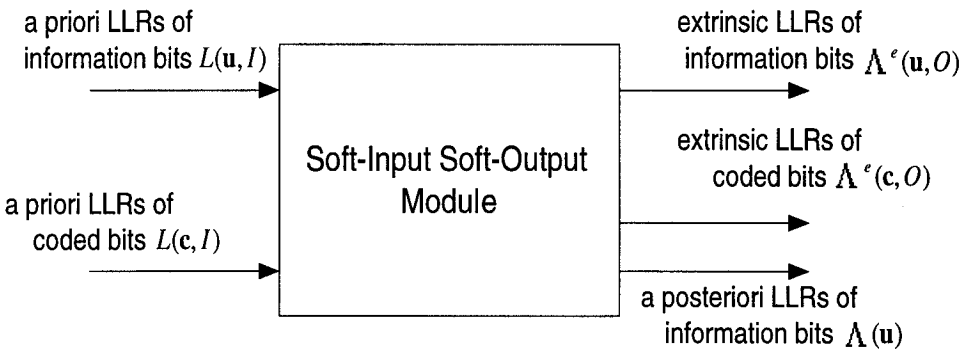

Figure 3.1: The SISO module

In Section 3.1, we first give a general description of a SISO a posteriori probability (APP) module for iterative decoding of concatenated codes. This model can be further extended for other functions in the receiver. Then we describe turbo principles, i.e. the way by which several SISO APP modules in the receiver cooperate iteratively, by using as examples the iterative decoders of parallel concatenated codes in Section 3.2 and of serially concatenated codes in Section 3.3. Finally, we present the optimum MAP and log-MAP algorithms, the suboptimum max-log-MAP algorithm and a general APP algorithm for the SISO APP module in Section 3.4.

3.1 Soft-Input Soft-Output APP Module

Parallel and serially concatenated codes have been shown to yield a remarkable coding gain close to the theoretical limits [Ben96a], [Ben98], [Ber96], [Div95], [Dum98], [Sas98], [Vit98b] while they have a relatively simple iterative decoding structure. The core of the iterative decoder is a soft-input soft-output APP module (Fig. 3.1), which is employed by each component decoder. The SISO APP module has two input ports accepting the a priori log-likelihood ratios (LLRs) of information bits and coded bits and two output ports forming extrinsic LLRs of these bits based on the code constraints. It can also

calculate the a posteriori LLRs of information bits at the output when the final decisions are required. Denote each information bit frame as $\mathbf{u} = [u_1, u_2, \ldots, u_Q]$, where Q is its length and the corresponding coded bit frame as $\mathbf{c} = [c_1, c_2, \ldots, c_F]$, where F is the coded bit frame length. The letters I and O refer to the input and output of the SISO module, respectively. The a priori LLRs of information bits $L(\mathbf{u}, I)$ and coded bits $L(\mathbf{c}, I)$ at the input are:

$$L(\mathbf{u}, I) = \{L(u_i, I), 1 \leq i \leq Q\}, \tag{3.1}$$

$$L(\mathbf{c}, I) = \{L(c_j, I), 1 \leq j \leq F\}, \tag{3.2}$$

where

$$L(u_i, I) \triangleq \log \frac{P(u_i = 1)}{P(u_i = 0)}, \tag{3.3}$$

and

$$L(c_j, I) \triangleq \log \frac{P(c_j = 1)}{P(c_j = 0)}. \tag{3.4}$$

The logarithm operation ($\log(\cdot)$) in this thesis refers to the natural logarithm of its argument. The extrinsic LLRs of information bits and coded bits at the output are:

$$\Lambda^e(\mathbf{u}, O) = \{\Lambda^e(u_i, O), 1 \leq i \leq Q\}, \tag{3.5}$$

$$\Lambda^e(\mathbf{c}, O) = \{\Lambda^e(c_j, O), 1 \leq j \leq F\}, \tag{3.6}$$

respectively. The output extrinsic LLR $\Lambda^e(u_i, O)$ of information bit u_i is computed based on the code constraints and a priori LLRs of information bits and coded bits except the a priori LLR of itself $L(u_i, I)$. Similarly, the extrinsic LLR $\Lambda^e(c_j, O)$ of coded bit c_j depends on the code constraints and a priori LLRs of information bits and coded bits except the a priori LLR of itself $L(c_j, I)$. That means, the extrinsic LLRs of information bit u_i and coded bit c_j are independent of their a priori LLRs $L(u_i, I)$ and $L(c_j, I)$,respectively. SISO APP blocks of component codes in the iterative decoder cooperate by exchanging extrinsic

LLRs of information bits or coded bits as a priori LLRs. The final decisions of information bits are based on the a posteriori LLRs of information bits $\Lambda(\mathbf{u}) = \{\Lambda(u_i), 1 \leq i \leq Q\}$ at the output of one SISO block.

There are the optimum MAP and log-MAP algorithms and the suboptimum max-log-MAP algorithm for the SISO module to calculate the extrinsic LLRs of information bits and coded bits, which will be briefly introduced in Section 3.4. In particular, in Subsection 3.4.3, we present a general algorithm to calculate the three soft outputs of the SISO module in Fig. 3.1.

The SISO module for the component code in concatenated coding systems can be extended for other functions in the receiver, such as multiuser detection or channel equalization, by replacing the code constraints by the multiple access channel constraints or the frequency-selective fading channel constraints, respectively. The SISO multiuser detection is the main topic of this thesis. In order to clearly describe how the SISO blocks in the receiver cooperate with each other, in the following two sections, we use iterative decoders for parallel concatenated codes and serially concatenated codes as examples.

3.2 Iterative Decoders for Parallel Concatenated Codes (PCC)

The well-known turbo codes belong to the category of parallel concatenated convolutional codes . In this section, we consider the encoder and iterative decoder of a basic turbo code [Ber96]. Fig. 3.2 shows the encoder structure of a basic turbo code. The data flow (d_k at time k) enters directly to a first component recursive systematic convolutional (RSC) encoder C_1 and after interleaving, it feeds (d_n at time k) a second component RSC encoder C_2. These two encoders are not necessarily identical. Data flow d_k is

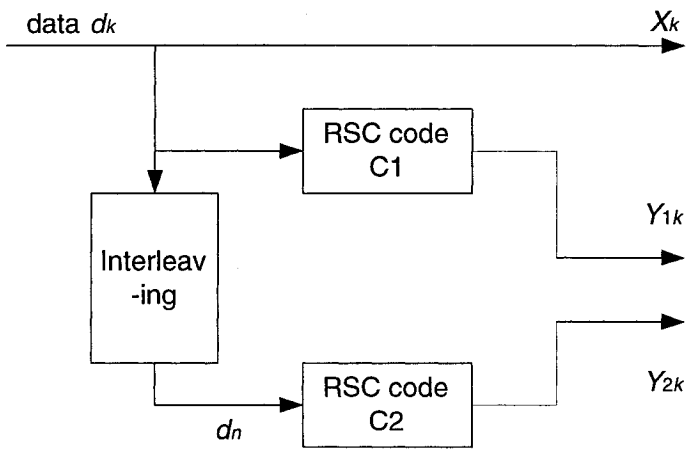

Figure 3.2: A basic turbo encoder

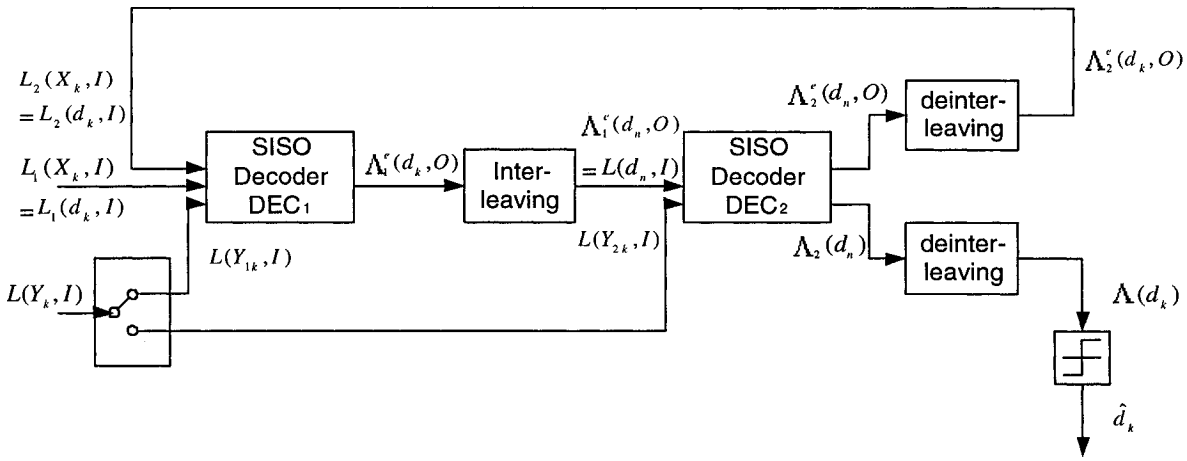

Figure 3.3: The iterative turbo decoding structure (without considering the delays introduced by two component SISO decoders, the interleaver and de-interleavers)

systematically transmitted as symbol X_k and redundancies Y_{1k} and Y_{2k} produced by C_1 and C_2 respectively may be completely transmitted or punctured for higher rates. The two component code rates R_1 and R_2 associated with C_1 and C_2, after puncturing, give a total rate R:

$$\frac{1}{R} = \frac{1}{R_1} + \frac{1}{R_2} - 1. \tag{3.7}$$

Fig. 3.3 shows the iterative turbo decoding structure, which does not consider the delays introduced by two component decoders and interleaver. For a discrete memoryless Gaussian channel and a binary modulation, the decoder input consists of two random variables x_k and y_k at time k:

$$x_k = (2X_k - 1) + i_k, \tag{3.8}$$

$$y_k = (2Y_k - 1) + q_k, \tag{3.9}$$

where i_k and q_k are two independent noises with the same variance σ^2. The redundant information y_k is demultiplexed and sent to decoder $\mathrm{DEC_1}$ when $Y_k = Y_{1k}$ and toward decoder DEC when $Y_k = Y_{2k}$.

The a priori LLRs $L_1(d_k, I)$ of information bit d_k and $L(Y_k, I)$ of redundancy bit Y_k are obtained from their channel soft values directly:

$$L_1(d_k, I) = \log\frac{p(x_k|d_k = 1)}{p(x_k|d_k = 0)} = \frac{2}{\sigma^2}x_k, \tag{3.10}$$

$$L(Y_k, I) = \log\frac{p(y_k|Y_k = 1)}{p(y_k|Y_k = 0)} = \frac{2}{\sigma^2}y_k. \tag{3.11}$$

The decoder shown in Fig. 3.3 is made up of two component decoders ($\mathrm{DEC_1}$ and $\mathrm{DEC_2}$) in a serial concatenation scheme. For the first component decoder, its input of a

priori LLR $L_2(d_k, I)$ of information bit d_k is fedback from the second component decoder, whose calculation will be shown later by (3.15).

$$L_2(d_k, I) = \Lambda_2^e(d_k, O) \tag{3.12}$$

The first SISO decoder calculates the a posteriori LLR value $\Lambda_1(d_k)$ of information bit d_k based on the code constraints and its soft inputs, which can be expressed as:

$$\Lambda_1(d_k) = L_1(d_k, I) + L_2(d_k, I) + W_{1k}, \tag{3.13}$$

where W_{1k} is a function of the a priori LLRs of other information bits $\{L_1(d_i, I), i \neq k\}$, $\{L_2(d_i, I), i \neq k\}$ and the redundancy bits $\{L(Y_{1i}, I)\}$. That means, W_{1k} is independent of the a priori LLR of information bit d_k. Since the a priori LLR $L_2(d_k, I)$ is fedback from the second SISO decoder, the extrinsic LLR of the first decoder $\Lambda_1^e(d_k, O)$ should be independent of it and is defined as:

$$\Lambda_1^e(d_k, O) \triangleq L_1(d_k, I) + W_{1k}. \tag{3.14}$$

After interleaving, the extrinsic LLRs $\Lambda_1^e(d_n, O)$ of information bits from the first decoder are output to the second decoder as the a priori LLRs $L(d_n, I)$. The second decoder calculates the a posteriori LLR $\Lambda_2(d_n)$ of information bit d_n, which can be expressed as:

$$\Lambda_2(d_n) = L(d_n, I) + \Lambda_2^e(d_n, O), \tag{3.15}$$

where $\Lambda_2^e(d_n, O)$ depends on the sequence $\{L(d_i, I), i \neq n\}$, $\{L(Y_{2k}, I)\}$ and the code constraints. Due to the presence of interleaving between the two component decoders, extrinsic LLRs $\{\Lambda_2^e(d_k, O)\}$ (i.e. the fedback a priori LLRs $\{L_2(d_k, I)\}$ of the first decoder) and the a priori information $\{L_1(d_k, I)\}$ and $\{L(Y_{1k}, I)\}$ are weakly correlated. Therefore, these three values can be used jointly by the first component decoder for carrying out a new decoding of bit d_k. The term turbo code is given for this iterative feedback decoding scheme with reference to the principle of the turbo engine.

The two SISO component decoders cooperate with each other by exchanging extrinsic LLRs of information bits. Note that these extrinsic LLRs provided by different SISO component decoders are independent, which ensures a fast convergence of the system performance to a desired one with additional iterations. After sufficient number of iterations, the final decisions on the information bits are given as hard decisions of a posteriori LLRs of information bits:

$$\hat{d}_k = \text{sign}[\Lambda(d_k)]. \tag{3.16}$$

3.3 Iterative Decoders for Serially Concatenated Codes (SCC)

Serial concatenation of component codes separated by interleavers has been shown to have higher interleaver gains and better performance at high signal-to-noise ratios than turbo codes [Ben98]. Similarly, serially concatenated codes can also be decoded iteratively [Ben96b], [Ben98]. Fig. 3.4 and Fig. 3.5 show the encoder and decoder structure for serially concatenated codes, respectively. Differently from turbo decoders, the component SISO decoders of serially concatenated codes calculate and exchange the extrinsic LLRs of not only information bits but also coded bits.

The a priori information of coded bits and information bits of the inner decoder is from its soft inputs: $L(\mathbf{c}^i, I)$ and $L(\mathbf{u}^i, I)$ respectively, which are log-likelihood ratios without considering the inner code constraints. $L(\mathbf{c}^i, I) = \{L(c_k^i, I), k\}$ and $L(\mathbf{u}^i, I) = \{L(u_k^i, I), k\}$, where k is the time index. The LLRs of coded bits $\{L(\mathbf{c}^i, I)\}$ are from the channel soft values directly. Under the assumption of BPSK modulation and an additive white Gaussian noise (AWGN) channel, the inner decoder receives the channel soft values y_k at time k as:

$$y_k = (2c_k^i - 1) + n_k, \tag{3.17}$$

Figure 3.4: The encoder structure of serially concatenated codes

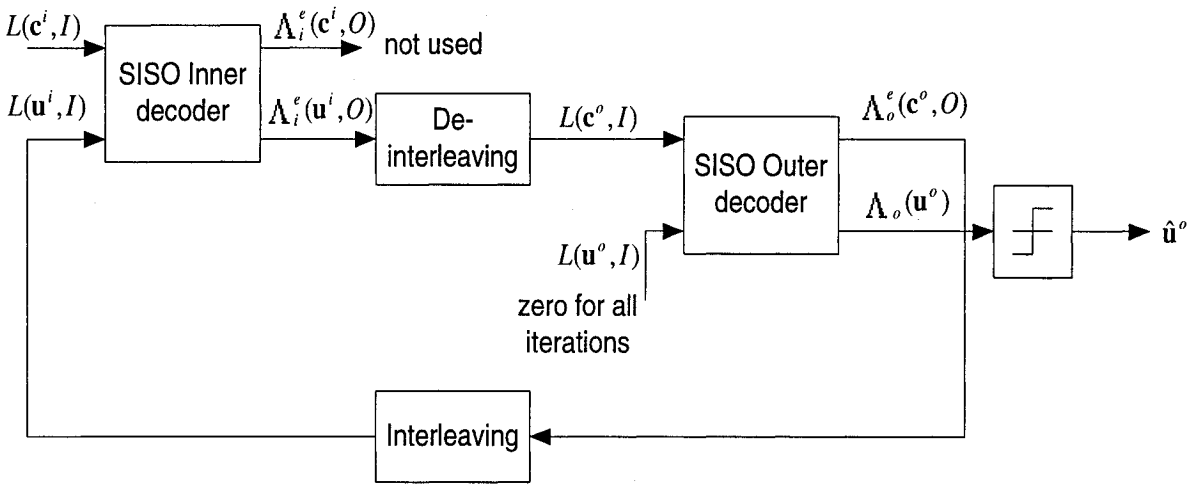

Figure 3.5: The iterative decoding structure for serially concatenated codes (without considering the delays introduced by two component SISO decoders, the interleaver and de-interleavers)

where n_k is a Gaussian random variable with zero-mean and variance σ^2. The a priori LLRs of coded bits are calculated as:

$$L(c_k^i, I) = \log\frac{p(y_k|c_k^i = 1)}{p(y_k|c_k^i = 0)} = \frac{2}{\sigma^2}y_k. \tag{3.18}$$

The a priori LLRs $L(\mathbf{u}^i, I)$ of information bits are fedback from the SISO outer decoder and initialized as zeros in the first iteration. Based on its soft inputs and the inner code constraints, the SISO inner decoder calculates the a posteriori LLRs $\Lambda_i(c_k^i)$ of coded bit c_k^i and $\Lambda_i(u_k^i)$ of information bit u_k^i, which can be expressed as:

$$\Lambda_i(c_k^i) = L(c_k^i, I) + \Lambda_i^e(c_k^i, O), \tag{3.19}$$

$$\Lambda_i(u_k^i) = L(u_k^i, I) + \Lambda_i^e(u_k^i, O). \tag{3.20}$$

The extrinsic LLRs $\Lambda_i^e(\mathbf{c}^i, O)$ of coded bits are not used in the decoder. For information bit u_k^i, its extrinsic LLR $\Lambda_i^e(u_k^i, O)$ is a function of the a priori LLRs of coded bits $L(\mathbf{c}^i, I)$, information bits excluding itself $\{L(u_j^i, I), j \neq k\}$ and the inner code constraints. That is, the extrinsic LLR $\Lambda_i^e(u_k^i, O)$ of information bit u_k^i is independent from its a priori LLR $L(u_k^i, I)$. These extrinsic LLRs of information bits are passed through the de-interleaver (denoted as π^{-1}), whose outputs correspond to the a priori LLRs of the coded bits of the outer code, i.e.,

$$L(\mathbf{c}^o, I) = \pi^{-1}[\Lambda_i^e(\mathbf{u}^i, O)]. \tag{3.21}$$

The a priori LLRs $L(\mathbf{u}^o, I)$ of information bits of the outer code are set to zeros. Based on its soft inputs, the SISO outer decoder calculates the a posteriori LLR $\Lambda_o(c_k^o)$ of coded bit c_k^o, which can be expressed as following:

$$\Lambda_o(c_k^o) = L(c_k^o, I) + \Lambda_o^e(c_k^o, O). \tag{3.22}$$

The extrinsic LLR $\Lambda_o^e(c_k^o, O)$ of coded bit c_k^o dependes on the a priori LLRs of all coded bits excluding itself and the outer code constraints. After being interleaved, these extrinsic LLRs are fedback to the SISO inner decoder as its soft inputs. The final hard decisions of information bits are based on their a posteriori LLRs $\Lambda_o(\mathbf{u}^o)$.

3.4 The Optimum MAP Algorithm and Suboptimum Algorithms

The maximum a posteriori symbol decoding algorithm is optimum in the sense of the minimum bit error probability. The BCJR algorithm [Bah74] is a MAP decoding algorithm. It calculates the a posteriori probability of an information bit or coded bit when the encoding can be expressed as a Markov process and the channel is discrete and memoryless. Furthermore, the BCJR algorithm can calculate the extrinsic information about information bits and coded bits, which is essentially required by iteratively decoding, such as turbo decoding.

In this section, for clear description, first we introduce the original BCJR algorithm [Bah74] in Subsection 3.4.1. However, the original BCJR algorithm is numerically unstable. Its implementation based on the log-likelihood algebra [Hag96], i.e. the log-MAP algorithm, resolves this problem. The detailed log-MAP algorithm is presented in Subsection 3.4.2. To further reduce the computational complexity of the optimum log-MAP algorithm, we review the suboptimum max-log-MAP algorithm. Then based on the BCJR algorithm, in Subsection 3.4.3 we present a general APP algorithm for the SISO module of Section 3.1.

Alternative soft output decoding algorithms include the weighted output decoding algorithm in [Bat79], [Bat89] and the soft output Viterbi algorithm (SOVA) in [Ber93b], [Hag89], [Hag95], which are simpler while suboptimum compared with the optimum MAP algorithm. Comparison of these optimum and suboptimum algorithms is presented in [Fos98], [Rob95], [Vit98a]. For detailed information, please refer to these references.

Figure 3.6: Block diagram of a transmission system

3.4.1 The Original BCJR algorithm

The original BCJR algorithm [Bah74] is the optimum algorithm to calculate the a posteriori probabilities of coded bits and information bits. Consider the transmission system diagram in Fig. 3.6. The encoder output is assumed to be a discrete-time finite-state Markov source. The M distinct states of the Markov source are indexed by the integer $m, m = 0, 1, \ldots, M-1$. The state of the encoder at time t is denoted by S_t and its output by X_t. A state sequence of the encoder extending from time t to t' is denoted by $\boldsymbol{S}_t^{t'} = S_t, S_{t+1}, \ldots, S_{t'}$, and the corresponding output sequence is $\boldsymbol{X}_t^{t'} = X_t, X_{t+1}, \ldots, X_{t'}$. The state transitions of the Markov source are:

$$p_t(m|m') = P\{S_t = m|S_{t-1} = m'\}. \tag{3.23}$$

Their output probabilities are denoted as

$$q_t(X|m', m) = P\{X_t = X|S_{t-1} = m'; S_t = m\} \tag{3.24}$$

where X belongs to some finite discrete alphabet.

The Markov source starts in the initial state $S_0 = 0$, and produces an output sequence $\boldsymbol{X}_1^\tau$ ending in the terminal state $S_\tau = 0$. $\boldsymbol{X}_1^\tau$ is the input to a noisy discrete memoryless channel whose output is the sequence $\boldsymbol{Y}_1^\tau = Y_1, Y_2, \ldots, Y_\tau$. The transition probabilities of the channel are defined by $R(\cdot|\cdot)$ so that for all $1 \leq t \leq \tau$

$$P\{\boldsymbol{Y}_1^t|\boldsymbol{X}_1^t\} = \prod_{j=1}^{t} R(Y_j|X_j). \tag{3.25}$$

In the following, first we consider the a posteriori probabilities of states and transitions of the Markov source. Then we apply these results to calculate the a posteriori LLRs of information bits and coded bits, and the extrinsic LLRs of coded bits for a linear encoder. The a posteriori probabilities of states and transitions are the conditional probabilities:

$$P\{S_t = m | \boldsymbol{Y}_1^\tau\} = P\{S_t = m; \boldsymbol{Y}_1^\tau\}/P\{\boldsymbol{Y}_1^\tau\}, \tag{3.26}$$

and

$$P\{S_{t-1} = m'; S_t = m | \boldsymbol{Y}_1^\tau\} = P\{S_{t-1} = m'; S_t = m; \boldsymbol{Y}_1^\tau\}/P\{\boldsymbol{Y}_1^\tau\}. \tag{3.27}$$

Since for a given $\boldsymbol{Y}_1^\tau$, $P\{\boldsymbol{Y}_1^\tau\}$ is a constant, we can first focus on calculating the joint probabilities $P\{S_t = m; \boldsymbol{Y}_1^\tau\}$ and $P\{S_{t-1} = m'; S_t = m; \boldsymbol{Y}_1^\tau\}$ and then normalize them to add up to 1 to obtain the same results as (3.26) and (3.27), respectively. Denote the joint probabilites as

$$\lambda_t(m) = P\{S_t = m; \boldsymbol{Y}_1^\tau\} \tag{3.28}$$

and

$$\sigma_t(m', m) = Pr\{S_{t-1} = m'; S_t = m; \boldsymbol{Y}_1^\tau\}. \tag{3.29}$$

To simplify the notation, we define the following probability functions:

$$\alpha_t(m) = P\{S_t = m; \boldsymbol{Y}_1^t\}, \tag{3.30}$$

$$\beta_t(m) = P\{\boldsymbol{Y}_{t+1}^\tau | S_t = m\}, \tag{3.31}$$

$$\gamma_t(m', m) = P\{S_t = m; Y_t | S_{t-1} = m'\}. \tag{3.32}$$

Using the property of the Markov source, i.e. the current output depends only on the current state and current input, we can obtain $\lambda_t(m)$ and $\sigma_t(m', m)$ as follows:

$$\lambda_t(m) = \alpha_t(m) \cdot \beta_t(m), \tag{3.33}$$

$$\sigma_t(m', m) = \alpha_{t-1}(m') \cdot \gamma_t(m', m) \cdot \beta_t(m). \tag{3.34}$$

The most important part of the algorithm is that $\alpha_t(m)$ and $\beta_t(m)$ can be calculated by forward and backward recursions, respectively.

$$\alpha_t(m) = \sum_{m'} \alpha_{t-1}(m') \cdot \gamma_t(m', m) \tag{3.35}$$

$$\beta_t(m) = \sum_{m'} \beta_{t+1}(m') \cdot \gamma_{t+1}(m, m') \tag{3.36}$$

Their boundary conditions are:

$$\alpha_0(m) = \begin{cases} 1, & \text{for } m = 0 \\ 0, & \text{otherwise} \end{cases} \tag{3.37}$$

$$\beta_\tau(m) = \begin{cases} 1, & \text{for } m = 0 \\ 0, & \text{otherwise} \end{cases} \tag{3.38}$$

$\gamma_t(m', m)$ is determined by the encoder trellis and the channel transition probability:

$$\gamma_t(m', m) = \sum_{X} p_t(m|m') \cdot q_t(X|m', m) \cdot R(Y_t|X). \tag{3.39}$$

The summation in (3.39) is over all possible output symbols X. Whenever a transition from state $S_{t-1} = m'$ to state $S_t = m$ exits and its output is X_t, the probability $\gamma_t(m', m)$ is reduced to:

$$\gamma_t(m', m) = R(Y_t|X_t) \cdot p(X_t). \tag{3.40}$$

Now we consider the application of the BCJR algorithm to decode a convolutional code. Of course, the algorithm can be applied to any code whose encoder can be expressed by a Markov process. Assume that a binary rate k_0/n_0 convolutional encoder with constraint length ν is employed. The input to the encoder at time t is the block

$U_t = (u_t^1, u_t^2, \ldots, u_t^{k_0})$ and the corresponding output is $X_t = (x_t^1, x_t^2, \ldots, x_t^{n_0})$. For a convolutional code without feedback, its state can be represented as a $k_0\nu$-tuple:

$$S_t = (s_t^1, s_t^2, \ldots, s_t^{k_0\nu}) = (U_t, U_{t-1}, \ldots, U_{t-\nu-1}). \tag{3.41}$$

The above equation means the informatin bits $\{u_t^i, 1 \leq i \leq k_0\}$ are contained in state S_t, that is:

$$s_t^i = u_t^i, \qquad i = 1, 2, \ldots, k_0. \tag{3.42}$$

Therefore, the a posteriori probability of information bit u_t^i is calculated by:

$$p(u_t^i = 0 | \boldsymbol{Y}_1^\tau) = \sum_{m \in \mathcal{A}_t^{i0}} \lambda_t(m)/a_t^i, \tag{3.43}$$

where $\mathcal{A}_t^{i0}$ is the set the states S_t such that $s_t^i = 0$ and a_t^i is the normalization constant. Similiarly, $\mathcal{A}_t^{i1}$ is defined. The a posteriori log-likelihood ratio of information bit u_t^i is:

$$\begin{aligned} \log\frac{P(u_t^i = 1 | \boldsymbol{Y}_1^\tau)}{P(u_t^i = 0 | \boldsymbol{Y}_1^\tau)} &= \log\frac{\sum_{m \in \mathcal{A}_t^{i1}} \lambda_t(m)}{\sum_{m \in \mathcal{A}_t^{i0}} \lambda_t(m)} \\ &= \log\frac{\sum_{m \in \mathcal{A}_t^{i1}} \alpha_t(m)\beta_t(m)}{\sum_{m \in \mathcal{A}_t^{i0}} \alpha_t(m)\beta_t(m)} \end{aligned} \tag{3.44}$$

The a posteriori probability of coded bit x_t^i is:

$$p(x_t^i = 0 | \boldsymbol{Y}_1^\tau) = \sum_{(m',m) \in \mathcal{B}_t^{i0}} \sigma_t(m', m)/b_t^i, \tag{3.45}$$

where $\mathcal{B}_t^{i0}$ is the set of transitions $S_{t-1} = m' \rightarrow S_t = m$ such that the ith output digit x_t^i on that transition is 0 and b_t^i is the normalization constant. Similiarly, define $\mathcal{B}_t^{i1}$. The a posteriori log-likelihood ratio of coded bit x_t^i is:

$$\begin{aligned} \log\frac{p(x_t^i = 1 | \boldsymbol{Y}_1^\tau)}{p(x_t^i = 0 | \boldsymbol{Y}_1^\tau)} &= \log\frac{\sum_{(m',m) \in \mathcal{B}_t^{i1}} \sigma_t(m', m)}{\sum_{(m',m) \in \mathcal{B}_t^{i0}} \sigma_t(m', m)} \\ &= \log\frac{\sum_{(m',m) \in \mathcal{B}_t^{i1}} \alpha_{t-1}(m')\beta_t(m)\gamma_t(m', m)}{\sum_{(m',m) \in \mathcal{B}_t^{i0}} \alpha_{t-1}(m')\beta_t(m)\gamma_t(m', m)}. \end{aligned} \tag{3.46}$$

Based on the property of the memoryless channel (3.25) and probability $\gamma_t(m', m)$ in (3.40), we have:

$$\log\frac{p(x_t^i = 1|\,\boldsymbol{Y}_1^\tau)}{p(x_t^i = 0|\,\boldsymbol{Y}_1^\tau)} = \log\frac{\sum_{(m',m)\in\mathcal{B}_t^{i1}} \alpha_{t-1}(m')\beta_t(m)\prod_{j=1}^{n_0} R(y_t^j|x_t^j)p(x_t^j)}{\sum_{(m',m)\in\mathcal{B}_t^{i0}} \alpha_{t-1}(m')\beta_t(m)\prod_{j=1}^{n_0} R(y_t^j|x_t^j)p(x_t^j)} \tag{3.47}$$

$$= \log\frac{p(x_t^i = 1)}{p(x_t^i = 0)} + \log\frac{R(y_t^i|x_t^i = 1)}{R(y_t^i|x_t^i = 0)} + \log\frac{\sum_{(m',m)\in\mathcal{B}_t^{i1}} \alpha_{t-1}(m')\beta_t(m)\prod_{j\neq i} R(y_t^j|x_t^j)p(x_t^j)}{\sum_{(m',m)\in\mathcal{B}_t^{i0}} \alpha_{t-1}(m')\beta_t(m)\prod_{j\neq i} R(y_t^j|x_t^j)p(x_t^j)}. \tag{3.48}$$

The first term in (3.48) is the a priori LLR of coded bit x_t^i, the second term is the LLR provided by the channel soft value y_t^i and the last term is the extrinsic LLR provided by the decoder.

3.4.2 The Log-MAP and Max-Log-MAP Algorithms

In this subsection, we present an implementation of the original MAP algorithm (the original BCJR algorithm) based on the log-likelihood algebra [Hag96]. Compared with the original MAP algorithm, the optimum log-MAP algorithm is more numerically stable. Furthermore the suboptimum max-log-MAP algorithm has reduced computational complexity.

Following the same notations as in Subsection 3.4.1, we define the following:

$$\hat{\alpha}_t(m) = \log\alpha_t(m) \tag{3.49}$$

$$\hat{\beta}_t(m) = \log\beta_t(m) \tag{3.50}$$

$$\hat{\gamma}_t(m', m) = \log\gamma_t(m', m) \tag{3.51}$$

The log-MAP algorithm consists of two generalized Viterbi algorithms [Vit98a], one operating with a forward recursion and the other working with a backward recursion.

For the forward recursion, a trellis $\hat{\alpha}_t(m)$ is initialized according to:

$$\hat{\alpha}_0(m) = \begin{cases} 0, & \text{for } m = 0 \\ -\infty, & \text{for } m \neq 0 \end{cases} \tag{3.52}$$

The remainder of the trellis is obtained by the generalized Viterbi algorithm, defined by the recursion relation:

$$\hat{\alpha}_t(m) = \max_{m'} *[\hat{\alpha}_{t-1}(m') + \hat{\gamma}_t(m', m)]. \tag{3.53}$$

In the above, the operator $\max*$ is defined by the Jacobian logarithm:

$$\begin{aligned} \max*(x, y) &= \log(e^x + e^y) \\ &= \max(x, y) + \log(1 + e^{-|x-y|}), \end{aligned} \tag{3.54}$$

and by the recursion relationship

$$\begin{aligned} \max*(x, y, z) &= \max*(\max*(x, y), z) \\ &= \log(e^x + e^y + e^z), \end{aligned} \tag{3.55}$$

where $\log(\cdot)$ is the natural logarithm. In a similar way, for the backward recursion, a trellis $\hat{\beta}_t(m)$ is initialized according to:

$$\hat{\beta}_\tau(m) = \begin{cases} 0, & \text{for } m = 0 \\ -\infty, & \text{for } m \neq 0 \end{cases} \tag{3.56}$$

The remainder of the trellis is obtained by a generalized Viterbi algorithm running according to the backward recursion:

$$\hat{\beta}_t(m) = \max_{m'} *[\hat{\beta}_{t+1}(m') + \hat{\gamma}_{t+1}(m, m')]. \tag{3.57}$$

Once the forward and backward recursions have been completed, the a posteriori log-likelihood ratio of information bit u_t^i is found by

$$\begin{aligned} \log\frac{P(u_t^i = 1 | \boldsymbol{Y}_1^\tau)}{P(u_t^i = 0 | \boldsymbol{Y}_1^\tau)} &= \max_{m \in \mathcal{A}_t^{i1}} *[\hat{\alpha}_t(m) + \hat{\beta}_t(m)] \\ &\quad - \max_{m \in \mathcal{A}_t^{i0}} *[\hat{\alpha}_t(m) + \hat{\beta}_t(m)]. \end{aligned} \tag{3.58}$$

The a posteriori LLR of coded bit x_t^i is:

$$\log\frac{p(x_t^i=1|\,\boldsymbol{Y}_1^\tau)}{p(x_t^i=0|\,\boldsymbol{Y}_1^\tau)} = \max_{(m',m)\in\mathcal{B}_t^{i1}} *[\hat{\alpha}_{t-1}(m')+\hat{\beta}_t(m)+\hat{\gamma}_t(m',m)] - \max_{(m',m)\in\mathcal{B}_t^{i0}} *[\hat{\alpha}_{t-1}(m')+\hat{\beta}_t(m)+\hat{\gamma}_t(m',m)]. \tag{3.59}$$

In order to further reduce the complexity of the log-MAP algorithm, we use the following approximation:

$$\log\sum_{j=1}^{n} e^{a_j} \approx \max_{j\in[1,n]} a_j, \tag{3.60}$$

where $\max_{j\in[1,n]}$ can be computed by successively calculating (n-1) maximization functions over only two values and $\log(\cdot)$ is the natural logarithm. Compared with (3.54), the approximation in (3.60) ignores the second term in (3.54). Based on this approximation, we have the suboptimum max-log-MAP algorithm. The forward and backward recursions can also be implemented by the two generalized Viterbi algorithms and are defined as following:

$$\hat{\alpha}_t(m) \approx \max_{m'}[\hat{\alpha}_{t-1}(m')+\hat{\gamma}_t(m',m)], \tag{3.61}$$

$$\hat{\beta}_t(m) \approx \max_{m'}[\hat{\beta}_{t+1}(m')+\hat{\gamma}_{t+1}(m,m')]. \tag{3.62}$$

The corresponding a posteriori LLRs of coded bit x_t^i and information bit u_t^i are:

$$\log\frac{p(x_t^i=1|\,\boldsymbol{Y}_1^\tau)}{p(x_t^i=0|\,\boldsymbol{Y}_1^\tau)} \approx \max_{(m',m)\in\mathcal{B}_t^{i1}}[\hat{\alpha}_{t-1}(m')+\hat{\beta}_t(m)+\hat{\gamma}_t(m',m)] - \max_{(m',m)\in\mathcal{B}_t^{i0}}[\hat{\alpha}_{t-1}(m')+\hat{\beta}_t(m)+\hat{\gamma}_t(m',m)], \tag{3.63}$$

$$\log\frac{P(u_t^i=1|\,\boldsymbol{Y}_1^\tau)}{P(u_t^i=0|\,\boldsymbol{Y}_1^\tau)} \approx \max_{m\in\mathcal{A}_t^{i1}}[\hat{\alpha}_t(m)+\hat{\beta}_t(m)] - \max_{m\in\mathcal{A}_t^{i0}}[\hat{\alpha}_t(m)+\hat{\beta}_t(m)], \tag{3.64}$$

respectively.

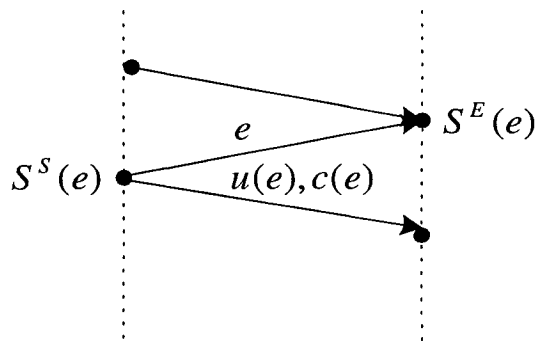

Figure 3.7: An edge of the trellis

3.4.3 A General Algorithm of the SISO APP Module

In this subsection, we present a general SISO APP algorithm [Ben97] for the SISO module introduced in Fig. 3.1 of Section 3.1 which is modified based on the original BCJR algorithm. This general algorithm works on trellis transitions ("edges"), rather than pairs of states in the original BCJR algorithm, and is capable of coping with parallel edges. In the following, we will show how to calculate the soft outputs of the SISO APP module (i.e. the extrinsic LLRs of information bits and coded bits, and the a posteriori LLRs of information bits) based on its soft inputs (i.e. a priori LLRs of these bits).

To each edge e on the trellis, the following functions are associated (see Fig. 3.7): the starting state $S^S(e)$; the ending state $S^E(e)$; the input symbol $u(e)$ and the output symbol $c(e)$. The relationship between these functions depends on the particular encoder.

Recall the time index $t \in [1, \tau]$. Based on LLRs $L(u_t^j, I)$ in (3.3) and $L(c_t^j, I)$ in (3.4) of the jth bit within each symbol at time t, we obtain the corresponding probabilities $p[u_t^j, I]$ and $p[c_t^j, I]$ respectively as following:

$$p[u_t^j, I] = \frac{e^{(2u_t^j - 1)L(u_t^j, I)}}{1 + e^{(2u_t^j - 1)L(u_t^j, I)}}, \tag{3.65}$$

$$p[c_t^j, I] = \frac{e^{(2c_t^j - 1)L(c_t^j, I)}}{1 + e^{(2c_t^j - 1)L(c_t^j, I)}}. \tag{3.66}$$

The a priori probabilities of bits $p[u_t^j(e), I]$ and $p[c_t^j(e), I]$ associated with the edge e can be calculated based on (3.65), (3.66) respectively and the edge e on the trellis. If the bits in each symbol associated with the edge e are independent, the a priori LLR of each symbol is:

$$P[u_t(e), I] = \prod_j p[u_t^j(e), I], \tag{3.67}$$

$$P[c_t(e), I] = \prod_j p[c_t^j(e), I]. \tag{3.68}$$

The a posteriori LLR $\Lambda(c_t^j)$ and $\Lambda(u_t^j)$ for the jth bit within each symbol at time t are computed as:

$$\Lambda(c_t^j) = \log \frac{\sum_{e:c_t^j(e)=1} A_{t-1}[S^S(e)]P[u_t(e), I]P[c_t(e), I]B_t[S^E(e)]}{\sum_{e:c_t^j(e)=0} A_{t-1}[S^S(e)]P[u_t(e), I]P[c_t(e), I]B_t[S^E(e)]}, \tag{3.69}$$

and

$$\Lambda(u_t^j) = \log \frac{\sum_{e:u_t^j(e)=1} A_{t-1}[S^S(e)]P[u_t(e), I]P[c_t(e), I]B_t[S^E(e)]}{\sum_{e:u_t^j(e)=0} A_{t-1}[S^S(e)]P[u_t(e), I]P[c_t(e), I]B_t[S^E(e)]}, \tag{3.70}$$

respectively. The quantities $A_t(\cdot)$ for $t = 1, \ldots, \tau$ and $B_t(\cdot)$ for $t = \tau - 1, \ldots, 0$ are obtained through the forward and backward recursions, respectively, as

$$A_t(S) = \sum_{e:S^S(e)=S} A_{t-1}[S^S(e)]P[u_t(e), I]P[c_t(e), I], \tag{3.71}$$

$$B_t(S) = \sum_{e:S^E(e)=S} B_{t+1}[S^E(e)]P[u_{t+1}(e), I]P[c_{t+1}(e), I], \tag{3.72}$$

with initial values $A_0(S) = 1$ if $S = S_0$ and $A_0(S) = 0$ otherwise; $B_\tau(S) = 1$ if $S = S_\tau$ and $B_\tau(S) = 0$, otherwise.

The a posteriori LLRs $\Lambda(u_t^j)$ and $\Lambda(c_t^j)$ of information bit u_t^j and coded bit c_t^j can also be expressed as:

$$\Lambda(u_t^j) = L(u_t^j, I) + \Lambda^e(u_t^j, O), \tag{3.73}$$

$$\Lambda(c_t^j) = L(c_t^j, I) + \Lambda^e(c_t^j, O), \tag{3.74}$$

where the extrinsic LLR $\Lambda^e(u_t^j, O)$ and $\Lambda^e(c_t^j, O)$ are:

$$\Lambda^e(u_t^j, O) = \log \frac{\sum_{e:u_t^j(e)=1} A_{t-1}[S^S(e)] \prod_{i \neq j} P[u_t^i(e), I] P[c_t(e), I] B_t[S^E(e)]}{\sum_{e:u_t^j(e)=0} A_{t-1}[S^S(e)] \prod_{i \neq j} P[u_t^i(e), I] P[c_t(e), I] B_t[S^E(e)]}, \tag{3.75}$$

$$\Lambda^e(c_t^j, O) = \log \frac{\sum_{e:c_t^j(e)=1} A_{t-1}[S^S(e)] P[u_t(e), I] \prod_{i \neq j} P[c_t^i(e), I] B_t[S^E(e)]}{\sum_{e:c_t^j(e)=0} A_{t-1}[S^S(e)] P[u_t(e), I] \prod_{i \neq j} P[c_t^i(e), I] B_t[S^E(e)]}. \tag{3.76}$$

Note that the extrinsic LLRs $\Lambda^e(u_t^j, O)$ and $\Lambda^e(c_t^j, O)$ are independent of the a priori LLRs $L(u_t^j, I)$ and $L(c_t^j, I)$, respectively.

3.5 Summary

The underlying principles of iterative turbo decoders, turbo principles, are introduced in this chapter. Component decoders for concatenated codes can be generalized as a SISO APP module with the a priori LLRs of information bits and coded bits as its soft inputs and the extrinsic LLRs of these bits and the a posteriori LLRs of information bits as its soft outputs. We showed the turbo principles, i.e. the way by which component SISO APP blocks cooperate iteratively in the receiver, by the decoding structures of parallel and serially concatenated codes. Finally, we gave some optimum and suboptimum APP algorithms for the SISO APP module.

Turbo principles can be applied by the receivers of coded multiuser systems, where we consider the multiuser detector as a SISO APP block. Thus, the receiver consists of several SISO APP blocks, including the SISO multiuser detector and single user SISO

decoders. These blocks can cooperate iteratively based on the turbo principles. The resulting system performance approaches to that of the single user system, while the computational complexity of the receiver is kept low. The following three chapters will focus on the SISO multiuser detection.

Chapter 4

Background on Soft-Input Soft-Output (SISO) Multiuser Detection for Coded Multiuser Systems

For multiuser systems with forward error correction (FEC) codes, the optimal receiver combines the trellises of both the multiuser detector and the individual FEC codes, which results in a prohibitive complexity of $O(2^{K\nu})$, where K is the number of users in the channel and ν is the code constraint length [Gia96a]. In [Gia96b], some low-complexity receivers, which perform multiuser symbol detection and decoding either separately or jointly, are studied.

In order to reduce the complexity of jointly detecting and decoding for coded multiuser systems, well-known turbo principles are employed in the receiver. The multiuser detector and single user decoders transfer the extrinsic soft information of coded symbols to one another in a turbo-like loop. The resulting iterative receiver can provide near single user

system performance with feasible computational complexity.

In this chapter, first we introduce a fundamental theory based on minimum cross-entropy (MCE) for the iterative receiver in Section 4.1. Then, we present a general iterative receiver structure based on turbo principles for coded multiuser systems in Section 4.2. In the following sections, we focus on iterative SISO multiuser detectors and a complete review of it is provided. In Section 4.3, we introduce optimum iterative SISO multiuser detectors. Based on some approximation, we can obtain simpler while suboptimum iterative SISO detectors which are reviewed in Section 4.4.

4.1 Theoretical Fundamentals of Iterative Multiuser Receivers – Minimum Cross-Entropy

The minimum cross-entropy framework [Moh93] – [Moh98c] provides information theory fundamentals for iterative receivers of coded multiuser systems. In this section, first we introduce the minimum cross-entropy solution for decoding [Moh93], [Moh97a] and then present its application on iterative receivers for coded multiuser systems [Moh97b] – [Moh98c].

4.1.1 Minimum Cross-Entropy (MCE)

Cross-entropy minimization is a statistical inference scheme. It estimates the probability distribution function of a random variable that satisfies given constraints on its moments and minimizes the cross-entropy with respect to an a priori distribution. Let $\mathbf{x}$ be a random vector with a priori distribution $q(\mathbf{x})$. The principle of cross-entropy minimization finds a distribution $p(\mathbf{x})$ which has the minimum cross-entropy with respect to $q(\mathbf{x})$, i.e.

$$p = \arg\{\min_{s} H[s, q]\}, \tag{4.1}$$

where $H[s,q]$ is the cross-entropy of two distributions s and q. The distribution $p(\mathbf{x})$ is subject to the following constraints:

$$\sum_{\mathbf{x}} p(\mathbf{x}) = 1, \tag{4.2}$$

which is a normalization constraint and

$$E_p[f_i(\mathbf{x})] = 0, \qquad i = 1, \ldots, P, \tag{4.3}$$

where E_p is the expectation over the distribution p, $\{f_i\}$ are functions in $\mathbf{x}$ that represent the equality constraints on the moments of $\mathbf{x}$ and P is the number of constraint functions.

The minimum cross-entropy distribution $p(\mathbf{x})$ in (4.1) is given by the product of the a priori distribution $q(\mathbf{x})$ and an exponential function of the constraints:

$$p(\mathbf{x}) = q(\mathbf{x})\exp\left[-\mu_0 - \sum_{k=1}^{P} \mu_k f_k(\mathbf{x})\right], \tag{4.4}$$

where $\{\mu_k\}$ are the Lagrange multipliers with μ_0 determined by (4.2) and the remaining μ_k determined from (4.3). That is,

$$\sum_{\mathbf{x}} q(\mathbf{x})\exp\left[-\mu_0 - \sum_{k=1}^{P} \mu_k f_k(\mathbf{x})\right] = 1, \tag{4.5}$$

$$\sum_{\mathbf{x}} f_i(\mathbf{x})q(\mathbf{x})\exp\left[-\mu_0 - \sum_{k=1}^{P} \mu_k f_k(\mathbf{x})\right] = 0. \qquad i = 1, \ldots, P. \tag{4.6}$$

By denoting

$$A = \exp[-\mu_0], \tag{4.7}$$

$$g_i(\mathbf{x}) = \exp[-\mu_i f_i(\mathbf{x})], \qquad i = 1, \ldots, P, \tag{4.8}$$

and based on (4.4), we have the MCE distribution expressed as:

$$p(\mathbf{x}) = Aq(\mathbf{x})g_1(\mathbf{x}) \cdots g_P(\mathbf{x}). \tag{4.9}$$

For coding applications, the constraint functions are parity equations of the code. The expression for $g_i(\mathbf{x})$ simplifies to $I_i(\mathbf{x})$, that is, the indicator function for a set of codewords that satisfy the ith parity equation. Now the MCE distribution is equivalent to the a posteriori codeword probability and equal to:

$$p(\mathbf{x}) = Aq(\mathbf{x})I_1(\mathbf{x}) \cdots I_P(\mathbf{x}). \tag{4.10}$$

The final decision of $\mathbf{x}$ has the maximum a posteriori probability over all possible probabilities of $\mathbf{x}$. Minimum cross-entropy decoding has the following two important properties. Let $\mathcal{J}$ represent the processing performed by the minimum cross-entropy decoder. Assume that the binary codeword length is F. Let $\mathbf{x}$ be a random vector with dimension F,

$$\mathbf{x} = \Big\{[x(1), x(2), \cdots, x(F)] : x(n) \in \{-1, +1\}\Big\}. \tag{4.11}$$

and $\mathbf{y}$ be the corresponding noisy measurement vector at the output of the channel.

- **Property 1:** Minimum cross-entropy decoding is lossless. That is,

  $$\mathcal{M}(\mathbf{x}; \mathbf{y}) = \mathcal{M}(\mathbf{x}; \mathcal{J}(\mathbf{y})), \tag{4.12}$$

  where $\mathcal{M}(\mathbf{x}; \mathbf{y})$ is the mutual information between $\mathbf{x}$ and $\mathbf{y}$.

- **Property 2:** Minimum cross-entropy decoding with only a subset of the constraints is lossless. That is,

  $$\mathcal{M}(\mathbf{x}; \mathbf{y}) = \mathcal{M}(\mathbf{x}; \mathcal{J}_1(\mathbf{y})), \tag{4.13}$$

  where $\mathcal{J}_1$ is the MCE processing based on only one subset of constraints.

Therefore, the MCE distribution in (4.10) can be obtained iteratively. In each iteration, only one subset of constraints are considered. The constraints are grouped into sets

$C_i(\mathbf{x}), i = 1, \cdots, V$ and each of the constraint set is considered separately. We use the notation $q_0(\mathbf{x}) \circ C_i(\mathbf{x})$ to represent the MCE distribution corresponding to the a priori distribution $q_0(\mathbf{x})$ and constraint set $C_i(\mathbf{x})$. Denote

$$g'_v(\mathbf{x}) = \exp\Big[-\mu_0 - \sum_{f_i \in C_v} \mu_i f_i(\mathbf{x}) \Big], \tag{4.14}$$

where the summation is over the constraints in the constraint set C_v. The serial implementation of the iterative MCE decoder is as follows:

1. set $p_1(\mathbf{x}) = q_0(\mathbf{x}) \circ C_1(\mathbf{x}) = c_1 q_0(\mathbf{x}) g'_1(\mathbf{x})$, where c_1 is the normalization constant;

2. determine $p_{j+1}(\mathbf{x})$ as the MCE distribution corresponding to the a priori distribution $p_j(\mathbf{x})$ and the constraint set $C_{(1+j) \bmod V}$:

$$p_{j+1}(\mathbf{x}) = p_j(\mathbf{x}) \circ C_{(1+j) \bmod V}(\mathbf{x}) = c_{j+1} p_j(\mathbf{x}) g'_{(1+j) \bmod V}(\mathbf{x}), \tag{4.15}$$

   where c_{j+1} is the normalization constant;

3. repeat step 2 until convergence occurs or a required number of repetitions have been done.

Actually, $p_j(\mathbf{x})$ converges to the unique MCE distribution with respect to the a priori distribution $q_0(\mathbf{x})$ and satisfies all of the constraints. $g'_v(\mathbf{x})$ is the extrinsic information obtained from the constraint set C_v.

Alternatively, the MCE decoder has a parallel implementation which is equivalent to the above serial implementation. Let $p_{serial}(\mathbf{x})$ be the result after V steps of the serial algorithm defined by (4.15). Let $p^v(\mathbf{x}) = q_0(\mathbf{x}) \circ C_v(\mathbf{x}) = q_0(\mathbf{x}) g'_v(\mathbf{x}), v = 1, \cdots, V$ be the V MCE distributions after one parallel step, then the distribution

$$p_{parallel}(\mathbf{x}) = c_{parallel} \frac{p^1(\mathbf{x}) p^2(\mathbf{x}) \cdots p^V(\mathbf{x})}{[q_0(\mathbf{x})]^{V-1}} = p_{serial}(\mathbf{x}), \tag{4.16}$$

where the constant $c_{parallel}$ normalizes the probability mass. Thus, for the decoding problem, the constraints can be applied in parallel rather than serially. Moreover, the parallel version converges to the same limit as the serial version.

It can also be shown that the a priori distribution to be used with the vth branch of the parallel implementation can be expressed as:

$$q^v(\mathbf{x}) = c^v q_0(\mathbf{x}) g'_1(\mathbf{x}) \cdots g'_{v-1}(\mathbf{x}) g'_{v+1}(\mathbf{x}) \cdots g'_V(\mathbf{x}), \tag{4.17}$$

where c^v is the appropriate normalization constant. Therefore, the a priori distribution of the vth branch consists of the initial probability $q_0(\mathbf{x})$ and the extrinsic information provided by all the other branches. The a posteriori distribution obtained by the vth branch is $p_v(\mathbf{x}) = q^v(\mathbf{x}) \circ C_v(\mathbf{x}) = c_v^{parallel} q^v(\mathbf{x}) g'_v(\mathbf{x})$. This is called the modified MCE algorithm.

4.1.2 An Iterative Multiuser Receiver Based on the MCE Algorithm

Based on the above parallel implementation of the modified MCE decoder, we show an iterative multiuser receiver structure for coded multiuser systems in Fig. 4.1. There are K active users in the system. Each user's information bits are encoded and then modulated. Let $\mathbf{b}_k$ denote one coded symbol frame of user k, $\mathbf{b}_k = [b_k(0), b_k(1), \ldots, b_k(F-1)]$, where F is the transmitted symbol frame length. The matrix $\mathbf{b}$ is the K-dimensional code vector corresponding to all users.

$$\mathbf{b} = \begin{pmatrix} \mathbf{b}_1 \\ \mathbf{b}_2 \\ \vdots \\ \mathbf{b}_K \end{pmatrix}_{K \times F} \tag{4.18}$$

The iterative multiuser receiver calculates the MCE distribution of coded symbols of all users, i.e. $\mathbf{b}$.

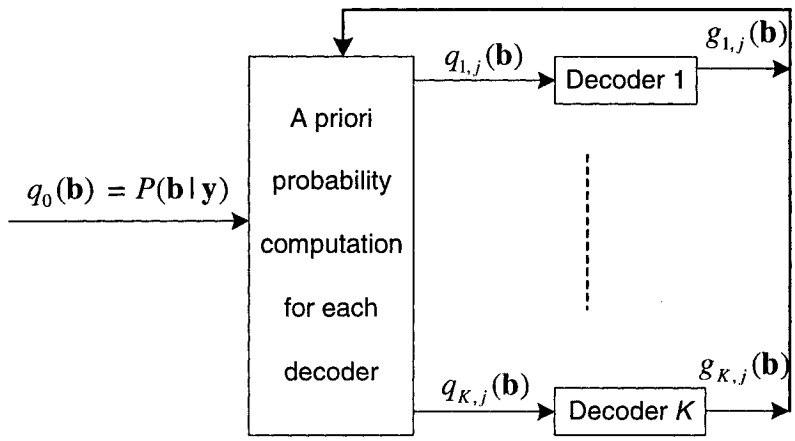

Figure 4.1: Iterative multiuser receiver structure based on the MCE algorithm

Fig. 4.1 shows the iterative receiver structure, where $\mathbf{y} = \mathbf{y}_{K\times F}$ is the output of K parallel filters matched to K users' waveforms respectively and j is the iteration index. $q_0(\mathbf{b})$ is the initial distribution of $\mathbf{b}$ obtained from the matched filter output $\mathbf{y}$.

$$q_0(\mathbf{b}) = P(\mathbf{b}|\mathbf{y}) = \frac{P(\mathbf{y}|\mathbf{b})\theta(\mathbf{b})}{\theta(\mathbf{y})} \equiv P(\mathbf{y}|\mathbf{b})\theta(\mathbf{b}) \tag{4.19}$$

where $\equiv$ denotes that both sides contain the same information of $\mathbf{b}$, $\theta(\mathbf{b})$ is the a priori probability of $\mathbf{b}$ before any decoding procedure, $\theta(\mathbf{y})$ is the a priori probability of $\mathbf{y}$ and $P(\mathbf{y}|\mathbf{b})$ is determined by the channel and it is assumed time-invariant. For an AWGN channel, it is a joint distribution of a set of $K \times F$ jointly Gaussian random variables. Denote $q_{k,j}(\mathbf{b})$ as the a priori probability of $\mathbf{b}$ for the kth decoder in the jth iteration. In the first iteration, $q_{k,j}(\mathbf{b})$ is initialized as $q_0(\mathbf{b})$ for all single user decoders. The kth decoder calculates the probability $p_{k,j}(\mathbf{b})$, which can be the a posteriori probability of $\mathbf{b}$ or the distribution of $\mathbf{b}$ which has the minimum cross-entropy with $q_{k,j}(\mathbf{b})$ by using the code constraints of the kth user. $g_{k,j}(\mathbf{b})$ is the extrinsic information provided only by the kth decoder which satisfies the following equation:

$$p_{k,j}(\mathbf{b}) = q_{k,j}(\mathbf{b}) \cdot g_{k,j}(\mathbf{b}). \tag{4.20}$$

In the jth iteration, the a priori probability of $\mathbf{b}$ is updated by the following equation for the kth decoder (done by the "A priori probability computation" block):

$$q_{k,j}(\mathbf{b}) = q_0(\mathbf{b}) \cdot g_{1,j-1}(\mathbf{b}) \cdots g_{k-1,j-1}(\mathbf{b}) \cdot g_{k+1,j-1}(\mathbf{b}) \cdots g_{K,j-1}(\mathbf{b}). \tag{4.21}$$

Equation (4.21) shows that the a priori probability of $\mathbf{b}$ for the kth decoder consists of the initial probability $q_0(\mathbf{b})$ and the extrinsic information provided by all the other decoders.

After employing all of the code constraints and enough number of iterations, the decoder gives the final decision $\hat{\mathbf{b}}$, which has the maximum MCE distribution $p(\mathbf{b})$ over all possible $\mathbf{b}$:

$$p(\mathbf{b}) = q_0(\mathbf{b}) g_1(\mathbf{b}) g_2(\mathbf{b}) \cdots g_K(\mathbf{b}), \tag{4.22}$$

$$\hat{\mathbf{b}} = \arg\{\max_{\mathbf{b}} p(\mathbf{b})\} = \arg\{\max_{\mathbf{b}} q_0(\mathbf{b}) g_1(\mathbf{b}) g_2(\mathbf{b}) \cdots g_K(\mathbf{b})\}. \tag{4.23}$$

The main drawback of this iterative receiver is its high computational complexity, since decoding is based on the multi-dimensional distribution of $\mathbf{b}$ which corresponds to 2^{KF} values. Therefore, we need to make some approximation to obtain simpler iterative multiuser receivers.

In the following, we introduce a practical iterative multiuser receiver with feasible complexity. Compared with the previous iterative receiver, the practical one is based on two simplifications. The first simplification is that in each single user decoder we can only consider its codewords, not the whole K dimensional code vector $\mathbf{b}_{K\times F}$, since in $\mathbf{b}_{K\times F}$ only the kth row $\mathbf{b}_k$ is the codeword of the kth single user encoder. The second simplification is that we employ the BCJR decoding algorithm instead of the MCE decoding algorithm in each single user decoder. Fig. 4.2 is one directly approximate receiver structure of Fig. 4.1, where j is still the iteration index.

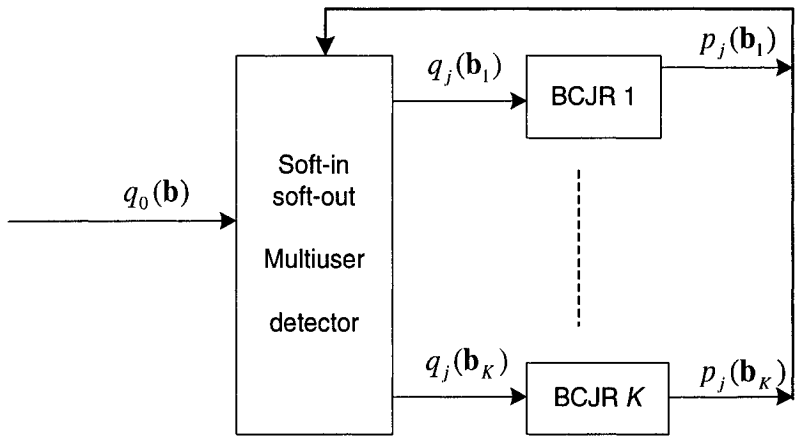

Figure 4.2: Simplified iterative multiuser receiver structure based on the MCE algorithm

In the practical iterative multiuser receiver, the kth single user decoder only needs the a priori information of $\mathbf{b}_k$, which is denoted by $q_j(\mathbf{b}_k)$ in the jth iteration. In the first iteration, this a priori information is the corresponding marginal distribution from $q_0(\mathbf{b})$ in (4.19):

$$q_0(\mathbf{b}_k) = \sum_{\mathbf{b} \in \mathcal{B}_k} q_0(\mathbf{b}), \tag{4.24}$$

where $\mathcal{B}_k$ is the set of $\mathbf{b}$ which has the kth row equal to $\mathbf{b}_k$. It will be updated in the later iterations.

Single user decoders perform K parallel BCJR decodings. In the jth iteration, the kth decoder performs BCJR decoding using $q_j(\mathbf{b}_k)$ as its input and produces the a posteriori distribution $p_j(\mathbf{b}_k)$ of $\mathbf{b}_k$, which can also be expressed as:

$$p_j(\mathbf{b}_k) = q_j(\mathbf{b}_k) g_j(\mathbf{b}_k), \tag{4.25}$$

where $g_j(\mathbf{b}_k)$ is the extrinsic information provided by the kth decoder in the jth iteration. In fact, the BCJR decoder calculates the a posteriori probability of each coded bit. Using

BCJR decoding instead of MCE decoding is under the assumption that the successive decoded bits are independent, which can be achieved by a random interleaver/de-interleaver pair for each user. In particular, that is:

$$p_j(\mathbf{b}_k) = \prod_{i=0}^{F-1} p_j(b_k(i)). \tag{4.26}$$

The a priori distribution $q_j(\mathbf{b}_k)$ for the kth decoder in the jth iteration is updated as:

$$\begin{aligned} q_j(\mathbf{b}_k) &= P_j(\mathbf{b}_k|\mathbf{y}) \\ &= \frac{P_j(\mathbf{y}|\mathbf{b}_k)\theta(\mathbf{b}_k)}{\theta(\mathbf{y})} \\ &= \frac{\theta(\mathbf{b}_k)}{c_{jk}} \sum_{\mathbf{b}\in\mathcal{B}_k} P(\mathbf{y}|\mathbf{b}) \cdot p_{j-1}(\mathbf{b}) \\ &= \frac{\theta(\mathbf{b}_k)}{c_{jk}} \sum_{\mathbf{b}\in\mathcal{B}_k} P(\mathbf{y}|\mathbf{b}) \cdot \prod_{i\neq k} p_{j-1}(\mathbf{b}_i), \end{aligned} \tag{4.27}$$

where c_{jk} is the appropriate normalization constant. Equation (4.27) holds only when $\{\mathbf{b}_i, i \neq k\}$ are independent. Furthermore, in order to keep independence between multiuser detection and single user decoding, which is required by turbo principles, we can replace $p_{j-1}(\mathbf{b}_i)$ in (4.27) by the extrinsic information $g_{j-1}(\mathbf{b}_i)$.

After the required number of iterations, the kth decoder gives the final decision $\hat{\mathbf{b}_k}$ which has the maximum a posteriori probability:

$$\hat{\mathbf{b}_k} = \arg\{\max_{\mathbf{b}_k}[p(\mathbf{b}_k)]\}. \tag{4.28}$$

To simplify the single user decoder, i.e. employ the BCJR decoding algorithm, the input coded bits to each decoder are required to be independent, which is achieved by the de-interleaving process. Thus, the soft information transferred between the multiuser

detector and a bank of single user decoders can be the a priori probability or the extrinsic information of each coded bit (instead of the coded bit sequence $\mathbf{b}_k$) and the final decision for each information bit is based on its a posteriori probability. In the following, we will use this approximation to review the iterative cooperation between multiuser detection and decoding and denote the soft information by the log-likelihood algebra in [Hag96].

4.2 A General Iterative Multiuser Detection and Decoding Structure for Coded Multiuser Systems

Fig. 4.3 shows a general iterative multiuser system structure where each user applies its own forward error correction code [Wan99]. The receiver shown in this figure is a detailed version of Fig. 4.2. One information bit frame of user k is denoted as $\mathbf{d}_k = [d_k(0), d_k(1), \ldots, d_k(Q-1)]$, where Q is the information frame length. The coded bits of each user are interleaved before modulation. The function of these interleavers will be explained later in Subsection 4.2.2. The modulation can be BPSK, M-ary quadrature amplitude modulation (M-QAM) or a higher dimensional modulation. For simplicity, here we assume BPSK modulation. The vector $\mathbf{b}_k = [b_k(0), b_k(1), \ldots, b_k(F-1)]$ is one modulated symbol frame of user k, where F is the transmitted symbol frame length. The receiver consists of two parts, a soft-input soft-output multiuser detector and a bank of K single user soft-input soft-output decoders, which are separated by de-interleavers and interleavers. These two parts cooperate iteratively by transferring updated extrinsic soft information of coded symbols between them. The notations of soft information in Fig. 4.3 will be explained in the following subsections by the log-likelihood algebra used in [Wan99].

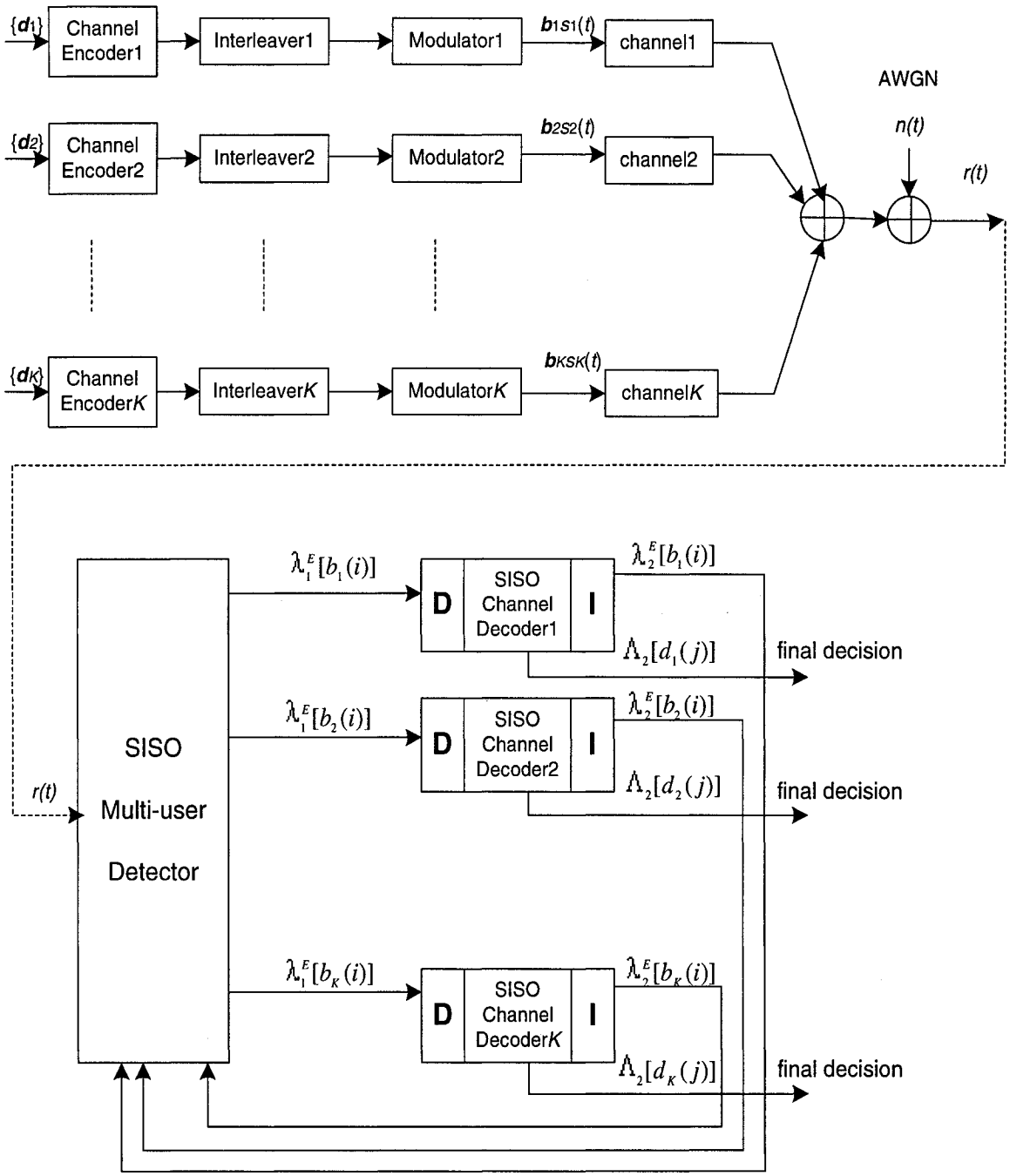

Figure 4.3: A general multiuser system structure with the iterative receiver (**D** and **I** denote de-interleavers and interleavers, respectively.)

4.2.1 SISO Multiuser Detectors

The SISO multiuser detector calculates the a posteriori log-likelihood ratio of a transmitted "+1" and a transmitted "-1" for every transmitted symbol of the kth user $b_k(i)$ (assuming binary modulation):

$$\Lambda_1[b_k(i)] \triangleq \log\frac{P[b_k(i)=+1|r(t)]}{P[b_k(i)=-1|r(t)]}, \quad k=1,\ldots,K; \quad i=0,\ldots F-1, \tag{4.29}$$

where K is the number of active users in the system and $r(t)$ is the received multiuser signal. Using the Bayes' rule, the above equation can be written as:

$$\begin{aligned}\Lambda_1[b_k(i)] &= \log\frac{P[r(t)|b_k(i)=+1]}{P[r(t)|b_k(i)=-1]} + \log\frac{P[b_k(i)=+1]}{P[b_k(i)=-1]} \\ &= \lambda_1^E[b_k(i)] + \lambda_2^P[b_k(i)],\end{aligned} \tag{4.30}$$

where

$$\lambda_1^E[b_k(i)] \triangleq \log\frac{P[r(t)|b_k(i)=+1]}{P[r(t)|b_k(i)=-1]} \tag{4.31}$$

is the extrinsic LLR of $b_k(i)$ provided only by the multiuser detector and

$$\lambda_2^P[b_k(i)] \triangleq \log\frac{P[b_k(i)=+1]}{P[b_k(i)=-1]} \tag{4.32}$$

is the a priori LLR of the coded bit $b_k(i)$, which is provided only by the channel decoder of the kth user in the previous iteration (assuming that the a priori LLR of $b_k(i)$ before any detection and decoding procedure is zero). The superscript ^{E} denotes the extrinsic information and ^{P} denotes the quantity obtained from the previous iteration. The extrinsic LLR $\lambda_1^E[b_k(i)]$, which is provided only by the multiuser detector, is obtained based on the received multiuser signal $r(t)$, the a priori information of the coded bits of all the other users, $\{\lambda_2^P[b_l(j)], l \neq k, 0 \leq j \leq F-1\}$, and the a priori information of the coded bits of the kth user other than the ith bit, $\{\lambda_2^P[b_k(j)], j \neq i\}$. Note that the extrinsic LLR $\lambda_1^E[b_k(i)]$ of $b_k(i)$ is independent of its a priori LLR $\lambda_2^P[b_k(i)]$, which makes sure that the resulting system performance converges quickly. The extrinsic LLRs

$\{\lambda_1^E[b_k(i)], 0 \leq i \leq F-1\}$ is then de-interleaved and fed into the kth user's channel decoder as a priori LLRs.

From (4.30), we can see that the main task of SISO multiuser detectors is to calculate the extrinsic LLR of each coded bit of each user $\{\lambda_1^E[b_k(i)], 0 \leq i \leq F-1, 1 \leq k \leq K\}$ based on the received multiuser signal $r(t)$ and the a priori LLRs of all the other coded bits $\{\lambda_2^P[b_l(j)], l \neq k, j \neq i\}$, excluding the one of $b_k(i)$. The probability $P[r(t)|b_k(i)]$ in calculating the extrinsic LLR in (4.30) can also be considered as the equivalent channel transition probability. How to calculate these extrinsic LLRs by SISO multiuser detectors is the main objective of this thesis.

4.2.2 A Bank of SISO Single User Decoders

In Fig. 4.3, the soft outputs about each user's coded symbols from the multiuser detector are first de-interleaved before they are passed into its decoder. Therefore, even when the channel has memory, the soft inputs into each single user decoder are independent of each other, which is required by the single user decoding algorithm described in the following. Thus, each decoder can work on each coded bit or each information bit separately. Furthermore, in [Pin03] interleavers are used as one additional way to separate multiple users. We will consider functions of interleavers/de-interleavers in the next subsection.

The kth user's SISO decoder computes the a posteriori log-likelihood ratio of each coded symbol $b_k(n)$ based on the a priori LLRs of all coded symbols provided by the multiuser detector and the code constraints:

$$\begin{aligned}\Lambda_2[b_k(n)] &\triangleq \log\frac{P[b_k(n)=+1|\{\lambda_1^P[b_k(n)]\}_{n=0}^{F-1}; \text{decoding}]}{P[b_k(n)=-1|\{\lambda_1^P[b_k(n)]\}_{n=0}^{F-1}; \text{decoding}]} \\ &= \lambda_2^E[b_k(n)] + \lambda_1^P[b_k(n)]. \end{aligned} \tag{4.33}$$

The above equation shows that the a posteriori LLR of each coded symbol is also

the sum of the extrinsic LLR $\lambda_2^E[b_k(n)]$ provided only by the decoder and the a priori LLR $\lambda_1^P[b_k(n)]$ provided only by the multiuser detector. The extrinsic LLR $\lambda_2^E[b_k(n)]$ of the coded bit $b_k(n)$ is obtained based on the a priori LLR of all the other coded bits $\{\lambda_1^P[b_k(m)], m \neq n\}$ and the trellis constraint of the code. The extrinsic LLRs delivered by K channel decoders $\{\lambda_2^E[b_k(n)], 1 \leq k \leq K, 0 \leq n \leq F-1\}$ are then interleaved and fed back to the SISO multiuser detector as a priori LLRs of coded symbols of all users in the next iteration.

After the required number of iterations, the single user decoders calculate the a posteriori LLR of every information bit $d_k(j)$:

$$\Lambda_2[d_k(j)] \triangleq \log \frac{P[d_k(j)=1|\{\lambda_1^P[b_k(n)]\}_{n=0}^{F-1}; \text{decoding}]}{P[d_k(j)=0|\{\lambda_1^P[b_k(n)]\}_{n=0}^{F-1}; \text{decoding}]}, \quad k=1,\ldots,K; \quad j=0,\ldots,Q-1, \tag{4.34}$$

based on which we make the final decision for each information bit. That is:

$$\hat{d}_k(j) = \text{sign}\big(\Lambda_2[d_k(j)]\big). \tag{4.35}$$

For the single user decoder, when the input coded bits are from a Markov source (for example, a convolutional encoder) and independent of each other, the a posteriori probability of each coded bit and each information bit can be calculated by the BCJR algorithm [Bah74], the soft output Viterbi algorithm [Hag95] or their modified variations [Ben96c], [Fra98], [Hue00], [Pap96], [Rob95], [Zhe00] based on the equivalent channel transition probabilities and the a priori probabilities of information bits or coded bits. Furthermore, for parallel concatenated convolutional codes (PCCC) and serially concatenated convolutional codes (SCCC) , their component decoders can cooperate iteratively with each other [Ben96b], [Hag96].

When the single user code is a powerful code, such as convolutional code (CC) , serially

concatenated convolutional code or parallel concatenated convolutional code, it is well known how to implement its decoder along with the multiuser detector in a turbo-like iterative way [Ale99], [Ree98], [Shi01], [Wan99]. References [Ale99] and [Wan99] show in greater detail that SISO single user convolutional decoders can successfully cooperate with the SISO multiuser detector iteratively. [Ree98] and [Shi01] deal with the cases when multiple users employ SCCCs and PCCCs, respectively.

4.2.3 Functions of Interleavers/De-interleavers for Iterative Multiuser Receivers

Interleavers/de-interleavers in the coded multiuser system are indispensable for the iterative multiuser receiver. Their important functions have been exploited by several authors.

In [Moh98a], the asymptotic multiuser efficiency of coded multiuser systems is derived. It is shown that the optimal asymptotic multiuser efficiency with coding and random interleaving is one. There will be a performance degradation when interleavers/de-interleavers are not employed in the multiuser system, which is confirmed by simulation results. Furthermore, in [Moh98a], the influence of the interleaver size on the system performance is also investigated. Based on simulation results, it is shown that the interleaver size clearly plays a role at low SNRs. In particular, the larger interleaver size improves performance in the range between the threshold and the single user system performance, while it has little effect on the threshold behavior of the detector and the rate of performance convergence.

The synchronous multiuser access channel can be considered as a convolutional code. Furthermore, in [Ale99], the asynchronous random CDMA channel is considered as a time-varying convolutional code. Thus, the coded multiuser system appears as a serially

concatenated coding system, for which we can employ a serially iterative turbo decoder. Therefore, interleavers are required based on the turbo principles to reduce correlations between two component decoders, i.e. the multiuser detector and single user decoders.

Interleavers can also be used to distinguish multiple users in a multiple access system. An asynchronous interleaver-division multiple-access (IDMA) scheme is proposed in [Pin03], where users are uniquely specified by different chip-level interleaving methods instead of by different signatures as in a conventional CDMA system. In the receiver, a very simple chip-by-chip iterative multiuser detector can provide nearly optimal performance for systems with a large number of users. The success of IDMA systems, i.e. the significant separation function of interleavers, is explained by using a factor graph approach. Interleavers reduce the number of short cycles in factor graphs of IDMA systems, which is essential for the success of a message passing process.

4.3 Optimum Iterative SISO Multiuser Detection

Optimum SISO multiuser detectors calculate the extrinsic LLR of each coded symbol of each user (4.31) directly from the received signal based on the a priori LLRs of other coded symbols. They can employ the minimum cross-entropy algorithm [Moh97a] – [Moh98c] or maximum a posteriori algorithm [Ale99], [Bah74]. However, the complexity of the optimum SISO multiuser detector in calculating extrinsic LLRs of coded symbols is exponentially proportional to the number of users K per iteration. In order to reduce the complexity, much effort has been given to efficient sub-optimum SISO detectors, which we will introduce in Section 4.4.

4.3.1 System Model

For a synchronous multiuser system with K active users on the AWGN channel, its system model has been given in Section 2.1. Here we briefly repeat it for the reference in the following sections. In the receiver, we use a bank of matched filters, which are matched to the K users' waveforms respectively, as the front end and sample each filter output at the symbol rate. The matched filter output vector during each symbol interval is:

$$\mathbf{y} = \mathbf{RAb} + \mathbf{n}, \tag{4.36}$$

where $\mathbf{R}$ is the $K \times K$ normalized cross-correlation matrix of multiple users' waveforms,

$$\mathbf{y} = [y_1, \ldots, y_K]^T, \tag{4.37}$$

$$\mathbf{b} = [b_1, \ldots, b_K]^T, \tag{4.38}$$

$$\mathbf{A} = diag\{A_1, \ldots, A_K\}, \tag{4.39}$$

where b_k and A_k are the kth user's transmitted binary symbol and signal amplitude respectively, and $\mathbf{n}$ is a zero-mean Gaussian random vector with covariance matrix equal to [Moh97a]:

$$E[\mathbf{n}\mathbf{n}^T] = \sigma^2\mathbf{R}, \tag{4.40}$$

where σ^2 is the double-sided power spectral density of the background Gaussian noise process. The output of the kth user's matched filter is:

$$y_k = A_k b_k + \sum_{j=1, j\neq k}^{K} \rho_{kj} A_j b_j + n_k, \tag{4.41}$$

where $\{\rho_{kj}, j = 1, \ldots, K\}$ is the kth row of $\mathbf{R}$ and $\rho_{kk} = 1$.

4.3.2 Maximum A Posteriori Algorithm

For a synchronous multiuser system, we can calculate probability $p(\mathbf{y}|b_k)$ in the extrinsic LLRs of coded symbols (4.31) by marginalizing the joint channel transition probabilitiy $p(\mathbf{y}|\mathbf{b})$ [Moh97a], [Ree98]. The equivalent channel transition probability of the matched filter output $\mathbf{y}$ conditioned on transmitted symbol b_k is:

$$\begin{aligned} p(\mathbf{y}|b_k) &= \sum_{\mathbf{b}\in\mathcal{B}^k} p(\mathbf{y}|\mathbf{b}) \times p(\mathbf{b}) \\ &= \sum_{\mathbf{b}\in\mathcal{B}^k} p(\mathbf{y}|\mathbf{b}) \times \prod_{i=1,i\neq k}^{K} p(b_i), \end{aligned} \tag{4.42}$$

where $\mathcal{B}^k$ is the set of all possible vectors $\mathbf{b}$ with the same b_k. Here we use the assumption that coded symbols of different users are independent.

Alternatively, since a multiple access channel can be considered as a convolutional code, the coded multiuser system appears as a serial concatenation of two coding systems. At the receiver, we can employ serial turbo decoding strategies. Therefore, in order to calculate the a posteriori probability of b_k, we can employ the optimum MAP algorithm (for example, the BCJR algorithm) [Bah74], log-MAP algorithm [Hag96], suboptimum SOVA algorithm [Hag95] or their variations based on the equivalent trellis of the multiuser channel. After subtracting the a priori LLR of b_k from its a posteriori LLR, we obtain the extrinsic LLR of b_k, which will be transferred to the kth user's decoder.

4.4 Sub-Optimum SISO Multiuser Detection

Due to the high complexity of optimum multiuser detection, there has been much work devoted to the simple while sub-optimum SISO multiuser detection techniques which are feasible in practical systems. In this section, several research directions are reviewed.

4.4.1 Reduced-Complexity Trellis-Based SISO Multiuser Detection

As seen in Subsection 4.3.2, the multiuser channel can be considered as a convolutional code, therefore represented by a trellis. Under some approximation, we can reduce the complexity of this trellis, thus obtain reduced-complexity SISO multiuser detection algorithms.

In [Ale99], an approximate BCJR algorithm is proposed for the equivalent time-varying convolutional code of the asynchronous random CDMA system. They use the M algorithm [Sch97] in the forward recursion and cut the recursion with length FK into FK recursions of depth two in the backward recursion, where F is the coded frame length and K is the number of active users. Finally, the complexity is reduced from $O(2^K)$ to $O(K)$.

In [Qin00a], [Qin01], the reduced-state T-MAP algorithm is used in the SISO multiuser detector, instead of the optimum MAP algorithm. The T-MAP multiuser detector keeps only the paths with the metrics which are within a threshold $T$of the maximum metric in the forward recursion of the BCJR algorithm. Then the backward recursion is performed only for the part of the trellis that survives after the forward recursion. In addition to have the reduced complexity, the T-MAP multiuser detector is adaptive to channel conditions. At low received signal-to-noise ratios, since most of the paths are kept, it is close to the full-complexity MAP detector. Therefore, it has the same worst case computational complexity as the MAP detector. However, the average number of extended nodes in the trellis is reduced.

4.4.2 Soft Interference Cancellation Detection

A soft interference cancellation detector has the minimum complexity ($\sim O(K^2)$ per symbol in each iteration) among other SISO multiuser detectors [Ale98], [Ket99], [Qin00b], [Shi01]. The detector first obtains soft symbol estimates based on soft inputs from a bank of single user decoders. Then it calculates the interfering signal for each user and cancels this interfering signal from each user's matched filter output. The output of soft interference cancellation consists of the desired signal, residual interference and the background Gaussian noise. By assuming that the residual interference is also a Gaussian random variable and independent of the background noise, the detector calculates and outputs extrinsic LLRs of coded symbols to single user decoders. Although soft interference cancellation detection is very simple, the resulting system has a severe performance penalty at low signal-to-noise ratios and low convergence speed, especially for highly correlated narrow-band systems and heavily loaded CDMA systems. We will compare its bit error rate performance with our proposed SISO decorrelator in Subsection 5.2.3.

In more detail, a soft interference canceller for a synchronous multiuser system is described as follows. Its soft inputs $\{\lambda_2^P(b_k), 1 \leq k \leq K\}$ (which are LLRs of coded symbols) are provided by a bank of single user decoders. The soft estimate of each coded symbol of each user is:

$$\hat{b}_k = E[b_k|\lambda_2^P(b_k)] = \tanh\left(\frac{\lambda_2^P(b_k)}{2}\right), \qquad k = 1, \ldots, K. \tag{4.43}$$

The interfering signal for each symbol of each user can be constructed and cancelled from its matched filter output:

$$\mathbf{z} = \mathbf{y} - (\mathbf{R} - \mathbf{I})\mathbf{A}\hat{\mathbf{b}} = \mathbf{A}\mathbf{b} + (\mathbf{R} - \mathbf{I})\mathbf{A}(\mathbf{b} - \hat{\mathbf{b}}) + \mathbf{n} \tag{4.44}$$

where $\hat{\mathbf{b}} = [\hat{b}_1, \ldots, \hat{b}_K]^T$ and $\mathbf{I}$ is the identity matrix. For the kth user, its output of soft interference cancellation is:

$$z_k = A_k b_k + \sum_{j=1, j\neq k}^{K} \rho_{kj} A_j (b_j - \hat{b}_j) + n_k. \tag{4.45}$$

The second term in (4.45) is the residual interference and can be assumed to be a Gaussian random variable which is independent of n_k. Thus the soft output of the multiuser detector can be calculated as:

$$\lambda_1^E[b_k] = \log\frac{P[z_k|b_k=+1]}{P[z_k|b_k=-1]} = \frac{2A_k z_k}{\sigma_k^2}, \qquad 1 \le k \le K, \tag{4.46}$$

where σ_k^2 is the variance of the sum of the residual interference and n_k and can be statistically estimated by the multiuser detector.

4.4.3 Improved Soft Interference Cancellation

In order to improve the performance of soft interference cancellation, an instantaneous linear minimum mean square error filter is applied on the output of soft interference cancellation [Can00], [Wan99], which further suppresses the residual interference. By Gaussian approximation of the MMSE filter output, the detector calculates soft outputs.

In the SISO MMSE detector for a synchronous multiuser system, first for each user k, a soft interference cancellation is performed on the matched filter output vector $\mathbf{y}$ at each symbol instant:

$$\mathbf{y}_k = \mathbf{y} - \mathbf{RA}\hat{\mathbf{b}}_k = \mathbf{RA}[\mathbf{b} - \hat{\mathbf{b}}_k] + \mathbf{n}, \qquad 1 \le k \le K, \tag{4.47}$$

where

$$\hat{\mathbf{b}}_k = [\hat{b}_1, \ldots, \hat{b}_{k-1}, 0, \hat{b}_{k+1}, \ldots, \hat{b}_K]^T. \tag{4.48}$$

Next, in order to further suppress the residual interference in $\mathbf{y}_k$, an instantaneous linear MMSE filter $(\mathbf{w}_k)_{K\times 1}$ is applied on $\mathbf{y}_k$. The filter output is denoted as:

$$x_k = \mathbf{w}_k^T \mathbf{y}_k. \tag{4.49}$$

The filter $\mathbf{w}_k$ is chosen to minimize the mean square error between the coded bit b_k and the filter output x_k, i.e.,

$$\mathbf{w}_k = \arg\min_{\mathbf{w}_k \in \mathcal{R}^K} E\left\{\left[b_k - \mathbf{w}_k^T \mathbf{y}_k\right]^2\right\}. \tag{4.50}$$

By assuming that different users' coded bits are independent of each other and using the statistical property of coded symbols indicated in (4.43), we have the following MMSE filter:

$$\mathbf{w}_k = \mathbf{A}_{kk}\mathbf{R}^{-1}\left[\mathbf{V}_k + \sigma^2\mathbf{R}^{-1}\right]^{-1}\mathbf{e}_k, \tag{4.51}$$

where

$$\mathbf{V}_k \triangleq \sum_{j\neq k}\mathbf{A}_{jj}^2\left[1-\hat{b}_j^2\right]\mathbf{e}_j\mathbf{e}_j^T + \mathbf{A}_{kk}^2\mathbf{e}_k\mathbf{e}_k^T, \tag{4.52}$$

and $\mathbf{e}_k$ is a K-dimensional column vector with the kth element as 1 and all other elements as zeros.

Soft outputs are calculated by assuming that the output of the soft instantaneous MMSE filter x_k represents the output of an equivalent additive white Gaussian noise channel having b_k as its input. That is:

$$x_k = \mu_k b_k + \eta_k, \tag{4.53}$$

where μ_k is the equivalent amplitude of the kth user's signal at the output, and $\eta_k \sim \mathcal{N}(0, v_k^2)$ is a Gaussian noise sample. The parameters μ_k and v_k^2 can be computed as follows:

$$\mu_k = E[x_k b_k] = \mathbf{A}_{kk}^2\left[\left[\mathbf{V}_k + \sigma^2\mathbf{R}^{-1}\right]^{-1}\right]_{kk}, \tag{4.54}$$

$$v_k^2 = \mathrm{var}[x_k] = \mu_k - \mu_k^2. \tag{4.55}$$

From (4.53) the soft output, i.e. the extrinsic LLR of b_k, delivered by the soft instantaneous MMSE filter is then

$$\lambda_1^E[b_k] = \log\frac{p[x_k|b_k=+1]}{p[x_k|b_k=-1]} = \frac{2x_k}{1-\mu_k}. \tag{4.56}$$

Employing the recursive algorithm to calculate the matrix inverse in (4.51), the computational complexity of this detector is $\sim O(K^3)$ per symbol in each iteration.

4.4.4 SISO Decision Feedback Detection

In [Bei02], [Gam00], [Lam99], a nonlinear MMSE filter consisting of a feedforward filter and a feedback filter is used. The feedforward part is applied on the matched filter output directly and the feedback part is on soft symbol estimates. We will introduce this detector in detail in Chapter 5 and compare it with our proposed SISO multiuser detector there.

4.5 Summary

In this chapter, first both theoretical fundamentals and practical implementation of iterative receivers for coded multiuser systems are provided based on the minimum cross-entropy algorithm. Then, based on turbo principles, we introduce a general iterative receiver structure. Finally, we focus on reviewing optimum and suboptimum iterative SISO multiuser detectors in detail. In the next chapter, we propose our new SISO multiuser detectors and compare them with those available in the literature.

Chapter 5

SISO Multiuser Detection for Synchronous Coded Multiuser Systems over AWGN Channels

In this chapter, we propose and derive three types of SISO multiuser detectors for synchronous multiuser systems over AWGN channels. The position and task of the SISO multiuser detector in the recursive receiver for coded multiuser systems are shown in Fig. 4.3. These SISO detectors are adapted from traditional (non-SISO) multiuser detection techniques [Ver98], such as, decorrelating detection, linear MMSE detection and parallel decision feedback detection. Based on the soft inputs of detectors which are fedback from a bank of SISO single user decoders, these detectors further exploit the a priori information of coded symbols in their detection. Moreover, they calculate soft outputs, which are extrinsic log-likelihood ratios of coded symbols, and output them to SISO single user decoders in turn. The resulting system performance approaches to that of the single user system after only a few iterations for moderate and high signal-to-noise ratios. Furthermore, their computational complexity is kept low, which is a cubic function of the number of users. For each type of SISO detector, performance analysis and simulation

results are provided. Performance comparison among these detectors is presented at the end of this chapter.

In Section 5.1, the system model of a synchronous multiuser system over the AWGN channel is given. We propose and analyze a SISO decorrelating detector in Section 5.2, a linear SISO MMSE detector in Section 5.3. The SISO parallel decision feedback detector in [Bei02], [Gam00] and [Lam99] is introduced in Section 5.4 for comparison purposes. Comparison among these three types of SISO multiuser detectors is provided in Section 5.5.

5.1 System Model

For clear description and simplicity we consider synchronous multiuser systems with K active users over the AWGN channel. We also assume that BPSK modulation is used by each user. This system model has been given in Section 2.1. In the following, we briefly repeat some of the relevant equations for convenience.

In the receiver, we use a bank of matched filters as the front end and sample the filter output at the symbol rate. The matched filter output vector during each symbol interval is:

$$\mathbf{y} = \mathbf{RAb} + \mathbf{n}, \tag{5.1}$$

where $\mathbf{R}$ is the $K \times K$ normalized cross-correlation matrix of multiuser waveforms, $\mathbf{y} = [y_1, \ldots, y_K]^T$ is the matched filter output vector, $\mathbf{b} = [b_1, \ldots, b_K]^T$ is the transmitted coded symbol vector, $\mathbf{A}$ is a diagonal matrix with diagonal elements as the amplitudes of multiple users' transmitted signals, $\mathbf{A} = diag\{A_1, \ldots, A_K\}$, and $\mathbf{n}$ is a zero-mean Gaussian random vector with covariance matrix equal to:

$$E[\mathbf{n}\mathbf{n}^T] = \sigma^2\mathbf{R}, \tag{5.2}$$

where $\sigma^2 = N_0/2$ is the double-sided power spectral density of the additive white Gaussian noise.

5.2 SISO Decorrelating Multiuser Detection

In this section, instead of an MMSE filter [Wan99] introduced in Section 4.4.3, we propose a novel SISO decorrelator which is applied to the output of the soft interference canceller (SIC) . Based on the updated soft inputs of the SISO detector which are fedback from a bank of single user decoders, the equivalent cross-correlation matrix of multiple users at the output of SIC is also updated and employed in each iteration. If we assume that the reliabilities of these soft inputs are improved from one iteration to the next, the cross-correlation matrix will have smaller cross correlation elements. Thus, noise enhancement introduced by decorrelating will be reduced as well. Because of negligible residual interference as well as reduced noise enhancement in successive iterations, we will show in this section that the performance of our iterative receiver approaches to that of the single user system only after a few iterations.

In the following, first we propose a novel SISO decorrelator in Subsection 5.2.1 and then analyze its performance in Subsection 5.2.2. Monte-Carlo simulation results are shown in Subsection 5.2.3 and compared with those of soft interference cancellers. Finally, the computational complexity of the SISO decorrelator is analyzed in Subsection 5.2.4.

5.2.1 SISO Decorrelating Multiuser Detectors

The soft inputs of the detector, which are provided by a bank of SISO single user decoders, are the a priori log-likelihood ratios $\{\lambda_{in}(b_k), 1 \leq k \leq K\}$ of coded symbols.

$$\lambda_{in}(b_k) = \log \frac{\Pr(b_k = +1 | \text{decoding in the previous iteration})}{\Pr(b_k = -1 | \text{decoding in the previous iteration})} \tag{5.3}$$

Based on them, we can obtain the soft estimate of each coded symbol of each user:

$$\hat{b}_k = E[b_k|\lambda_{in}(b_k)] = \tanh\left(\frac{\lambda_{in}(b_k)}{2}\right), \quad k = 1, \ldots, K. \tag{5.4}$$

The sign of soft symbol estimate $\hat{b}_k$ is the hard decision of b_k and its absolute value $|\hat{b}_k|$ is the reliability of this hard decision. Then the interfering signal for each symbol of each user can be constructed and cancelled from its matched filter output:

$$\begin{aligned} \mathbf{z} &= \mathbf{y} - (\mathbf{R} - \mathbf{I})\mathbf{A}\hat{\mathbf{b}} \\ &= \mathbf{RAb} - (\mathbf{R} - \mathbf{I})\mathbf{A}\hat{\mathbf{b}} + \mathbf{n} \\ &= \mathbf{Ab} + (\mathbf{R} - \mathbf{I})\mathbf{A}(\mathbf{b} - \hat{\mathbf{b}}) + \mathbf{n}, \end{aligned} \tag{5.5}$$

where $\mathbf{I}$ is the identity matrix.

The output $\mathbf{z}$ of the soft interference canceller in (5.5) still has a residual interference which is shown by the second term in the third equation. Furthermore, it has a new equivalent cross-correlation matrix $\mathbf{R}_u$ of multiple users' waveforms. We can express $\mathbf{z}$ in an alternative way:

$$\mathbf{z} = \mathbf{R}_u\mathbf{Ab} + \mathbf{n}, \tag{5.6}$$

where

$$\mathbf{R}_u = \mathbf{R} \cdot \mathbf{C} + \mathbf{D}. \tag{5.7}$$

Both $\mathbf{C}$ and $\mathbf{D}$ are diagonal matrices and can be expressed as:

$$\mathbf{C} = \begin{pmatrix} \frac{b_1 - \hat{b}_1}{b_1} & & \mathbf{0} \\ & \frac{b_2 - \hat{b}_2}{b_2} & \\ \mathbf{0} & & \ddots \\ & & & \frac{b_K - \hat{b}_K}{b_K} \end{pmatrix}_{K \times K}, \tag{5.8}$$

$$\mathbf{D} = \begin{pmatrix} \frac{\hat{b}_1}{b_1} & & & \mathbf{0} \\ & \frac{\hat{b}_2}{b_2} & & \\ & & \ddots & \\ \mathbf{0} & & & \frac{\hat{b}_K}{b_K} \end{pmatrix}_{K \times K}, \tag{5.9}$$

$$\mathbf{C} = \mathbf{I} - \mathbf{D}. \tag{5.10}$$

For example, a multiuser system with three users has a symmetric cross-correlation matrix $\mathbf{R}$:

$$\mathbf{R} = \begin{pmatrix} 1 & \rho_{12} & \rho_{13} \\ \rho_{12} & 1 & \rho_{23} \\ \rho_{13} & \rho_{23} & 1 \end{pmatrix}. \tag{5.11}$$

The equivalent cross-correlation matrix $\mathbf{R}_u$ for the output of the soft interference canceller is equal to:

$$\mathbf{R}_u = \begin{pmatrix} 1 & \rho_{12} \cdot \frac{b_2 - \hat{b}_2}{b_2} & \rho_{13} \cdot \frac{b_3 - \hat{b}_3}{b_3} \\ \rho_{12} \cdot \frac{b_1 - \hat{b}_1}{b_1} & 1 & \rho_{23} \cdot \frac{b_3 - \hat{b}_3}{b_3} \\ \rho_{13} \cdot \frac{b_1 - \hat{b}_1}{b_1} & \rho_{23} \cdot \frac{b_2 - \hat{b}_2}{b_2} & 1 \end{pmatrix}. \tag{5.12}$$

However, from (5.7) - (5.9), we can see that $\mathbf{R}_u$ depends on $\{b_k, 1 \leq k \leq K\}$, which we have not yet recovered. Therefore, we need some reasonable approximation here. For (5.8) and (5.9), we need to estimate:

$$\hat{b}_k / b_k, \quad k = 1, \ldots, K. \tag{5.13}$$

For BPSK modulated symbols $b_k \in \{-1, +1\}$, we have the following equations:

$$\hat{b}_k / b_k = \hat{b}_k \cdot b_k, \quad k = 1, \ldots, K. \tag{5.14}$$

When the hard decision based on $\hat{b}_k$ is correct, that is $b_k = \text{sgn}(\hat{b}_k)$, we will have:

$$\hat{b}_k / b_k = \hat{b}_k \cdot b_k = |\hat{b}_k|, \quad k = 1, \ldots, K. \tag{5.15}$$

Assuming (5.15) is correct, we can approximate cross-correlation matrix $\mathbf{R}_u$ in (5.7) by the following $\hat{\mathbf{R}}_u$:

$$\hat{\mathbf{R}}_u = \mathbf{R} \cdot \hat{\mathbf{C}} + \hat{\mathbf{D}}, \tag{5.16}$$

where

$$\hat{\mathbf{C}} = \begin{pmatrix} 1-|\hat{b}_1| & & & \mathbf{0} \\ & 1-|\hat{b}_2| & & \\ \mathbf{0} & & \ddots & \\ & & & 1-|\hat{b}_K| \end{pmatrix}_{K\times K}, \tag{5.17}$$

$$\hat{\mathbf{D}} = \begin{pmatrix} |\hat{b}_1| & & & \mathbf{0} \\ & |\hat{b}_2| & & \\ \mathbf{0} & & \ddots & \\ & & & |\hat{b}_K| \end{pmatrix}_{K\times K}. \tag{5.18}$$

The corresponding approximate $\hat{\mathbf{R}}_u$ of $\mathbf{R}_u$ in (5.12) is:

$$\hat{\mathbf{R}}_u = \begin{pmatrix} 1 & \rho_{12}\cdot(1-|\hat{b}_2|) & \rho_{13}\cdot(1-|\hat{b}_3|) \\ \rho_{12}\cdot(1-|\hat{b}_1|) & 1 & \rho_{23}\cdot(1-|\hat{b}_3|) \\ \rho_{13}\cdot(1-|\hat{b}_1|) & \rho_{23}\cdot(1-|\hat{b}_2|) & 1 \end{pmatrix}. \tag{5.19}$$

In order to further reduce the residual interference in $\mathbf{z}$, we decorrelate $\mathbf{z}$ by multiplying it with $\hat{\mathbf{R}}_u^{-1}$. Assume that $\hat{\mathbf{R}}_u \approx \mathbf{R}_u$ and its inverse $\hat{\mathbf{R}}_u^{-1}$ exists, the output of decorrelating $\mathbf{z}$ will be:

$$\mathbf{x}^{DEC} = \hat{\mathbf{R}}_u^{-1} \cdot \mathbf{z} = \hat{\mathbf{R}}_u^{-1}\mathbf{R}_u\mathbf{A}\mathbf{b} + \hat{\mathbf{R}}_u^{-1} \cdot \mathbf{n} \approx \mathbf{A}\mathbf{b} + \mathbf{n}_u, \tag{5.20}$$

where $\hat{\mathbf{R}}_u^{-1}\mathbf{R}_u \approx \mathbf{I}$ and $\hat{\mathbf{R}}_u^{-1} \cdot \mathbf{n} = \mathbf{n}_u$. The equivalent noise vector $\mathbf{n}_u$ is still a vector of Gaussian random variables and has the following covariance matrix:

$$\begin{aligned} E[\mathbf{n}_u\mathbf{n}_u^T] &= E[(\hat{\mathbf{R}}_u^{-1}\mathbf{n})(\hat{\mathbf{R}}_u^{-1}\mathbf{n})^T] \\ &= \sigma^2\hat{\mathbf{R}}_u^{-1}\mathbf{R}(\hat{\mathbf{R}}_u^{-1})^T. \end{aligned} \tag{5.21}$$

The corresponding noise variable n_{uk} for the kth user's output x_k^{DEC} is a Gaussian random variable with the distribution $\mathcal{N}(0, \sigma_{uk}^2)$, where σ_{uk}^2 is the kth diagonal element of the covariance matrix in (5.21) and can be calculated directly by the detector. Therefore, the soft output of the SISO decorrelator during each symbol interval is:

$$\lambda_o^{DEC}[b_k] = \log\frac{P[x_k^{DEC}|b_k = +1]}{P[x_k^{DEC}|b_k = -1]} = \frac{2A_k x_k^{DEC}}{\sigma_{uk}^2}, \quad 1 \le k \le K. \tag{5.22}$$

Compared with the soft interference canceller in [Ale98] and [Shi01], our proposed SISO decorrelator does not consider the possible residual interference which may be introduced by the approximate $\hat{\mathbf{R}}_u$. In the next subsection, we will show that it is reasonable to ignore the possible residual interference introduced by $\hat{\mathbf{R}}_u$.

5.2.2 Performance Analysis

In this subsection, we analyze the performance of the SISO decorrelator under the assumption that the reliabilities $\{|\hat{b}_k|\}$ of coded symbols are improved in successive iterations at moderate to high signal-to-noise ratios, which is usually true for iterative receivers.

Using the approximate $\hat{\mathbf{R}}_u$ under (5.15), if one hard decision based on soft symbol estimate $\hat{b}_k$ is not correct, decorrelating $\mathbf{z}$ by $\hat{\mathbf{R}}_u^{-1}$ will introduce some residual interference. However, consider that soft estimates are based on soft inputs from single user decoders in (5.4), equation (5.15) does not hold only when the symbol estimate's reliability is low,

i.e. $|\hat{b}_k|$ is small. The resulting difference between $\hat{\mathbf{R}}_u$ and $\mathbf{R}_u$ is small. Therefore, the introduced residual interference will also be small. Moreover, since the symbol estimate reliabilities increase on successive iterations, the approximate cross-correlation matrix $\hat{\mathbf{R}}_u$ tends to $\mathbf{R}_u$. Thus we can ignore the residual interference which may be introduced by the approximate $\hat{\mathbf{R}}_u$. However, the detector performance in each iteration does depend on both hard decisions $\{\text{sgn}(\hat{b}_k)\}$ and reliabilities $\{|\hat{b}_k|\}$ of soft symbol estimates.

Since $|\hat{b}_k| \in [0,1], k = 1,\ldots,K$, absolute values of elements in $\mathbf{R}_u$ except diagonal ones are less than or equal to the corresponding ones in $\mathbf{R}$, which means that cross correlations between multiple users are reduced. Moreover, since symbol estimates have improved reliabilities (i.e. larger $|\hat{b}_k|$) from one iteration to the next, multiple users will have less cross correlations. Thus, we make good use of the soft inputs from a bank of single user decoders in both soft interference cancellation and the decorrelating process.

One main disadvantage of decorrelating detection is noise enhancement introduced by multiplying the inverse of the cross-correlation matrix. In the following, we will analyze noise variances at the output of the SISO decorrelator. The noise variance σ_{uk}^2 of the output noise variable n_{uk} of the SISO decorrelator for user k is the kth diagonal element of the covariance matrix (5.21). Denote

$$\xi_i = 1 - |\hat{b}_i|, \quad 1 \le k \le K, \quad \xi_i \in [0,1]. \tag{5.23}$$

Based on (5.7), (5.15) and (5.21), given the system cross-correlation matrix $\mathbf{R}$, σ_{uk}^2 is a function with multiple arguments $\{\xi_i, 1 \le i \le K\}$. Under the assumption that with additional iterations the reliability of each coded symbol $|\hat{b}_i|$ increases, ξ_i decreases. In the first iteration, we have no a priori information of coded symbols, (i.e. $\{|\hat{b}_i| = 0, 1 \le i \le K\}$), thus $\{\xi_i = 1, 1 \le i \le K\}$. The SISO decorrelator is now a traditional decorrelator with noise enhancement. Ideally, all coded symbols would have nearly perfect reliabilities, (i.e. $\{|\hat{b}_i| \to 1, 1 \le i \le K\}$), thus $\{\xi_i = 0, 1 \le i \le K\}$. At this time, $\sigma_{uk}^2 = N_0/2$ and

there is no noise enhancement introduced by the SISO decorrelator. The relationship between σ_{uk}^2 and intermediate values of $\{\xi_i, 1 \leq i \leq K\}$ is determined by simulation. It is determined that in general, σ_{uk}^2 is an increasing function of $\{\xi_i, 1 \leq i \leq K\}$ respectively, for moderate and large $\{\xi_i\}$. While for small $\{\xi_i\}$, it remains small and changes slowly. In Appendix A, we show the simulation results to confirm this conclusion. Therefore, with additional iterations, the noise enhancement of the SISO decorrelator will be reduced or remains low.

In summary, if we assume the reliabilities of coded symbols based on soft inputs are improved in successive iterations, the possible residual interference introduced by the appropriate cross-correlation matrix $\hat{\mathbf{R}}_u$ can be ignored and the noise enhancement due to decorrelating can be reduced or kept small. Therefore, the resulting system performance will approach fast to that of the single user system, which will be confirmed by Monte-Carlo simulation results shown in the next subsection.

5.2.3 Simulation Results

For simplicity, in this subsection, we consider a synchronous K-symmetric multiuser system. Its cross-correlation matrix $\mathbf{R}$ has only one parameter ρ, indicating the cross correlation between any pair of users.

$$\mathbf{R} = \begin{pmatrix} 1 & \rho & \cdots & \rho \\ \rho & 1 & \cdots & \rho \\ \vdots & & \ddots & \\ \rho & \cdots & \rho & 1 \end{pmatrix} \tag{5.24}$$

Since it is difficult to analyze the system performance by a closed expression of bit error probability for iterative receivers, we use the Monte-Carlo technique to obtain the bit error rate performance. The number of users, K, is 5 or 10. The cross correlation ρ

between any two users is equal. We use ρ values of 0.5, 0.7, or 0.9 for $K = 5$ and 0.3 for $K = 10$.

In the simulation, all users employ the same rate 1/2 convolutional code with constraint length 7 and the following generators [1011011], [1111001]. Iterative SISO single user decoders are based on the log-MAP algorithm [Hag96] [Bah74]. Different users have different constant block interleavers which are randomly selected. No effort is taken to optimize these interleavers. The frame size of information bits is 500 and the total number of simulated information frames is 10,000. Except the specific notation, we assume that the received amplitudes of all users' signals are equal and normalized to be unity. In this case, since all the users have the same performance, without loss of generality, we only show bit error rates of the first user.

In the following, we will compare the system performance provided by the SISO decorrelator and by the soft interference canceller in [Ale98], [Shi01], which has been introduced in subsection 4.4.2. The soft interference canceller has the lowest complexity, compared with other SISO detectors considered in this chapter. Performance-versus-complexity of these detectors are listed in Table 5.1 at the end of this chapter. In the first iteration, there is no soft information fedback from single user decoders. Therefore, at this time, our SISO decorrelating detector follows traditional (non-SISO) decorrelating detection, while the soft interference canceller follows conventional multiuser detection. Fig. 5.1 and Fig. 5.2 show comparison of bit error rate performances between the soft interference canceller and the SISO decorrelator for two K-symmetric multiuser systems with $K = 5$, $\rho = 0.5$ and $K = 10$, $\rho = 0.3$ respectively. Solid curves denote bit error rates of user 1 provided by the soft interference canceller, while dotted curves are provided by the SISO decorrelator. The performance of the single user system is also shown in these figures. Compared with the soft interference canceller, our proposed SISO decorrelator

has a faster convergence speed towards the single user system performance and better bit error rates at low SNRs.

Fig. 5.3 and Fig. 5.4 show the bit error rate performances of user 1 in the multiuser systems with $K = 5$ and higher cross correlations of 0.7 and 0.9, respectively. Since the soft interference canceller does not work for these highly correlated systems, we employ traditional decorrelating detection at the first iteration for both the soft interference canceller as well as the SISO decorrelator. Our proposed SISO decorrelator still has a better performance than the soft interference canceller. However, the difference between these two types of SISO detectors is smaller than those shown in Fig. 5.1 and Fig. 5.2, since for these highly correlated systems, the decorrelating process at the first iteration provides a key function. Simulation results of SISO decorrelating detectors and their comparison with those of soft interference cancellers confirm our analysis in Subsection 5.2.2.

Near-far resistance of the SISO decorrelating detector is also investigated. Fig. 5.5 shows and compares the bit error rate performances of strong users and weak users in one near-far situation, where $K = 5, \rho = 0.7$ and three users have 3dB more energy than the other two users. Since the users with the same energy in the system have almost the same bit error rate performance, we only show the performance of any of them. Bit error rates in the first five iterations are simulated and shown in the figure. Note that signal-to-noise ratios of strong users and weak users have 3dB difference and are marked by red color and blue color respectively in the figure. Signal-to-noise ratios of the single user are also indicated in blue. From Fig. 5.5, we can see that the performance of weak users can converge to that of the single user system after additional iterations. For strong users, they have 3dB more power. Their performance is worse than that of the single user at the same E_b/N_o values. That means, lower power users benefit from the strong

interference while higher power users suffer a performance loss from the weak interference. Furthermore, without power control in the receiver, multilple users' power difference will be higher. Fig. 5.6 shows the bit error rate performances of weak users in the fifth iteration under several near-far scenarios: power difference ranges from 3dB to 23dB. We can see that in all cases, their performance remains almost the same. Therefore, our SISO decorrelator has good near-far resistance for lower power users.

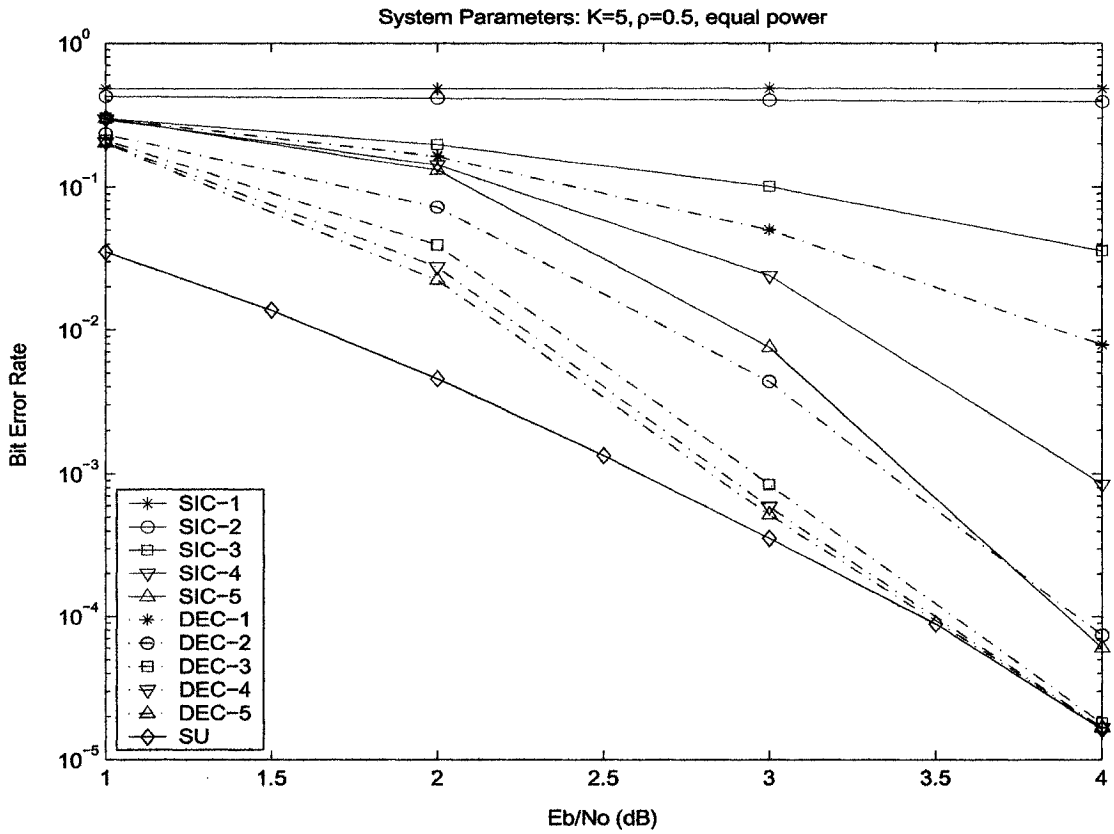

Figure 5.1: Comparison of bit error rate performances between the soft interference canceller in the first five iterations (SIC-1 – SIC-5), the SISO decorrelator (DEC-1 – DEC-5) and the single user system (SU) for $K = 5$, $\rho = 0.5$ and equal power users.

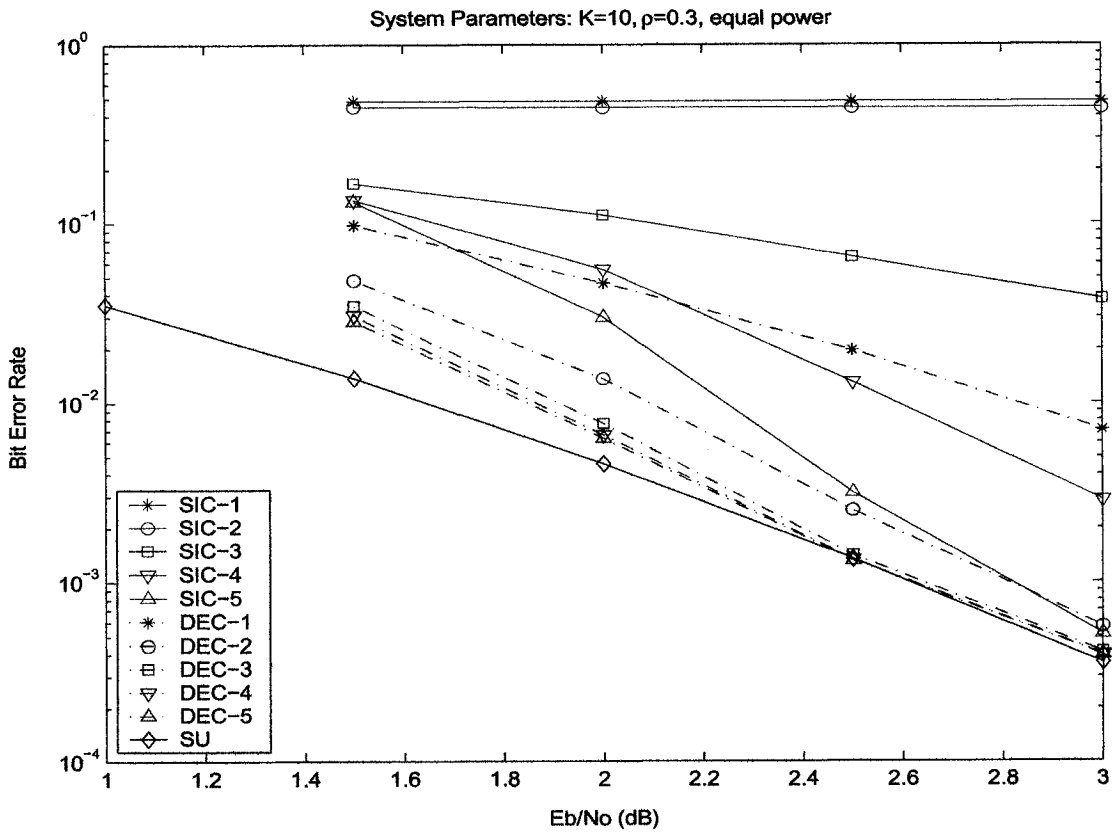

Figure 5.2: Comparison of bit error rate performances between the soft interference canceller in the first five iterations (SIC-1 – SIC-5), the SISO decorrelator (DEC-1 – DEC-5) and the single user system (SU) for $K = 10$, $\rho = 0.3$ and equal power users.

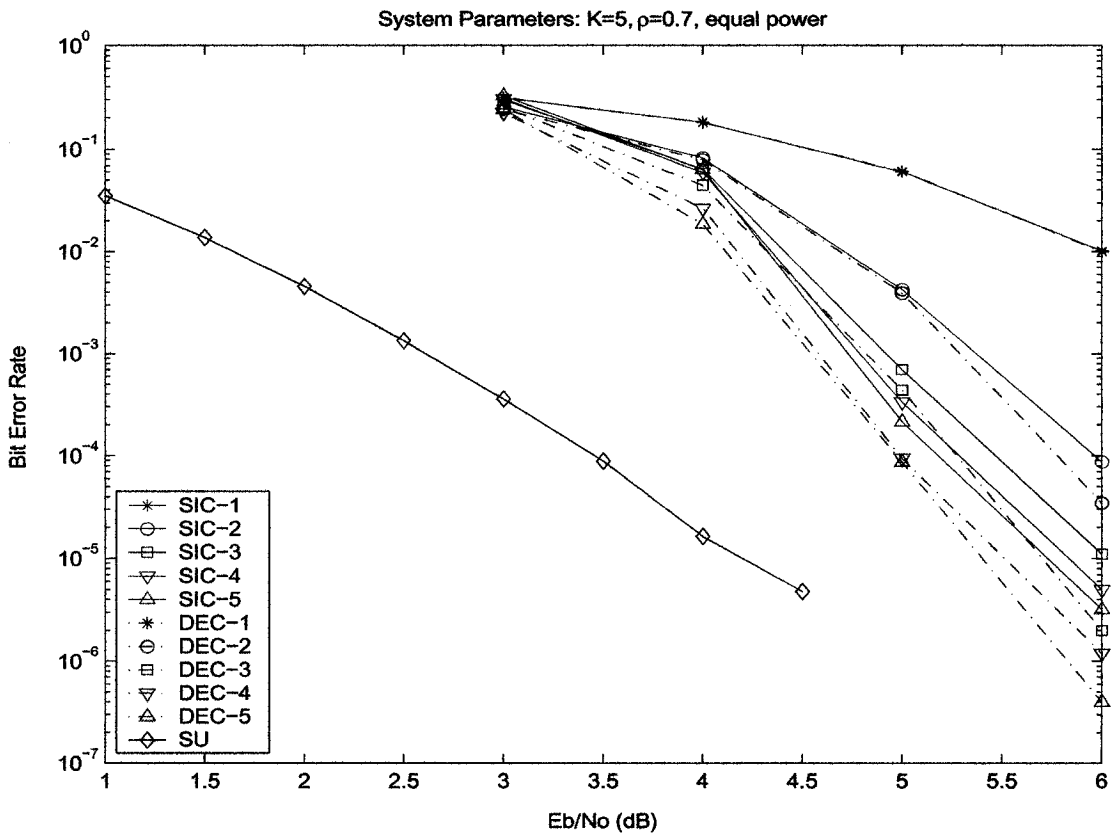

Figure 5.3: Comparison of bit error rate performances between the soft interference canceller in the first five iterations (SIC-1 – SIC-5), the SISO decorrelator (DEC-1 – DEC-5) and the single user system (SU) for $K = 5$, $\rho = 0.7$ and equal power users.

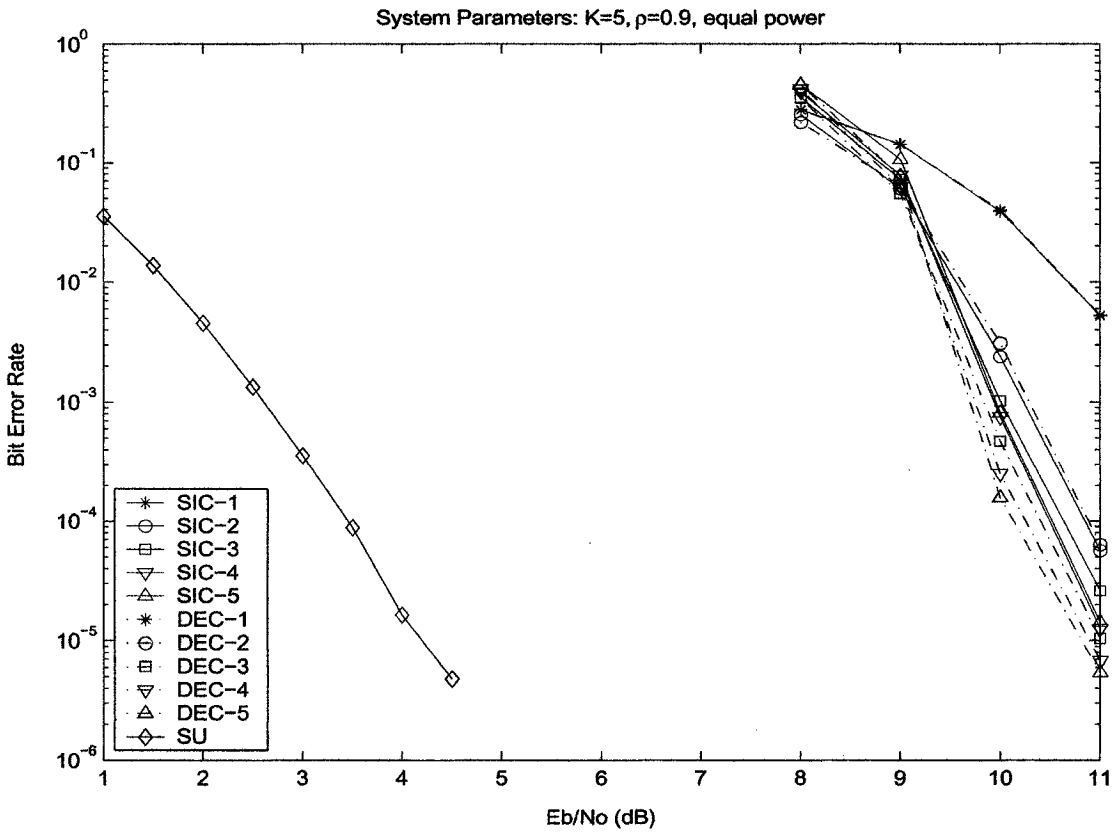

Figure 5.4: Comparison of bit error rate performances between the soft interference canceller in the first five iterations (SIC-1 – SIC-5), the SISO decorrelator (DEC-1 – DEC-5) and the single user system (SU) for $K = 5$, $\rho = 0.9$ and equal power users.

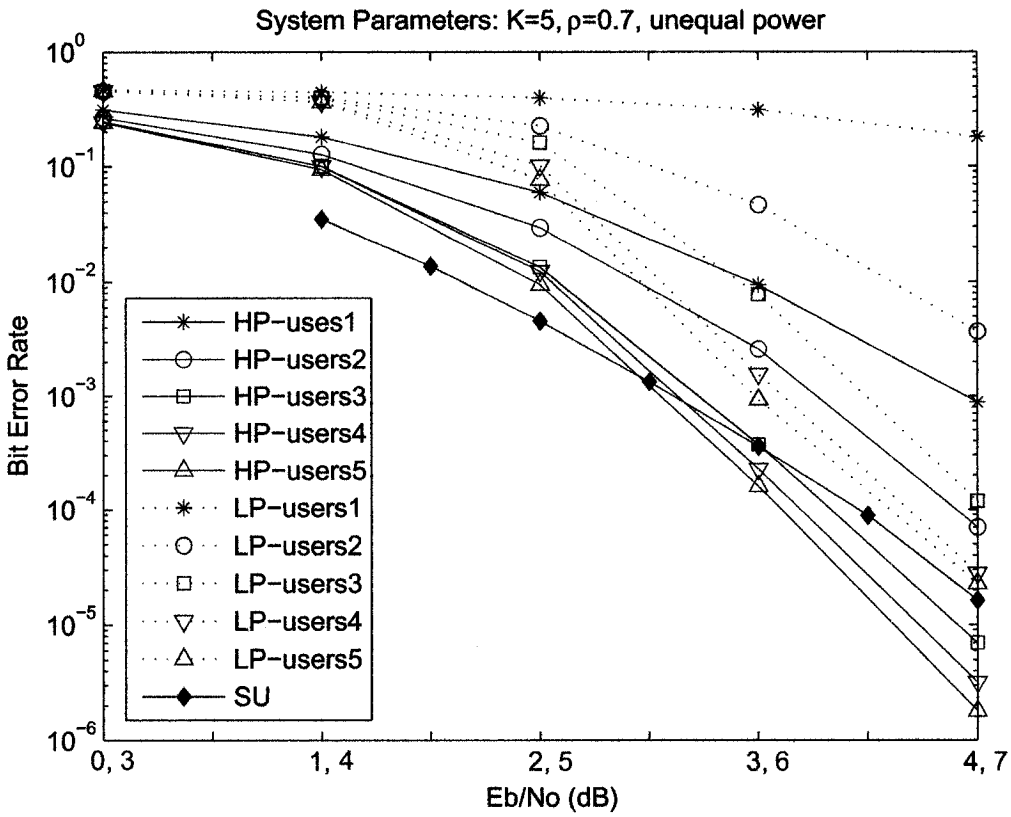

Figure 5.5: Comparison of bit error rate performances between higher power users in the first five iterations (HP-users1 – HP-users5), lower power users (LP-users1 – LP-users5) under SISO decorrelating detection and the single user system (SU). System parameters: $K = 5$, $\rho = 0.7$, three users have 3dB more energy than the other two. Signal-to-noise ratios of higher power users and lower power users are marked by red and blue colors, respectively. Signal-to-noise ratios of the single user system are indicated in blue.

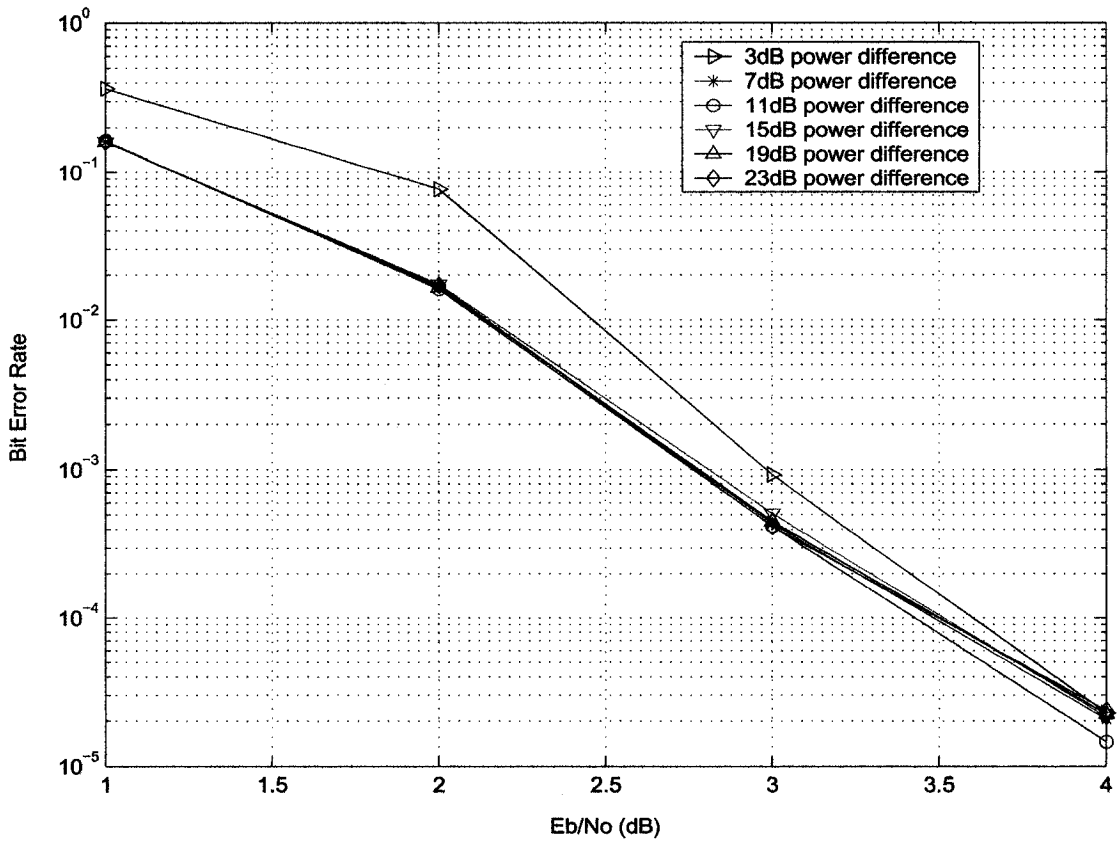

Figure 5.6: Bit error rate performances of lower power users under several power differences, provided by the SISO decorrelator in the fifth iteration. System parameters: $K = 5$, $\rho = 0.7$, three users have more power than the other two users.

5.2.4 Computational Complexity Analysis

Compared with the soft interference canceller, our proposed SISO decorrelator performs some extra computations at each iteration. Our detector must additionally compute the inverse of the updated cross-correlation matrix $\hat{\mathbf{R}}_u$, decorrelate the output of soft interference cancellation, compute variances of Gaussian noise random variables in $\mathbf{x}^{DEC}$, and calculate the soft outputs. In order to reduce the complexity of calculating the matrix inverse $\hat{\mathbf{R}}_u^{-1}$, we can employ a recursive method. Based on (5.16), we can express $\hat{\mathbf{R}}_u$ as:

$$\begin{aligned}\hat{\mathbf{R}}_u &= \mathbf{R}\cdot\hat{\mathbf{C}}+\hat{\mathbf{D}} \\ &= \mathbf{E}+\sum_{j=1}^{K}|\hat{b}_j|\cdot\mathbf{e}_j\cdot\mathbf{e}_j^T,\end{aligned} \tag{5.25}$$

where $\mathbf{E}\triangleq\mathbf{R}\cdot\hat{\mathbf{C}}$ and $\mathbf{e}_j$ denotes a K-dimensional column vector of all zeros, except for the jth element, which is 1.

In the following, we present a recursive algorithm to calculate the matrix inverse $\hat{\mathbf{R}}_u^{-1}$. Denote

$$\mathbf{\Phi}^{(0)}=\mathbf{E}^{-1}=\hat{\mathbf{C}}^{-1}\cdot\mathbf{R}^{-1}, \tag{5.26}$$

$$\mathbf{\Phi}^{(k)}=\left(\mathbf{E}+\sum_{j=1}^{k}|\hat{b}_j|\cdot\mathbf{e}_j\cdot\mathbf{e}_j^T\right)^{-1},\quad 1\le k\le K. \tag{5.27}$$

Therefore, we have

$$\hat{\mathbf{R}}_u^{-1}=\mathbf{\Phi}^{(K)}. \tag{5.28}$$

Using the matrix inverse lemma in [Gol96], we can calculate $\mathbf{\Phi}^{(k)}$ recursively as for $k=1,2,\ldots,K$.

$$\begin{aligned}\mathbf{\Phi}^{(k)} &= \left((\mathbf{\Phi}^{(k-1)})^{-1}+|\hat{b}_k|\cdot\mathbf{e}_k\cdot\mathbf{e}_k^T\right)^{-1} \\ &= \mathbf{\Phi}^{(k-1)}-\frac{1}{|\hat{b}_k|^{-1}+\left(\mathbf{\Phi}^{(k-1)}\right)_{kk}}\cdot\mathbf{\Phi}^{(k-1)}\cdot\mathbf{e}_k\cdot\mathbf{e}_k^T\cdot\mathbf{\Phi}^{(k-1)}\end{aligned} \tag{5.29}$$

Now we analyze the computational complexity of the SISO decorrelating detector. For DSP-based implementation, we assume three types of computation: summation (ADD), multiplication (MUL) and multiply and accumulation (MAC), each of which involves one floating-point operation. For matrix inverse computation, each recursive step (5.29) consists of K^2 MAC and K^2 MUL. Totally there are K recursions, the whole number of operations are $2K^3$ at each iteration for K users. Decorrelating procedure and calculation of noise variances for all K users involve K^2 and $(K^3 + K^2 + K)$ MAC, respectively. In addition, soft interference cancellation involves $(K^2 + 2K)$ MAC operations for K users. Table B.1 in Appendix B shows the number of operations required in each step of the SISO decorrelator. For each coded symbol interval per iteration, the detector needs $(3K^3 + 4K^2 + 6K)$ operations, which is a cubic function of the number of users K.

5.3 Linear SISO MMSE Multiuser Detection

In this section, we propose a linear SISO MMSE multiuser detector which applies an optimum linear MMSE filter to the matched filter output vector $\mathbf{y}$ for each user, under the criterion of minimum mean square error between the desired symbol and the MMSE filter output. In particular, the detector employs the available statistic information of coded symbols, which is provided by a bank of SISO single user decoders, in searching for optimum MMSE filters. First, in Subsection 5.3.1 we derive a linear SISO MMSE detector. Its performance analysis is presented in Subsection 5.3.2. In Subsection 5.3.3, we show its simulation results and compare them with those of the SISO decorrelator. Its computational complexity is analyzed at the end of this section.

5.3.1 Linear SISO MMSE Multiuser Detectors

In traditional linear MMSE multiuser detection [Ver98], we assume that there is no a priori information of coded symbols $\mathbf{b}$, that is,

$$E[\mathbf{b}] = \mathbf{0}, \tag{5.30}$$

where $\mathbf{0}$ is a K-dimensional column vector of all zeros.

However, in the SISO multiuser detector, we do have the a priori information of coded symbols, which consists of a priori log-likelihood ratios of coded symbols, $\{\lambda_{in}(b_k), 1 \leq k \leq K\}$ in (5.3), and is fedback from a bank of SISO single user decoders. Different users' coded symbols are assumed independent of one another. In summary, we have the following a priori statistical values of coded symbols for the kth user, which are useful in the design of the MMSE filter.

$$E[b_k] = 0, \tag{5.31}$$

$$E[b_i|\lambda_{in}(b_i)] = \hat{b}_i, \quad i \neq k, \tag{5.32}$$

$$E[b_i \cdot b_j|\lambda_{in}(b_i), \lambda_{in}(b_j)] = \hat{b}_i \cdot \hat{b}_j, \quad i \neq j, \tag{5.33}$$

$$E[b_j^2] = 1, \quad 1 \leq j \leq K, \tag{5.34}$$

where (5.34) is followed by the BPSK modulation assumption and $\hat{b}_i$ is the soft symbol estimate defined in (5.4).

Based on the above a priori statistics of coded symbols, we design a linear filter $\{\mathbf{m}_k\}_{K\times 1}$ with K taps for each user k, $1 \leq k \leq K$, under the minimum mean square error criterion:

$$\mathbf{M} = \begin{pmatrix} \mathbf{m}_1^T \\ \mathbf{m}_2^T \\ \cdots \\ \mathbf{m}_K^T \end{pmatrix}$$

$$= \arg\left\{\min_{\mathbf{M}^*} \mathrm{E}\left[\| \mathbf{b} - \mathbf{M}^*\mathbf{y} - \mathbf{U} \|^2\right]\right\}, \tag{5.35}$$

where $\mathbf{U}$ is a constant column vector which keeps an unbiased estimation for $\mathbf{b}$.

$$\mathbf{U} = E[\mathbf{b} - \mathbf{M}\mathbf{y}] = E[\mathbf{b}] - \mathbf{M}E[\mathbf{y}] \tag{5.36}$$

From (5.35), the MMSE filter $\mathbf{m}_k$ of user k satisfies the following minimum mean square error criterion:

$$\mathbf{m}_k = \arg\left\{\min_{\mathbf{m}_k^*} E\left[b_k - \mathbf{m}_k^{*T} \cdot (\mathbf{y} - E[\mathbf{y}]_k)\right]^2\right\}, \tag{5.37}$$

where introducing $E[\mathbf{y}]_k$ is to obtain an unbiased estimate of b_k and

$$E[\mathbf{y}]_k = \mathbf{R}\mathbf{A}E[\mathbf{b}]_k, \tag{5.38}$$

$$E[\mathbf{b}]_k = [\hat{b}_1, \hat{b}_2, \ldots, \hat{b}_{k-1}, 0, \hat{b}_{k+1}, \ldots, \hat{b}_K]^T. \tag{5.39}$$

In the following, we derive the expression of $\mathbf{m}_k$. The covariance matrix $\mathbf{R}_y$ of $(\mathbf{y} - E[\mathbf{y}]_k)$:

$$\mathbf{R}_y = E\left[(\mathbf{y} - E[\mathbf{y}]_k) \cdot (\mathbf{y} - E[\mathbf{y}]_k)^T\right] = E\left[\mathbf{y} \cdot \mathbf{y}^T\right] - E[\mathbf{y}]_k \cdot E[\mathbf{y}]_k^T, \tag{5.40}$$

where,

$$\begin{aligned} E\left[\mathbf{y} \cdot \mathbf{y}^T\right] &= E\left[(\mathbf{R}\mathbf{A}\mathbf{b} + \mathbf{n}) \cdot (\mathbf{b}^T\mathbf{A}^T\mathbf{R}^T + \mathbf{n}^T)\right] \\ &= E\left[\mathbf{R}\mathbf{A}\mathbf{b} \cdot \mathbf{b}^T\mathbf{A}^T\mathbf{R}^T + \mathbf{n} \cdot \mathbf{n}^T\right] \\ &= \mathbf{R}\mathbf{A}E\left[\mathbf{b} \cdot \mathbf{b}^T\right]\mathbf{A}^T\mathbf{R}^T + \sigma^2\mathbf{R}, \end{aligned} \tag{5.41}$$

$$E[\mathbf{y}]_k \cdot E[\mathbf{y}]_k^T = \mathbf{R}\mathbf{A}E[\mathbf{b}]_k \cdot E[\mathbf{b}]_k^T\mathbf{A}^T\mathbf{R}^T. \tag{5.42}$$

In (5.41), we have used the fact that coded symbols are independent of noise vector $\mathbf{n}$. Both $\mathbf{R}$ and $\mathbf{A}$ are symmetric matrices. Therefore,

$$\mathbf{R}_y = \mathbf{R}\mathbf{A}\mathbf{\Lambda}_k\mathbf{A}\mathbf{R} + \sigma^2\mathbf{R}, \tag{5.43}$$

where

$$\mathbf{\Lambda}_k \triangleq E\left[\mathbf{b}\cdot\mathbf{b}^T\right] - E[\mathbf{b}]_k \cdot E[\mathbf{b}]_k^T = \begin{pmatrix} 1-\hat{b}_1^2 & & & \\ & \ddots & \mathbf{0} & \\ & & 1_{kk} & \\ & \mathbf{0} & & \ddots \\ & & & 1-\hat{b}_K^2 \end{pmatrix}. \tag{5.44}$$

The correlation between $(\mathbf{y} - E[\mathbf{y}]_k)$ and b_k is:

$$\mathbf{p}_k = E\left[(\mathbf{y} - E[\mathbf{y}]_k)\cdot b_k\right] = \mathbf{RA}E\left[(\mathbf{b} - E[\mathbf{b}]_k)\cdot b_k\right] = \mathbf{RAe}_k, \tag{5.45}$$

where $\mathbf{e}_k$ denotes a K-dimensional column vector of all zeros, except for the kth element, which is 1. Based on the optimum linear solution for the Wiener-Hopf equation in (5.37) [Hay96], the optimum MMSE filter $\mathbf{m}_k$ for the kth user is:

$$\begin{aligned} \mathbf{m}_k &= \mathbf{R}_y^{-1}\cdot\mathbf{p}_k \\ &= \left[\mathbf{RA\Lambda}_k\mathbf{AR} + \sigma^2\mathbf{R}\right]^{-1}\cdot\mathbf{RAe}_k \\ &= \left[\mathbf{A\Lambda}_k\mathbf{AR} + \sigma^2\mathbf{I}\right]^{-1}\cdot\mathbf{Ae}_k \\ &= A_{kk}\mathbf{R}^{-1}(\mathbf{A\Lambda}_k\mathbf{A} + \sigma^2\mathbf{R}^{-1})^{-1}\mathbf{e}_k. \end{aligned} \tag{5.46}$$

The output of this MMSE filter is:

$$\begin{aligned} x_k^{MMSE} &= \mathbf{m}_k^T\cdot(\mathbf{y} - E[\mathbf{y}]_k) = \mathbf{m}_k^T\cdot\mathbf{RA}\cdot\begin{pmatrix} b_1-\hat{b}_1 \\ \vdots \\ b_k \\ \vdots \\ b_K-\hat{b}_K \end{pmatrix} + \mathbf{m}_k^T\cdot\mathbf{n} \\ &= (\mathbf{m}_k^T\mathbf{RA})_k\cdot b_k + \sum_{i=1,i\neq k}^{K}(\mathbf{m}_k^T\mathbf{RA})_i\cdot(b_i-\hat{b}_i) + \mathbf{m}_k^T\cdot\mathbf{n}. \end{aligned} \tag{5.47}$$

We can see that in (5.47) the first term is the desired signal, the second term is the residual interference after soft interference cancellation and the last one is the background

noise. After assuming that the second term is also a Gaussian random variable which is independent of the background noise, we can express x_k^{MMSE} as follows:

$$x_k^{MMSE} = \mu_k b_k + \eta_k, \tag{5.48}$$

where

$$\begin{aligned}\mu_k &= (\mathbf{m}_k^T \mathbf{R}\mathbf{A})_k \\ &= A_{kk}^2 \left[(\mathbf{A}\mathbf{\Lambda}_k \mathbf{A} + \sigma^2 \mathbf{R}^{-1})^{-1} \right]_{kk},\end{aligned} \tag{5.49}$$

and η_k is a Gaussian random variable with the distribution $\mathcal{N}(0, \sigma_k^2)$, where σ_k^2 is given by

$$\begin{aligned}\sigma_k^2 &= E\left[\sum_{i=1, i\neq k}^{K} (\mathbf{m}_k^T \mathbf{R}\mathbf{A})_i \cdot (b_i - \hat{b}_i) + \mathbf{m}_k^T \cdot \mathbf{n} \right]^2 \\ &= \sum_{i=1, i\neq k}^{K} (\mathbf{m}_k^T \mathbf{R}\mathbf{A})_i^2 \cdot (1 - \hat{b}_i^2) + \sigma^2 \mathbf{m}_k^T \mathbf{R}\mathbf{m}_k \\ &= \sum_{i=1}^{K} (\mathbf{m}_k^T \mathbf{R}\mathbf{A})_i^2 \cdot (1 - \hat{b}_i^2) + \sigma^2 \mathbf{m}_k^T \mathbf{R}\mathbf{m}_k - (\mathbf{m}_k^T \mathbf{R}\mathbf{A})_k^2 \\ &= \mathbf{m}_k^T \mathbf{R}\mathbf{A} \cdot \mathbf{\Lambda}_k \cdot (\mathbf{m}_k^T \mathbf{R}\mathbf{A})^T + \sigma^2 \mathbf{m}_k^T \mathbf{R}\mathbf{m}_k - (\mathbf{m}_k^T \mathbf{R}\mathbf{A})_k^2 \\ &= \mathbf{m}_k^T \mathbf{R}\mathbf{A}\mathbf{\Lambda}_k \mathbf{A}\mathbf{R}\mathbf{m}_k + \sigma^2 \mathbf{m}_k^T \mathbf{R}\mathbf{m}_k - \mu_k^2 \\ &= \mathbf{m}_k^T [\mathbf{R}\mathbf{A}\mathbf{\Lambda}_k \mathbf{A}\mathbf{R} + \sigma^2 \mathbf{R}]\mathbf{m}_k - \mu_k^2 \\ &= \mathbf{m}_k^T [\mathbf{R}\mathbf{A}\mathbf{\Lambda}_k \mathbf{A}\mathbf{R} + \sigma^2 \mathbf{R}] \cdot [\mathbf{R}\mathbf{A}\mathbf{\Lambda}_k \mathbf{A}\mathbf{R} + \sigma^2 \mathbf{R}]^{-1} \mathbf{R}\mathbf{A}\mathbf{e}_k - \mu_k^2 \\ &= \mathbf{m}_k^T \mathbf{R}\mathbf{A}\mathbf{e}_k - \mu_k^2 \\ &= \mu_k - \mu_k^2.\end{aligned} \tag{5.50}$$

For the second equation in (5.50), we assume that different users' symbols are independent of one another and they are also independent of the background noise vector $\mathbf{n}$. The extrinsic LLR of b_k, i.e., the soft output of b_k is:

$$\begin{aligned}\lambda_o^{MMSE}[b_k] &= \log \frac{P[x_k^{MMSE} | b_k = +1]}{P[x_k^{MMSE} | b_k = -1]} \\ &= \frac{2 x_k^{MMSE} \mu_k}{\sigma_k^2}\end{aligned}$$

$$= \frac{2x_k^{MMSE}}{1-\mu_k}, \quad 1 \leq k \leq K. \tag{5.51}$$

By comparing the above linear SISO MMSE detector with the detector consisting of soft interference cancellation followed by an instantaneous linear MMSE filter in [Wan99], we can see that they have exactly the same MMSE filter for each user and the same soft outputs.

5.3.2 Performance Analysis

Since the output of a non-SISO MMSE filter can be assumed to be a Gaussian random variable [Poo97] and from (5.47) the output of the SISO MMSE filter only consists of residual multiuser interference, we can assume that x_k^{MMSE} is also a Gaussian random variable, given by (5.48). The signal to residual interference-plus-noise ratio in x_k^{MMSE} is:

$$\text{SNR}_k = \frac{\mu_k^2}{\sigma_k^2} = \frac{\mu_k}{1-\mu_k}. \tag{5.52}$$

Here, we are interested in the relationship between SNR_k for each user k $(1 \leq k \leq K)$ and the number of iterations in the receiver. Under the same assumption as that in Subsection 5.2.2, which is that reliabilities of soft symbol estimates $\{|\hat{b}_k|, 1 \leq k \leq K\}$ increase with additional iterations, in the following we will show that $\{\text{SNR}_k, 1 \leq k \leq K\}$ also increase with the increased number of iterations. That is, each user's performance will be improved and approach to that of the single user system as we increase the number of iterations.

Based on (5.52), SNR_k is a strictly mono-increasing function of μ_k with $0 \leq \mu_k \leq 1$ in (5.49).

$$\begin{aligned} \mu_k &= (\mathbf{m}_k^T \mathbf{R} \mathbf{A})_k \\ &= (\mathbf{\Lambda}_k + \sigma^2 \mathbf{A}^{-1} \mathbf{R}^{-1} \mathbf{A}^{-1})_{kk}^{-1} \end{aligned} \tag{5.53}$$

We denote $\mathbf{\Lambda}_k$ in (5.44) by the following matrix:

$$\mathbf{\Lambda}_k \triangleq \begin{pmatrix} \zeta_1 & & \mathbf{0} & \\ & \zeta_2 & & \\ & & \ddots & \\ \mathbf{0} & & & \zeta_K \end{pmatrix}, \tag{5.54}$$

where

$$\zeta_i = 1 - \hat{b}_i^2, \quad 1 \leq i \leq K, i \neq k, \tag{5.55}$$

$$\zeta_k = 1. \tag{5.56}$$

Therefore, μ_k is a function with multiple arguments $\{\zeta_i, 1 \leq i \leq K, i \neq k\}$. In the following, we will find the relationship between μ_k and its arguments by using the recursive algorithm to calculate the matrix inverse in (5.53). Denote

$$\mathbf{\Phi}^{(0)} \triangleq 1/\sigma^2 \mathbf{ARA}, \tag{5.57}$$

$$\mathbf{\Phi}^{(j)} \triangleq \left(\sigma^2 \mathbf{A}^{-1}\mathbf{R}^{-1}\mathbf{A}^{-1} + \sum_{i=1}^{j} \zeta_i \mathbf{e}_i \mathbf{e}_i^T\right)^{-1}, \quad 1 \leq j \leq K. \tag{5.58}$$

Therefore, we have

$$\mathbf{\Phi}^{(K)} \triangleq \left(\sigma^2 \mathbf{A}^{-1}\mathbf{R}^{-1}\mathbf{A}^{-1} + \sum_{i=1}^{K} \zeta_i \mathbf{e}_i \mathbf{e}_i^T\right)^{-1}. \tag{5.59}$$

Using the matrix inverse lemma [Gol96], we can calculate $\mathbf{\Phi}^{(j)}$ recursively as for $j = 1, 2, \ldots, K$.

$$\begin{aligned} \mathbf{\Phi}^{(j)} &= \left((\mathbf{\Phi}^{(j-1)})^{-1} + \zeta_j \mathbf{e}_j \mathbf{e}_j^T\right)^{-1} \\ &= \mathbf{\Phi}^{(j-1)} - \frac{\mathbf{\Phi}^{(j-1)} \mathbf{e}_j \mathbf{e}_j^T \mathbf{\Phi}^{(j-1)}}{1/\zeta_j + (\mathbf{\Phi}^{(j-1)})_{jj}}, \quad 1 \leq j \leq K \end{aligned} \tag{5.60}$$

For the kth diagonal element of (5.60), the corresponding recursive algorithm is:

$$(\mathbf{\Phi}^{(j)})_{kk} = (\mathbf{\Phi}^{(j-1)})_{kk} - \frac{(\mathbf{\Phi}^{(j-1)})_{kj}^2}{1/\zeta_j + (\mathbf{\Phi}^{(j-1)})_{jj}}, \quad 1 \leq j \leq K. \tag{5.61}$$

Since $(\mathbf{\Phi}^{(j-1)})_{kk}$, $(\mathbf{\Phi}^{(j-1)})_{jj}$ and $(\mathbf{\Phi}^{(j-1)})_{kj}$ are values obtained in the $(j-1)$th recursive loop, they are independent of ζ_j. Therefore, $(\mathbf{\Phi}^{(j)})_{kk}$ is a strictly mono-decreasing function of ζ_j, for $1 \leq j \leq K$. After K recursive loops, $(\mathbf{\Phi}^{(K)})_{kk}$ is a strictly mono-decreasing function of ζ_K. We also note that the above recursive algorithm to calculate $\mathbf{\Phi}^{(K)}$ can have any recursive order with respect to i in (5.59), while give the same result. Thus, $(\mathbf{\Phi}^{(K)})_{kk}$, i.e. μ_k, is a strictly mono-decreasing function with respect to $\{\zeta_i, 1 \leq i \leq K, i \neq k\}$, respectively.

Under the assumption that with the increased number of iterations the reliabilities of soft symbol estimates increase, $\{\zeta_i, 1 \leq i \leq K, i \neq k\}$ will decrease respectively, which results in an increasing μ_k. Therefore, with additional iterations SNR_k will increase, which means that the kth user's performance will be improved and approach to that of the single user system.

5.3.3 Simulation Results

In this subsection, we use the same system parameters and Monte-Carlo simulation scenarios as those in Subsection 5.2.3, except that we employ the linear SISO MMSE detector here. In addition, we compare system performances provided by the SISO decorrelator and those provided by the linear SISO MMSE detector.

At the first iteration, we assume that there is no a priori information of coded symbols. That is, $\{\hat{b}_i = 0, 1 \leq i \leq K\}$ in (5.44) and $\mathbf{\Lambda}_k = \mathbf{I}$. The MMSE filter $\mathbf{m}_k$ is reduced to:

$$\begin{aligned} \mathbf{m}_k &= (\mathbf{RAAR} + \sigma^2\mathbf{R})^{-1} \cdot \mathbf{RAe}_k \\ &= (\mathbf{R} + \sigma^2\mathbf{A}^{-2})^{-1} \cdot \mathbf{A}^{-1}\mathbf{e}_k, \end{aligned} \tag{5.62}$$

which is a traditional linear MMSE filter in (2.54). Therefore, the linear SISO MMSE detector just follows the traditional linear MMSE detector at the first iteration. Fig. 5.7

- Fig. 5.10 show the bit error rate performances provided by the linear SISO MMSE detector and the SISO decorrelator in the first five iterations for the four K-symmetric multiuser systems in Subsection 5.2.3 respectively, where all users have the equal received power. We can see that the system performance provided by the linear SISO MMSE detector approaches to that of the single user system with only a few iterations and increased SNRs as well. These figures also show performance comparisons between the linear SISO MMSE detector and the SISO decorrelator. The linear SISO MMSE detector is shown to have a slightly better bit error rate performance than the SISO decorrelator. The explanation will be provided in Section 5.5.

For the near-far resistance of the linear SISO MMSE detector, we simulate bit error rates of unequal power users in the system with $K = 5, \rho = 0.7$ and show the result in Fig. 5.11, where three users have 3dB more energy than the other two. Note that signal-to-noise ratios of strong users and weak users have 3dB difference and are marked by red color and blue color respectively in that figure. Signal-to-noise ratios of the single user system are also indicated in blue. The linear SISO MMSE multiuser detector is also near-far resistant for lower power users since their performance converges to that of the single user system. While for high power users, their performance is worse than that of the single user system at the same E_b/N_o values.

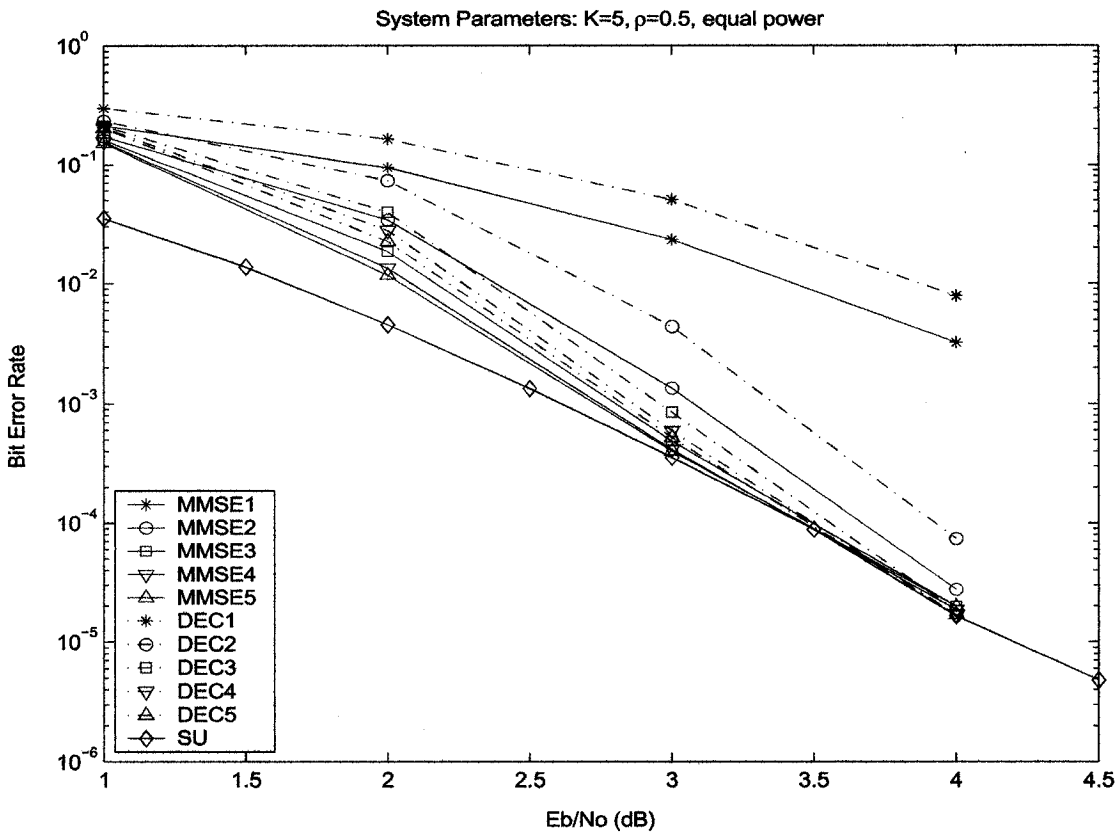

Figure 5.7: Comparison of bit error rate performances between the linear SISO MMSE detector at the first five iterations (MMSE1 – MMSE5), the SISO decorrelator (DEC1 – DEC5) and the single user system (SU) for $K = 5$, $\rho = 0.5$ and equal power users.

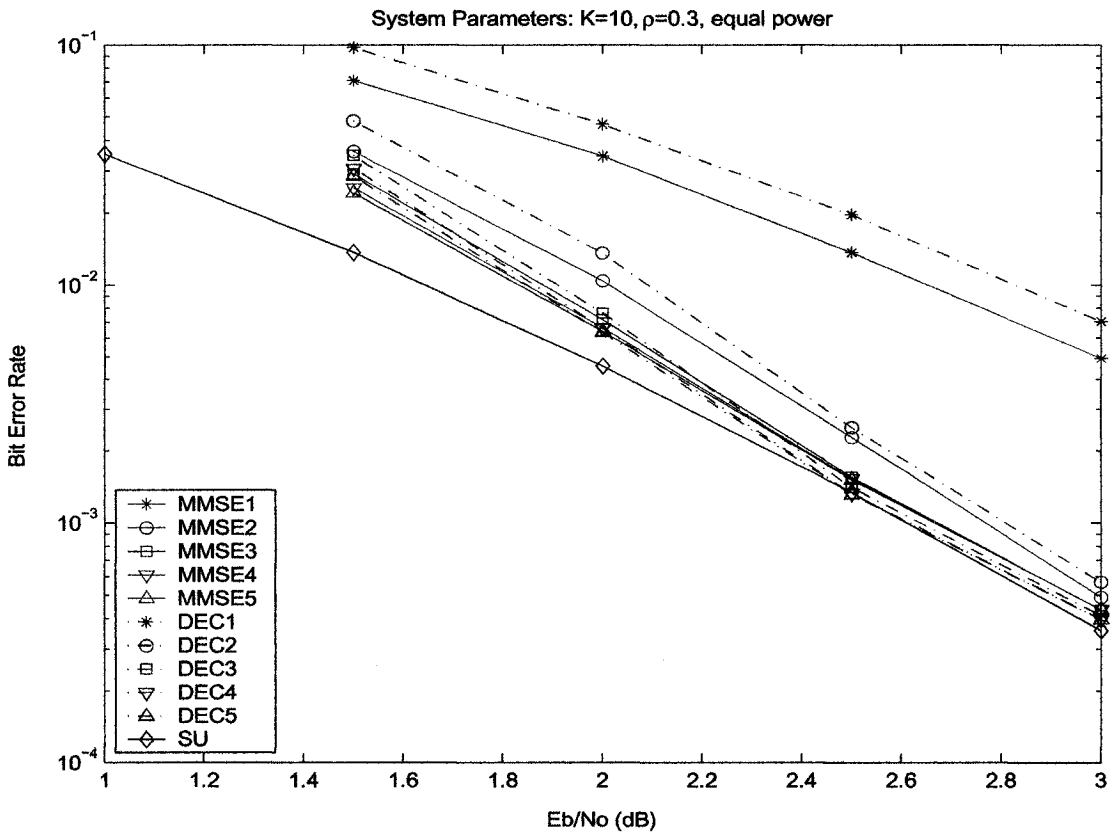

Figure 5.8: Comparison of bit error rate performances between the linear SISO MMSE detector at the first five iterations (MMSE1 – MMSE5), the SISO decorrelator (DEC1 – DEC5) and the single user system (SU) for $K = 10$, $\rho = 0.3$ and equal power users.

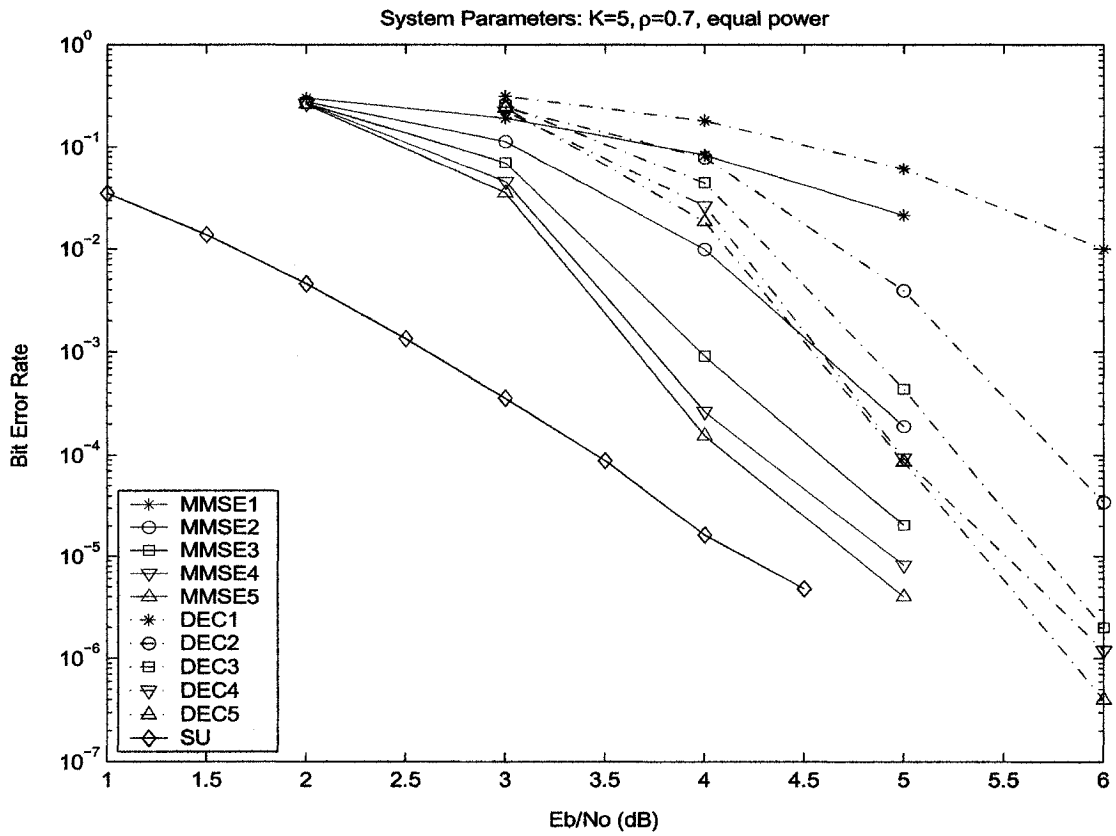

Figure 5.9: Comparison of bit error rate performances between the linear SISO MMSE detector at the first five iterations (MMSE1 – MMSE5), the SISO decorrelator (DEC1 – DEC5) and the single user system (SU) for $K = 5$, $\rho = 0.7$ and equal power users.

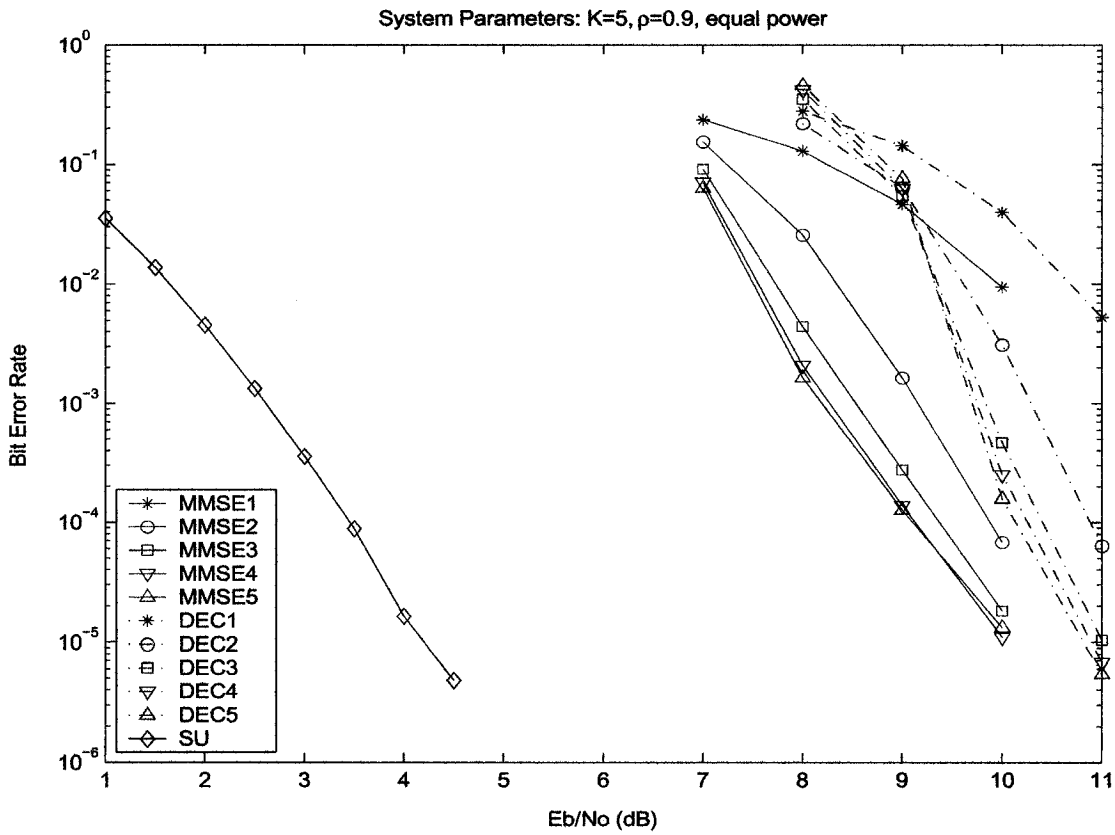

Figure 5.10: Comparison of bit error rate performances between the linear SISO MMSE detector at the first five iterations (MMSE1 – MMSE5), the SISO decorrelator (DEC1 – DEC5) and the single user system (SU) for $K = 5$, $\rho = 0.9$ and equal power users.

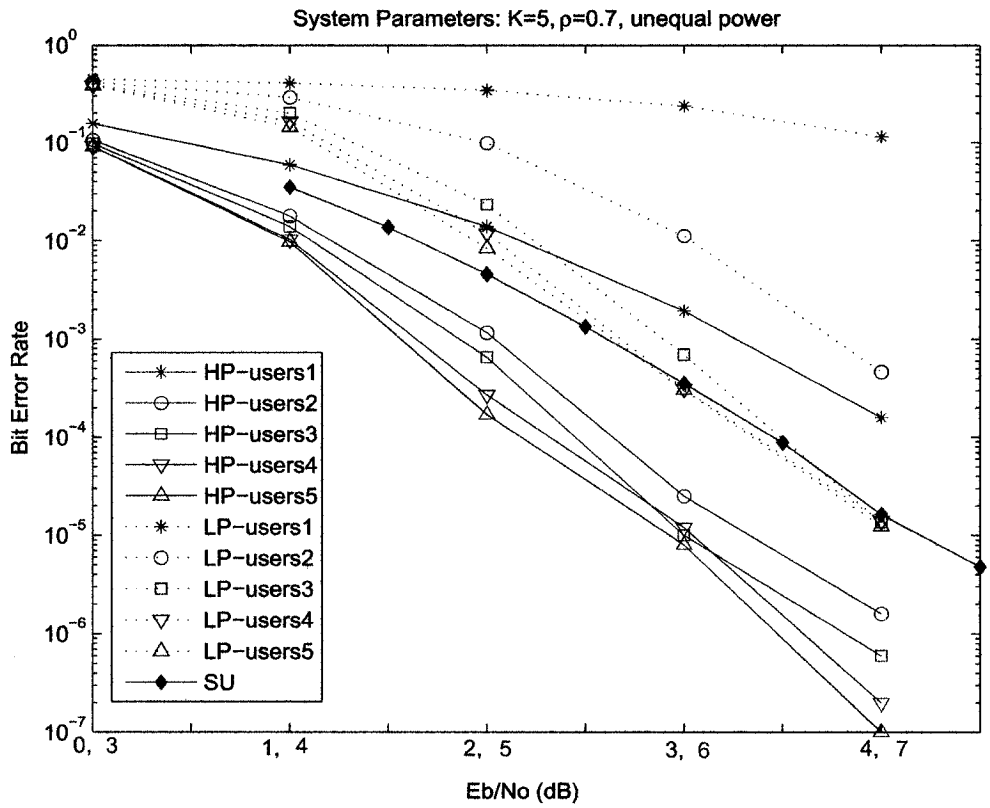

Figure 5.11: Comparison of bit error rate performances between higher power users in the first five iterations (HP-users1 – HP-users5), lower power users (LP-users1 – LP-users5) under linear SISO MMSE detection and the single user system (SU). System parameters: $K = 5$, $\rho = 0.7$, three users have 3dB more energy than the other two. Signal-to-noise ratios of higher power users and lower power users are marked by red and blue colors, respectively. Signal-to-noise ratios of the single user system are also indicated in blue.

5.3.4 Computational Complexity Analysis

Now we calculate the total number of operations needed by the linear SISO MMSE detector. The detection process for each symbol of each user includes: (1) calculating the optimum filter $\mathbf{m}_k$ for each user k; (2) computing the output x_k^{MMSE} of the MMSE filter; and finally (3) obtaining the soft output.

Table C.1 in Appendix C shows the number of operations required in each step of the linear SISO MMSE detector. In each iteration, for each symbol duration, the detector needs $4K^3 + 5K^2 + 3K$ operation, which is also a cubic function of the number of users.

5.3.5 Reduced-Complexity Linear SISO MMSE Detection

In this subsection, we introduce a reduced-complexity alternative to the linear SISO MMSE detector.

At the first iteration, since there is no a priori information of coded symbols, the linear SISO MMSE detector follows traditional linear MMSE detection. In particular, we apply a constant linear MMSE filter to all coded symbols of each user. For the second and subsequent iterations, the a priori information of coded symbols is available. After employing this information in the design of the MMSE filter for each user, we obtain the linear SISO MMSE detector in Section 5.3.1. However, to further reduce the computational complexity, we assume that for user k the soft estimates of interfering symbols are perfect. That is:

$$\hat{b}_i^2 = 1, \quad 1 \leq i \leq K, i \neq k. \tag{5.63}$$

Substituting (5.63) in (5.44), we have:

$$\mathbf{\Lambda}_k = \mathbf{e}_k \mathbf{e}_k^T. \tag{5.64}$$

Under this assumption, $\mathbf{\Lambda}_k$ is all zeros except for a 1 in the kth diagonal element. The MMSE filter of user k in (5.46) is reduced to:

$$\mathbf{m}_k = \left[\mathbf{RAe}_k\mathbf{e}_k^T\mathbf{AR} + \sigma^2\mathbf{R}\right]^{-1} \cdot \mathbf{RAe}_k, \tag{5.65}$$

which is constant for all symbols of user k in all iterations. Furthermore, by using the matrix inverse lemma in [Gol96], we can express the matrix inverse in (5.65) as:

$$\left[\mathbf{RAe}_k\mathbf{e}_k^T\mathbf{AR} + \sigma^2\mathbf{R}\right]^{-1} = \sigma^{-2}\mathbf{R}^{-1} - \frac{\sigma^{-2}A_k^2}{\sigma^2 + A_k^2} \cdot \mathbf{e}_k\mathbf{e}_k^T. \tag{5.66}$$

By substituting (5.66) into (5.65), we can express $\mathbf{m}_k$ as:

$$\begin{aligned}\mathbf{m}_k &= (\sigma^{-2}\mathbf{R}^{-1} - \frac{\sigma^{-2}A_k^2}{\sigma^2 + A_k^2} \cdot \mathbf{e}_k\mathbf{e}_k^T) \cdot \mathbf{RAe}_k \\ &= \frac{A_k}{\sigma^2 + A_k^2} \cdot \mathbf{e}_k,\end{aligned} \tag{5.67}$$

which has only one nonzero element at the kth row. Therefore, in the detector we calculate the MMSE filter $\mathbf{m}_k$ of user k only once and apply it to all symbols of user k in all iterations. In contrast, in the linear SISO MMSE detection, we need to update the MMSE filter $\mathbf{m}_k$ for each symbol of user k in each iteration. Thus, the computational complexity of the detector is reduced much.

The output of the reduced-complexity SISO MMSE detector of the kth user, x_{rk}^{MMSE}, is:

$$x_{rk}^{MMSE} = \mathbf{m}_k^T[\mathbf{y} - E(\mathbf{y})_k]. \tag{5.68}$$

By using Gaussian assumption of this output, similarly to (5.48), we can express x_{rk}^{MMSE} as:

$$x_{rk}^{MMSE} = \mu_k b_k + \eta_k, \tag{5.69}$$

where (5.49) and (5.50) still hold and

$$\mu_k = \frac{A_k^2}{\sigma^2 + A_k^2}. \tag{5.70}$$

The soft output is also calculted by (5.51).

In (5.68), $[\mathbf{y} - E(\mathbf{y})_k]$ is the output vector of soft interference cancellation and $\mathbf{m}_k$ only has one nonzero element at the kth row as shown in (5.67). Therefore, the reduced-complexity SISO MMSE detector is a scaled soft interference canceller in the second and subsequent iterations. It has a slower convergence speed compared with the linear SISO MMSE detector. Fig. 5.12 shows the performance comparison between the linear SISO MMSE detector and the reduced-complexity detector for the multiuser system with $K = 5, \rho = 0.7$. At the first iteration, both detectors have the same performance since they follow traditional MMSE detection. We can see that at the following iterations, the reduced-complexity MMSE detector has a slower convergence speed with additional iterations. Furthermore, there is a considerable performance difference between these two types of detectors.

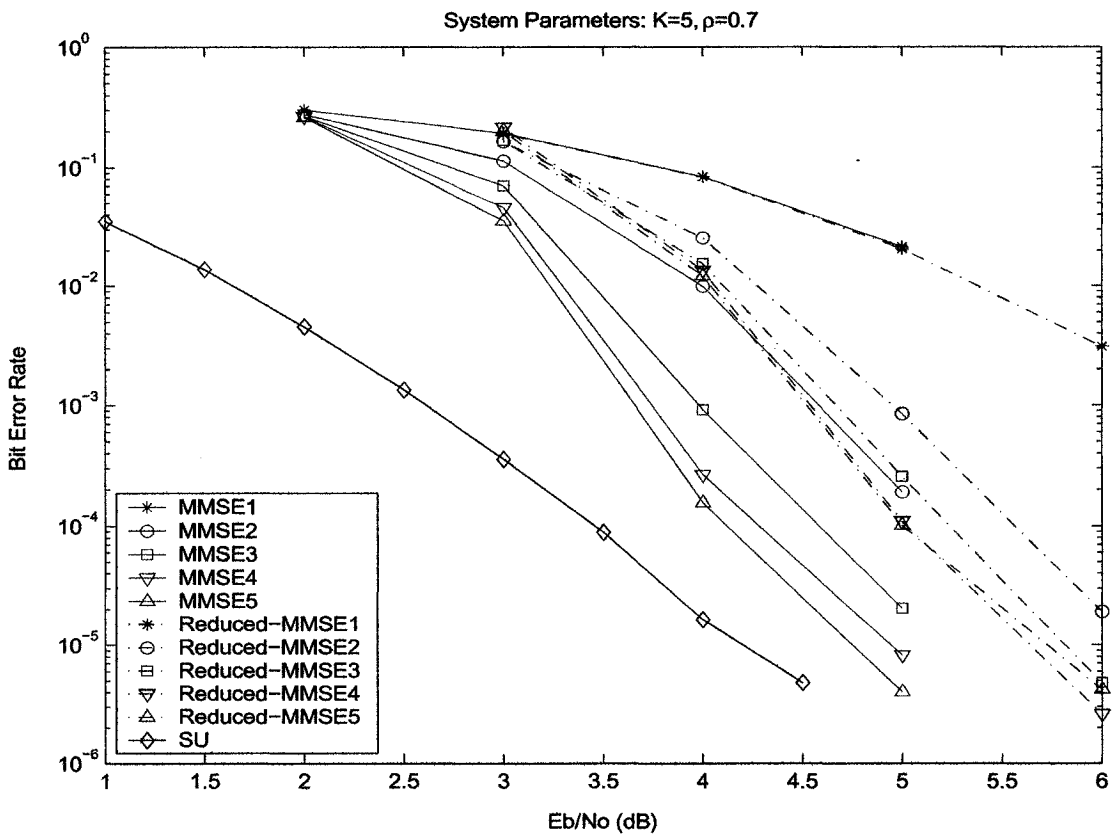

Figure 5.12: Comparison of bit error rate performances between the linear SISO MMSE detector at the first five iterations (MMSE1 – MMSE5), the reduced-complexity SISO MMSE detector (Reduced-MMSE1 – Reduced-MMSE5) and the single user system (SU) for $K = 5$, $\rho = 0.7$ and equal power users.

5.4 SISO Parallel Decision Feedback Multiuser Detectors

In this section, we use the same a priori information of coded symbols as that in Section 5.3 to derive the optimum feedforward filter $\mathbf{m}_{fk}$ and feedback filter $\mathbf{m}_{bk}$ of user k based on the minimum mean square error criterion. A similar derivation can also be found in [Gam00]. For the kth user, the optimum feedforward filter $\mathbf{m}_{fk(K\times 1)}$ and feedback filter $\mathbf{m}_{bk(K\times 1)}$ satisfy the following MMSE criterion:

$$\min_{\mathbf{m}_{fk},\mathbf{m}_{bk}} E\left[b_k - \mathbf{m}_{fk}^T\mathbf{y} - \mathbf{m}_{bk}^T\hat{\mathbf{b}}_k\right]^2, \tag{5.71}$$

where $\hat{\mathbf{b}}_k = \left[\hat{b}_1,\ldots,\hat{b}_{k-1},0,\hat{b}_{k+1}\ldots,\hat{b}_K\right]^T$ only consists of the fedback decisions of interfering users. Based on the soft inputs from single user decoders, these decisions are soft symbol estimates shown in (5.4). By constructing two new vectors as follows:

$$\mathbf{m} = \begin{pmatrix} \mathbf{m}_{fk} \\ \mathbf{m}_{bk} \end{pmatrix}, \tag{5.72}$$

$$\mathbf{v} = \begin{pmatrix} \mathbf{y} \\ \hat{\mathbf{b}}_k \end{pmatrix}, \tag{5.73}$$

the MMSE criterion in (5.71) is equal to:

$$\min_{\mathbf{m}} E\left[b_k - \mathbf{m}^T\mathbf{v}\right]^2. \tag{5.74}$$

Applying the Wiener-Hopf solutions [Hay96], we have the optimum $\mathbf{m}_{opt}$:

$$\mathbf{R}_v \cdot \mathbf{m}_{opt} = \mathbf{q}_k, \tag{5.75}$$

where

$$\begin{aligned}\mathbf{R}_v &= E\left[\mathbf{v}\cdot\mathbf{v}^T\right] \\ &= \begin{pmatrix} E\left[\mathbf{y}\cdot\mathbf{y}^T\right] & E\left[\mathbf{y}\cdot\hat{\mathbf{b}}_k^T\right] \\ E\left[\hat{\mathbf{b}}_k\cdot\mathbf{y}^T\right] & \hat{\mathbf{b}}_k\cdot\hat{\mathbf{b}}_k^T \end{pmatrix},\end{aligned} \tag{5.76}$$

$$\mathbf{q}_k = E[\mathbf{v} \cdot b_k]. \tag{5.77}$$

Using the same a priori information as in (5.31) - (5.34) and the assumption that multiple users' symbols are independent of the noise vector, we can calculate the elements in (5.76) as follows:

$$E\left[\mathbf{y} \cdot \mathbf{y}^T\right] = \mathbf{R}\mathbf{A}E\left[\mathbf{b} \cdot \mathbf{b}^T\right]\mathbf{A}\mathbf{R} + \sigma^2\mathbf{R}, \tag{5.78}$$

$$E\left[\mathbf{y} \cdot \hat{\mathbf{b}}^T\right] = \mathbf{R}\mathbf{A}\hat{\mathbf{b}}\hat{\mathbf{b}}^T, \tag{5.79}$$

$$E\left[\hat{\mathbf{b}} \cdot \mathbf{y}^T\right] = \hat{\mathbf{b}}\hat{\mathbf{b}}^T\mathbf{A}\mathbf{R}, \tag{5.80}$$

$$\mathbf{q}_k = \left[(\mathbf{R}\mathbf{A}\mathbf{e}_k)^T \quad 0^T\right]^T. \tag{5.81}$$

Substitute (5.76) and (5.77) into (5.75), we obtain the optimum filter as follows:

$$\mathbf{m}_{fk} = (\mathbf{R}\mathbf{A}\mathbf{\Lambda}_k\mathbf{A}\mathbf{R} + \sigma^2\mathbf{R})^{-1}\mathbf{R}\mathbf{A}\mathbf{e}_k, \tag{5.82}$$

$$\mathbf{m}_{bk} = -\mathbf{A}\mathbf{R}\mathbf{m}_{fk}. \tag{5.83}$$

The output of the SISO parallel decision feedback detector is:

$$\begin{aligned} x_k^{PDFD} &= \mathbf{m}_{fk}^T \cdot \mathbf{y} + \mathbf{m}_{bk}^T \cdot \hat{\mathbf{b}}_k \\ &= \mathbf{m}_{fk}^T \cdot \mathbf{y} - \mathbf{m}_{fk}^T \cdot \mathbf{R}\mathbf{A}\hat{\mathbf{b}}_k \\ &= \mathbf{m}_{fk}^T \cdot (\mathbf{y} - E[\mathbf{y}]_k). \end{aligned} \tag{5.84}$$

Comparing (5.82) with (5.46), we can see that the feedforward filter is the same as the linear SISO MMSE filter for each user. Therefore, for this specific case (i.e. soft symbols of all interfering users are fedback), the output of the SISO parallel decision feedback detector (5.84) is exactly the same as that of the linear SISO MMSE filter (5.47).

5.5 Comparison of the Three Types of SISO Detectors

In this section, we compare the three types of SISO multiuser detectors presented in the previous three sections. All of these detectors consist of soft interference cancellation, which makes use of soft inputs of detectors provided by a bank of SISO single user decoders. In addition, they further successfully exploit these soft inputs in their own ways. This is confirmed by their performance analysis and simulation results, which show that the resulting system performance approaches to that of the single user system quickly with the increased number of iterations. Furthermore, all types of SISO detectors have roughly the same computational complexity $\sim O(K^3)$ per symbol at each iteration, which is a cubic function of the number of users K.

It is well known that the traditional decorrelator has a worse performance compared with the traditional linear MMSE detector [Ver98]. Therefore, the conclusion we obtained in Section 5.3.3, which is that the SISO decorrelator has a slightly worse performance than the linear SISO MMSE detector, is intuitive. Another possible reason is explained as follows. Based on (5.52), (5.49) and (5.46), SNR_k of user k at the output of the linear SISO MMSE detector depends only on reliabilities $\{|\hat{b}_i|, i \neq k\}$ of soft symbol estimates, excluding their hard decisions $\{\text{sgn}(\hat{b}_i), i \neq k\}$. While for the SISO decorrelator, its approximate cross-correlation matrix $\hat{\mathbf{R}}_u$ in (5.16) is based on both reliabilities and hard decisions of soft symbol estimates. Therefore, the linear SISO MMSE detector is more robust against soft inputs with low reliabilities than the SISO decorrelator.

Comparing the computational complexity of the SISO decorrelator in Subsection 5.3.4 and that of the SISO MMSE detector in Subsection 5.2.4, we can see that the SISO decorrelator requires roughly 25% less computation than the SISO MMSE detector per

coded symbol duration in each iteration.

Although the output of the SISO parallel decision feedback detector for each user is the same as that of the linear SISO MMSE detector, the implementation of these two types of detectors are different for some specific cases. In linear SISO MMSE detection, we first cancel the soft interference for each user and then apply a linear MMSE filter on the output of the soft interference canceller to further suppress the residual multiple access interference (MAI) and background Gaussian noise in the MMSE sense. However, soft interference cancellation needs the interfering users' information, such as their received waveforms. In contrast, for the SISO parallel decision feedback detector, if we don't know the received waveforms of multiple users, we can apply adaptive algorithms to update and obtain the filter coefficients [Hon00], [Hon01] and [Rap99b]. Adaptive SISO multiuser detection is the main topic of Chapter 6.

5.6 Summary

Traditional multiuser detectors, such as decorrelating detectors, linear MMSE detectors and parallel decision feedback detectors, are successfully adapted to be SISO detectors, which can cooperate iteratively with a bank of SISO single user decoders. The resulting system performance approaches to that of the single user system after only a few iterations for moderate and high signal-to-noise ratios. Furthermore, the computational complexity of these SISO detectors is a cubic function of the number of users, making these detectors far less complex than optimum SISO multiuser detectors. Comparison of these three types of SISO multiuser detectors has also been shown in this chapter.

For easy reference, Table 5.1 shows the performance-versus-complexity of all the SISO multiuser detectors discussed in this chapter.

Table 5.1: Performance-versus-complexity of SISO multiuser detectors for synchronous multiuser systems. (K - number of users)

SISO Multiuser Detectors	Performance (required Eb/No(dB) at the 5th iteration, at BER 10^{-3}, for K-symmetric system with $K = 5$)		Complexity (number of operations per symbol interval per iteration)
	$\rho = 0.5$	$\rho = 0.7$	
1. Soft interference canceller	3.4	—	$K^2 + 5K$
2. SISO decorrelator	2.8	—	$3K^3 + 4K^2 + 6K$
3. SISO MMSE detector	2.7	3.6	$4K^3 + 5K^2 + 3K$
4. SISO parallel decision feedback detector	2.7	3.6	$4K^3 + 5K^2 + 3K$
5. Reduced-complexity SISO MMSE detector	—	4.5	$2K^2 + 9K$

Chapter 6

Adaptive SISO Multiuser Detection

6.1 Introduction

From Chapter 4 and Chapter 5, we see that the optimum and many suboptimum SISO multiuser detectors require a priori information of the multiuser system, such as all users' transmitted waveforms, relative delays and the channel impulse response. However, sometimes this information is not available. For example, in practical situations, this information may not be easily obtainable for time-varying fading channels. Due to unknown multipath fading channels, the received waveforms of all users and their relative delays are not available to the receiver.

Fortunately, if system parameters are constant or slowly varying, adaptive detectors (non-SISO) can successfully track them directly from the received signal [Hon98], [Poo95], [Rap94]. In many cases, a training sequence is required and transmitted before the transmission of actual data or inserted in the transmitted data stream. The receiver uses an adaptive algorithm to adjust its detector when the training sequence is being sent. While in the data transmission duration, the training sequence is replaced by symbol decisions made by the detector and the receiver is switched to the decision-directed

mode. When the receiver does not require the training sequence, we call this as blind detection which is the topic of [Hon95] and [Wan98].

In general, adaptive multiuser detectors have two main advantages. One is that by using adaptive detection, the receiver does not require the knowledge of the desired user's waveform and delay, the interfering users' waveforms and relative delays, or the fading channel coefficients. The adaptive detector can track this information from the received signal directly. The other advantage is that adaptive detectors may have a reduced computational complexity. For example, in a time varying environment, the non-adaptive decorrelator and linear MMSE detector need to recalculate a matrix inverse for each symbol, which has a high computational complexity. While in the adaptive detector, we can avoid calculating these matrix inverses. In [Che94] and [Xue99], an adaptive decorrelator and an adaptive linear MMSE detector are presented, respectively. Moreover, since the received signal is used as the desired signal, no training sequence is required. By applying the least squares or MMSE criterion to the desired signal and reconstructed signal, we can obtain the adaptive decorrelator or adaptive linear MMSE detector.

In [Rap94], adaptive linear and centralized decision feedback receiver structures for coherent demodulation in asynchronous DS-CDMA systems over multipath fading channels are proposed. These adaptive receivers have no knowledge of the signature waveforms and relative delays of all users as well as the channel impulse response. A training sequence is required by each user. Each user has its own single user detector, which is an adaptive filter with the length at least equal to the spreading gain. Moreover, in order to make the receiver insensitive to the differences in the signal arrival times of various users, the detector uses a fractionally spaced filter for each user. Based on the same a priori information as that in [Rap94], [Bor01] and [Rap99a] present an optimum adaptive

multiuser detector in the weighted least squares (WLS) sense, which consists of a bank of linear fractionally chip-spaced MMSE filters and a nonlinear WLS metric minimizer. The first part can be implemented by a bank of adaptive parallel decision feedback detectors, which obtain sufficient statistics for the following minimizer. The WLS metric minimizer exploits and suppresses the multiple access interference and intersymbol interference (ISI) in the received signal by optimum maximum likelihood sequence detection.

In the downlink, each user's detector usually knows its own waveform and delay, while without the information of other interfering users' waveforms and relative delays. Based on this a priori information, [Lee96], [Mad94], [Sin99], [Str94] propose single user adaptive filters with the length less than the spreading gain, which follow some preprocessing on the received signal. Therefore, detectors will have a faster convergence speed and less computational complexity, compared with those with the length at least equal to the spreading gain.

In the uplink of a multiple access network, usually all users' waveforms and relative delays are known to the base station. When all users' waveforms and relative delays are known while the channel coefficients are not available, the complexity and convergence speed of the adaptive detector can be further reduced and improved respectively, compared with adaptive detectors in the downlink. In [Nag99], by making use of the knowledge of the signal space for demodulation of all users' signals, the receiver substantially reduces the length of adaptive linear filters. For a good review of adaptive multiuser detection, please refer to [Woo98] and [Kua03].

For SISO multiuser detectors, [Hon00] presents an adaptive SISO parallel decision feedback multiuser detector for synchronous DS-CDMA systems with short spreading sequences. The receiver requires only a training sequence and timing for estimating all

filter coefficients for each user. By using an approximate least square algorithm and soft symbol estimates, the detector exploits the joint statistics of soft symbol estimates and transmitted symbols. The resulting system performance converges to the single user bound with relative low SNRs. In [Hon01], an adaptive SISO successive decision feedback detector is proposed for synchronous DS-CDMA systems and compared with the parallel decision feedback detector.

In this chapter, we want to employ adaptive algorithms in the SISO multiuser detector in order to avoid the a priori information of users' transmitted waveforms, relative delays and the channel impulse response, which is required by the optimum and suboptimum SISO multiuser detectors. A system model is introduced in Section 6.2.

In Section 6.3, we first derive the optimum SISO parallel decision feedback detector for synchronous DS-CDMA systems over the additive white Gaussian noise channel. These detectors need the knowledge of all users' transmitted waveforms and relative delays. Secondly, we propose two adaptive SISO parallel decision feedback detectors based on the normalized least mean square (NLMS) and the recursive least squares (RLS) algorithms, respectively. We assume that all users employ randomly selected short spreading sequences, which are unknown to the receiver. A training sequence is required for each user. Compared with traditional (non-SISO) adaptive detectors, our SISO adaptive detectors effectively exploit the a priori information of coded symbols, which is based on soft inputs of detectors provided by a bank of single user decoders, to further improve their convergence performance. Monte-Carlo simulation results of these two adaptive detectors are presented and compared. We can show that the resulting system performance converges to that of the single user system as we increase the number of iterations or signal-to-noise ratios. The adaptive detector based on the RLS algorithm has a better bit error rate performance than the detector based on the NLMS algorithm and requires

fewer training symbols, at the expense of increased computational complexity. Furthermore, both adaptive SISO parallel decision feedback detectors are shown to be near-far resistant.

In Section 6.4, we consider asynchronous DS-CDMA systems over the AWGN channel. For adaptive implementation of the SISO parallel decision feedback detector (PDFD), we select practical finite feedforward and feedback filter lengths to obtain a good trade-off between the system performance and computational complexity of the receiver. We propose three adaptive SISO parallel decision feedback detectors for asynchronous DS-CDMA systems where all users' waveforms and relative delays are unknown to the receiver. The feedforward filters of these adaptive detectors have the same length, which covers a two-symbol duration, while the feedback filters have different lengths. That is, their feedback filters try to cancel different amount of interference for the interested symbol. Based on the Monte-Carlo simulation results, the resulting system performance is still shown to approach to that of the single user system with additional iterations and increased signal-to-noise ratios as well. Furthermore, the adaptive SISO detector with more feedback filter taps provides a better bit error rate performance.

Finally, in Section 6.5 we extend our adaptive SISO parallel decision feedback detectors to asynchronous DS-CDMA systems over slow frequency nonselective Rayleigh fading channels. In addition to unknown multiple users' transmitted waveforms and relative delays, we assume that the channel impulse response is also unknown to the receiver. Adaptive detectors and simulation results for this case are presented and analyzed.

6.2 System Model

A general coded DS-CDMA system with an iterative and adaptive receiver is shown in Fig. 6.1. There are K active users in the system. The information bits of each user

are first encoded, then interleaved, modulated and spread before they are transmitted over the channel. The iterative receiver consists of two parts, an adaptive soft-input soft-output multiuser detector and a bank of SISO single user decoders, which are separated by de-interleavers and interleavers. These two parts cooperate iteratively by transferring updated extrinsic soft information of coded symbols between them.

In this section, we consider a general single-cellular DS-CDMA system in [Bor01]. The received signal is:

$$r(t) = \sum_{k=1}^{K} \sum_{i=1}^{N_b} b_k(i) s_k(t - iT - \tau_k) + n(t), \tag{6.1}$$

where K is the number of active users in the cell of interest, N_b is the number of symbols transmitted by each user, $b_k(i)$ is the ith symbol of the kth user, $s_k(t)$ and τ_k are its received signature waveform and transmission delay respectively, T is the symbol period and $n(t)$ is the background white Gaussian noise. Here we assume BPSK modulation, i.e. $b_k(i) \in \{+1, -1\}$. The received signature waveform of the kth user $s_k(t)$ is the convolution of its transmitted signature waveform $f_k(t)$ and the channel impulse response $h_k(t)$ for user k:

$$s_k(t) = f_k(t) \otimes h_k(t), \tag{6.2}$$

where $f_k(t)$ is a normalized waveform which is non-zero in $[0, T]$. We can express the impulse response of a multipath fading channel as follows:

$$h_k(t) = \sum_{l=1}^{L} h_{kl} \delta(t - \tau_{kl}), \tag{6.3}$$

where L is the number of multiple paths, h_{kl} is the path gain and τ_{kl} is the path delay of the lth path of the kth user, $\delta(\cdot)$ is the Dirac delta function. The channel gain is normalized so that the signal power levels at the output and input of the channel are the same. That is,

$$\sum_{l=1}^{L} |h_{kl}|^2 = 1. \tag{6.4}$$

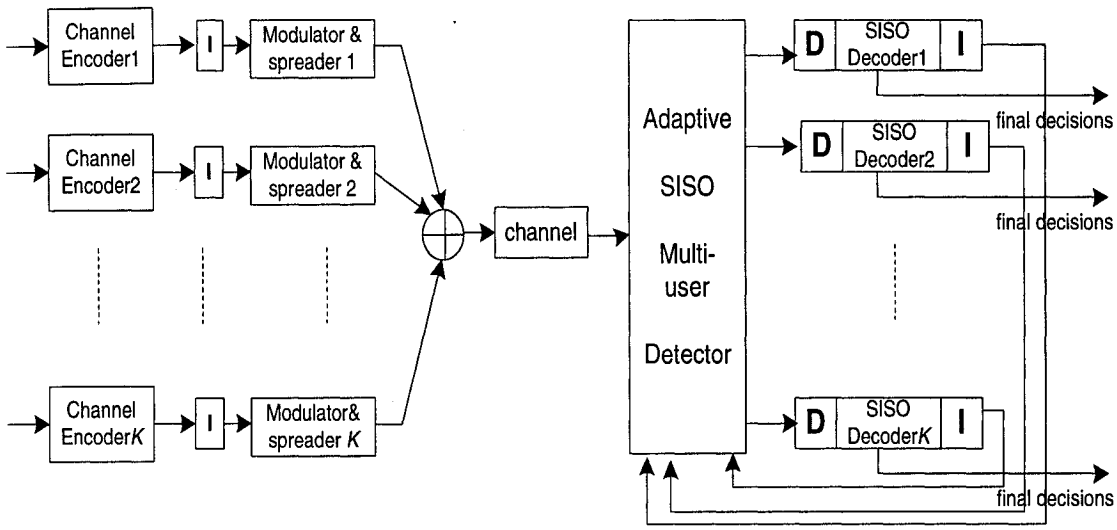

Figure 6.1: A general coded DS-CDMA system with an iterative and adaptive receiver (**I** and **D** denote interleavers and de-interleavers, respectively.)

The multiple path gains are assumed to be time-invariant or very slowly time-varying in comparison to the convergence speed of the adaptive algorithm employed.

In this chapter, we first assume a synchronous DS-CDMA system over the AWGN channel in Section 6.3, where the equivalent baseband received signal is:

$$r(t) = \sum_{k=1}^{K} \sum_{i=1}^{N_b} b_k(i) s_k(t - iT) + n(t), \tag{6.5}$$

and $s_k(t) = f_k(t)$. We will consider asynchronous DS-CDMA systems in Section 6.4. In the receiver, we employ a chip-matched filter which is matched to the chip waveform on the received signal $r(t)$ and sample its output at the rate f_s, where $f_s = p/T_c$, p is an integer and T_c is the chip duration. Thus, the fractionally chip-spaced output vector $\mathbf{r}$ during one symbol interval has the size of $N_s \times 1$ ($N_s = p \cdot N$, N is the spreading gain) and can be expressed by the equivalent discrete-time signals:

$$\mathbf{r} = \mathbf{S} \cdot \mathbf{b} + \mathbf{n} = \mathbf{s}_k b_k + \mathbf{S}^{(K/k)} \mathbf{b}^{(K/k)} + \mathbf{n}, \tag{6.6}$$

where

$$\mathbf{S} = [\mathbf{s}_1 \mathbf{s}_2 \cdots \mathbf{s}_K]_{N_s \times K}, \tag{6.7}$$

$$\mathbf{S}^{(K/k)} = [\mathbf{s}_1 \cdots \mathbf{s}_{k-1} \mathbf{s}_{k+1} \cdots \mathbf{s}_K]_{N_s \times (K-1)}, \tag{6.8}$$

$$\mathbf{b} = [b_1 b_2 \cdots b_K]^T, \tag{6.9}$$

$$\mathbf{b}^{(K/k)} = [b_1 \cdots b_{k-1} b_{k+1} \cdots b_K]^T. \tag{6.10}$$

The kth user's signature vector $\mathbf{s}_k$ is a column vector with size $N_s \times 1$ and $\mathbf{n}$ is a complex Gaussian noise vector with zero mean and covariance matrix:

$$\mathbf{R}_n = E[\mathbf{n} \cdot \mathbf{n}^H] = \sigma_n^2 \mathbf{I}_{N_s \times N_s}, \tag{6.11}$$

where σ_n^2 is the variance of each complex Gaussian random variable and $\mathbf{I}$ is the identity matrix.

6.3 SISO Parallel Decision Feedback Detectors (PDFDs) for Synchronous DS-CDMA Systems over AWGN Channels

In this section, we first derive the optimum feedforward and feedback filters of a SISO parallel decision feedback detector for synchronous DS-CDMA multiuser systems over the AWGN channel in Subsection 6.3.1. We use the soft symbol estimates, obtained from a bank of single user decoders, as the fedback decisions in the derivation of these optimum filters. Furthermore, the resulting SISO PDFD can be proven to be the same as the linear SISO MMSE detector. However, the SISO PDFD is preferable in some cases since it can be implemented adaptively even when some system parameters, such as transmitted signatures and relative delays of users and/or the multipath fading channel coefficients, are not available in the receiver. Then, we propose two adaptive SISO PDFDs based on the normalized least mean square and recursive least squares algorithms in Subsection 6.3.2. All users employ randomly selected short spreading sequences, which are unknown to the receiver. A training sequence is required for each user. Finally, Monte-Carlo simulation results of these two adaptive detectors are presented and compared in Subsection 6.3.3.

6.3.1 Non-Adaptive Optimum SISO PDFDs

As we have described in Subsection 5.3.1, for a SISO multiuser detector, it has soft inputs $\{\lambda_{in}(b_k), 1 \leq k \leq K\}$ which are extrinsic log-likelihood ratios provided by a bank of single user decoders of K users. Based on these soft inputs, we can obtain the a priori information of coded symbols which is indicated by (5.31), (5.32) and (5.34) for user k and is repeated in the following:

$$E[b_k] = 0, \tag{6.12}$$

$$E[b_j|\lambda_{in}(b_j)] = \hat{b}_j = \tanh\left(\frac{\lambda_{in}(b_j)}{2}\right), \quad j \neq k, 1 \leq j \leq K, \tag{6.13}$$

$$E[b_i^2] = 1, \quad 1 \leq i \leq K. \tag{6.14}$$

The value $\hat{b}_j$ obtained in (6.13) is called the soft symbol estimate. Equation (6.14) is due to our BPSK modulation assumption. We also assume that different users' coded symbols are independent of one another. That is,

$$E[b_i \cdot b_j | \lambda_{in}(b_i), \lambda_{in}(b_j)] = E[b_i | \lambda_{in}(b_i)] \cdot E[b_j | \lambda_{in}(b_j)], \quad i \neq j. \tag{6.15}$$

For synchronous systems over AWGN channels, the receiver can focus on one symbol duration since there is no ISI. In the parallel decision feedback detector, we use $N_s \times 1$ column vector $\mathbf{m}_{fk}$ and $(K\text{-}1)\times 1$ column vector $\mathbf{m}_{bk}$ to denote the feedforward and feedback filter of user k, respectively. The output of the parallel decision feedback detector of user k is:

$$x_k^{PDFD} = \mathbf{m}_{fk}^H \cdot \mathbf{r} + \mathbf{m}_{bk}^H \cdot \hat{\mathbf{b}}^{(K/k)}, \tag{6.16}$$

where $\hat{\mathbf{b}}^{(K/k)}$ is a vector consisting of the soft symbol estimates of $(K\text{-}1)$ interfering users in the interested cell. The optimum feedforward and feedback filters are derived based on the following MMSE criterion:

$$\min_{\mathbf{m}_{fk},\mathbf{m}_{bk}} E[b_k - x_k^{PDFD}]^2 = \min_{\mathbf{m}_{fk},\mathbf{m}_{bk}} E\left[b_k - \mathbf{m}_{fk}^H \cdot \mathbf{r} - \mathbf{m}_{bk}^H \cdot \hat{\mathbf{b}}^{(K/k)}\right]^2. \tag{6.17}$$

In order to obtain the solution of (6.17), we construct two larger matrices $\mathbf{m}_{dfdk}$ and $\mathbf{r}_{dfdk}$ as follows:

$$\mathbf{m}_{dfdk} = \begin{pmatrix} \mathbf{m}_{fk} \\ \mathbf{m}_{bk} \end{pmatrix}, \tag{6.18}$$

$$\mathbf{r}_{dfdk} = \begin{pmatrix} \mathbf{r} \\ \\ \hat{\mathbf{b}}^{(K/k)} \end{pmatrix}. \tag{6.19}$$

Thus, the MMSE criterion in (6.17) is equal to:

$$\min_{\mathbf{m}_{fk},\mathbf{m}_{bk}} E[b_k - \mathbf{m}_{dfdk}^H \cdot \mathbf{r}_{dfdk}]^2. \tag{6.20}$$

In order to have simple notations, we give the following definitions:

$$\mathbf{R}_k = \mathbf{s}_k \mathbf{s}_k^H, \tag{6.21}$$

$$\mathbf{R}_{(K/k)} = \mathbf{S}^{(K/k)}\left[\mathbf{I} - \mathrm{diag}(\hat{\mathbf{b}}^{(K/k)}\hat{\mathbf{b}}^{(K/k)H})\right]\mathbf{S}^{(K/k)H}. \tag{6.22}$$

The covariance matrix of $\mathbf{r}_{dfdk}$ is:

$$\begin{aligned}\mathbf{R}_{rdfd} &= E\left(\mathbf{r}_{dfdk} \cdot \mathbf{r}_{dfdk}^H\right) \\ &= \begin{pmatrix} E[\mathbf{r} \cdot \mathbf{r}^H] & E\left[\mathbf{r} \cdot \hat{\mathbf{b}}^{(K/k)H}\right] \\ E\left[\hat{\mathbf{b}}^{(K/k)} \cdot \mathbf{r}^H\right] & E\left[\hat{\mathbf{b}}^{(K/k)} \cdot \hat{\mathbf{b}}^{(K/k)H}\right] \end{pmatrix} \\ &= \begin{pmatrix} \left(\mathbf{R}_k + \mathbf{S}^{(K/k)} E\left[\mathbf{b}^{(K/k)}\mathbf{b}^{(K/k)H}\right]\mathbf{S}^{(K/k)H} + \sigma_n^2\mathbf{I}\right) & \mathbf{S}^{(K/k)}\hat{\mathbf{b}}^{(K/k)}\hat{\mathbf{b}}^{(K/k)H} \\ \hat{\mathbf{b}}^{(K/k)}\hat{\mathbf{b}}^{(K/k)H}\mathbf{S}^{(K/k)H} & \hat{\mathbf{b}}^{(K/k)}\hat{\mathbf{b}}^{(K/k)H} \end{pmatrix}.\end{aligned} \tag{6.23}$$

The cross correlation between $\mathbf{r}_{dfdk}$ and b_k is:

$$\mathbf{p}_{dfdk} = E[\mathbf{r}_{dfdk} \cdot b_k] = \begin{pmatrix} \mathbf{s}_k \\ \mathbf{0}_{(K-1)\times 1} \end{pmatrix}. \tag{6.24}$$

The Wiener-Hopf equation for the MMSE criterion in (6.20) is:

$$\mathbf{R}_{rdfd} \cdot \mathbf{m}_{dfdk} = \mathbf{p}_{dfdk}. \tag{6.25}$$

Substitute (6.18), (6.24) and (6.24) in (6.25), we have the following optimum solutions for the feedforward and feedback filters:

$$\mathbf{m}_{fk} = (\mathbf{R}_k + \mathbf{R}_{(K/k)} + \sigma_n^2\mathbf{I})^{-1} \cdot \mathbf{s}_k, \tag{6.26}$$

$$\mathbf{m}_{bk} = -\mathbf{S}^{(K/k)H} \cdot \mathbf{m}_{fk}. \tag{6.27}$$

From (6.26), we can see that the feedforward filter in the SISO PDFD suppresses the residual interference due to imperfect cancellation provided by the feedback filter and the background Gaussian noise. The output of the parallel decision feedback detector of user k is:

$$\begin{aligned} x_k^{PDFD} &= \mathbf{m}_{fk}^H \cdot \mathbf{r} + \mathbf{m}_{bk}^H \cdot \hat{\mathbf{b}}^{(K/k)} \\ &= \mathbf{m}_{fk}^H \cdot \mathbf{r} - \mathbf{m}_{fk}^H \cdot \mathbf{S}^{(K/k)} \hat{\mathbf{b}}^{(K/k)}. \end{aligned} \tag{6.28}$$

For the comparison purpose, we present the linear SISO MMSE multiuser detector in the following. By using the same a priori information of coded symbols (6.12) – (6.15) as those used in the SISO parallel decision feedback detector, we derive the optimum linear MMSE filter $\mathbf{m}_k$ with the size of $N_s \times 1$, which is applied on the received signal vector $\mathbf{r}$ directly and satisfies the following MMSE criterion:

$$\min_{\mathbf{m}_k} E\Big[b_k - \mathbf{m}_k^H \cdot (\mathbf{r} - E[\mathbf{r}]_k)\Big]^2, \tag{6.29}$$

where introducing $E[\mathbf{r}]_k$ is to obtain an unbiased MMSE estimate.

$$\begin{aligned} E[\mathbf{r}]_k &= E[\mathbf{s}_k b_k + \mathbf{S}^{(K/k)} \mathbf{b}^{(K/k)} + \mathbf{n}] \\ &= \mathbf{S}^{(K/k)} \hat{\mathbf{b}}^{(K/k)} \end{aligned} \tag{6.30}$$

Applying the Wiener-Hopf solutions to (6.29), the optimum MMSE filter $\mathbf{m}_k$ is:

$$\mathbf{m}_k = \mathbf{R}_r^{-1} \cdot \mathbf{p}_k. \tag{6.31}$$

In the following, $\mathbf{R}_r$ and $\mathbf{p}_k$ are calculated based on the a priori information of coded symbols (6.12) – (6.15).

$$\begin{aligned} \mathbf{R}_r &= E\Big[(\mathbf{r} - E(\mathbf{r})_k) \cdot (\mathbf{r} - E(\mathbf{r})_k)^H\Big] \\ &= E[\mathbf{r} \cdot \mathbf{r}^H] - E[\mathbf{r}]_k \cdot E[\mathbf{r}]_k^H, \end{aligned} \tag{6.32}$$

where

$$E[\mathbf{r}\cdot\mathbf{r}^H] = \mathbf{s}_k\mathbf{s}_k^H + \mathbf{S}^{(K/k)}E[\mathbf{b}^{(K/k)}\mathbf{b}^{(K/k)H}]\mathbf{S}^{(K/k)H} + \sigma_n^2\mathbf{I}, \tag{6.33}$$

$$E[\mathbf{b}^{(K/k)}\mathbf{b}^{(K/k)H}] = \mathbf{I}_{(K-1)\times(K-1)} + \hat{\mathbf{b}}^{(K/k)}\hat{\mathbf{b}}^{(K/k)H} - \mathrm{diag}(\hat{\mathbf{b}}^{(K/k)}\hat{\mathbf{b}}^{(K/k)H}), \tag{6.34}$$

$$E[\mathbf{r}]_k\cdot E[\mathbf{r}]_k^H = \mathbf{S}^{(K/k)}\hat{\mathbf{b}}^{(K/k)}\hat{\mathbf{b}}^{(K/k)H}\mathbf{S}^{(K/k)H}. \tag{6.35}$$

Therefore,

$$\begin{aligned}\mathbf{R}_r &= \mathbf{s}_k\mathbf{s}_k^H + \mathbf{S}^{(K/k)}[\mathbf{I} - \mathrm{diag}(\hat{\mathbf{b}}^{(K/k)}\hat{\mathbf{b}}^{(K/k)H})]\mathbf{S}^{(K/k)H} + \sigma_n^2\mathbf{I} \\ &= (\mathbf{R}_k + \mathbf{R}_{(K/k)} + \sigma_n^2\mathbf{I})^{-1},\end{aligned} \tag{6.36}$$

$$\mathbf{p}_k = E[\mathbf{r}\cdot b_k] = \mathbf{s}_k, \tag{6.37}$$

where in (6.36), we use the notations (6.21) and (6.22). Substitute (6.36) and (6.37) into (6.31), we obtain the optimum MMSE filter $\mathbf{m}_k$ for user k:

$$\mathbf{m}_k = \mathbf{R}_r^{-1}\cdot\mathbf{p}_k = (\mathbf{R}_k + \mathbf{R}_{(K/k)} + \sigma_n^2\mathbf{I})^{-1}\mathbf{s}_k. \tag{6.38}$$

The output of the MMSE filter is:

$$x_k^{MMSE} = \mathbf{m}_k^H\cdot[\mathbf{r} - E(\mathbf{r})_k] = \mathbf{m}_k^H\cdot\mathbf{r} - \mathbf{m}_k^H\cdot\mathbf{S}^{(K/k)}\hat{\mathbf{b}}^{(K/k)}. \tag{6.39}$$

By comparing (6.38) and (6.26), (6.39) and (6.28), we can see that the linear SISO MMSE multiuser detector and the SISO parallel decision feedback detector have exactly the same output. However, the implementation of these two types of detectors is different. In the linear SISO MMSE multiuser detector, we first cancel the soft interference for each user in the interested cell and then apply a linear MMSE filter on the output of soft interference cancellation to further suppress the residual MAI from the interfering users due to imperfect cancellation and the background Gaussian noise in the MMSE sense. However, soft interference cancellation needs the received signatures of interfering

users. Sometimes, we do not know the transmitted signatures of these users and/or the channel impulse response in the receiver. Thus, we cannot realize soft interference cancellation. On the other hand, for the SISO parallel decision feedback detector, if the received signatures of users are not available in the receiver, we can apply adaptive algorithms to update and obtain filter coefficients.

6.3.2 Adaptive SISO PDFDs

In this subsection, we assume that each user has a short spreading code, which is randomly selected and unknown to the receiver. Two adaptive algorithms, normalized LMS and RLS algorithms, are used in adaptive SISO parallel decision feedback detection to update the feedforward and feedback filters. Moreover, the a priori information of coded symbols is employed efficiently to improve the performance of the adaptive detector. The adaptive SISO PDFD only needs a training sequence for each user to estimate all the filter coefficients, and even does not know the background noise level.

The adaptive detector based on the normalized LMS algorithm for the MMSE criterion (6.17) updates the feedforward and feedback filters of user k as follows for m=0, 1, 2, ...:

$$\mathbf{m}_{fk}(m+1) = \mathbf{m}_{fk}(m) - \frac{\tilde{\mu}_f}{a + \|\mathbf{r}(m)\|^2} |\tilde{b}_k(m)| e_k^*(m) \mathbf{r}(m), \tag{6.40}$$

$$\mathbf{m}_{bk}(m+1) = \mathbf{m}_{bk}(m) - \frac{\tilde{\mu}_b}{a + \|\tilde{\mathbf{b}}^{(K/k)}(m)\|^2} |\tilde{b}_k(m)| e_k^*(m) \tilde{\mathbf{b}}^{(K/k)}(m), \tag{6.41}$$

where m is the recursive index and also the time index, $\tilde{\mu}_f$ and $\tilde{\mu}_b$ are $\in (0, 2)$ and are the step sizes for the feedforward and feedback filters, respectively. a is a small positive constant. The error signal in the mth recursion is:

$$e_k(m) = \tilde{b}_k(m) - \mathbf{m}_{fk}^H(m) \cdot \mathbf{r}(m) - \mathbf{m}_{bk}^H(m) \cdot \tilde{\mathbf{b}}^{(K/k)}(m), \tag{6.42}$$

where $\tilde{\mathbf{b}}^{(K/k)} = [\tilde{b}_1 \ldots \tilde{b}_{k-1}\tilde{b}_{k+1} \ldots \tilde{b}_K]^T$, $\{\tilde{b}_i(m) = b_i(m), 1 \leq i \leq K\}$ in the training mode and $\{\tilde{b}_i(m) = \hat{b}_i(m), 1 \leq i \leq K\}$ in the decision directed mode. $\hat{b}_i(m)$ is the soft symbol estimate of $b_i(m)$ in (6.13). In the decision directed mode, $|\hat{b}_k(m)|$ is used as the reliability of the error signal $e_k(m)$ in (6.40) and (6.41). Both filters are updated per symbol and their initial states are $\mathbf{m}_{fk}(0) = \mathbf{0}$ and $\mathbf{m}_{bk}(0) = \mathbf{0}$.

If the adaptive detector applies the RLS algorithm, we denote $\mathbf{w}_k(m) = [\mathbf{m}_{fk}^H(m)\ \mathbf{m}_{bk}^H(m)]^H$ and $\mathbf{u}(m) = [\mathbf{r}^H(m)\ \tilde{\mathbf{b}}^{(K/k)H}(m)]^H$. Then the feedforward and feedback filters of user k are updated for m=0, 1, 2, ...:

$$\mathbf{g}_k(m+1) = \frac{\lambda^{-1}\mathbf{P}_k(m)\mathbf{u}(m+1)}{1+\lambda^{-1}\mathbf{u}^H(m+1)\mathbf{P}_k(m)\mathbf{u}(m+1)}, \tag{6.43}$$

$$\xi_k(m+1) = \tilde{b}_k(m+1) - \mathbf{w}_k^H(m)\mathbf{u}(m+1), \tag{6.44}$$

$$\mathbf{w}_k(m+1) = \mathbf{w}_k(m) + \mathbf{g}_k(m+1)|\tilde{b}_k(m+1)|\xi_k^*(m+1), \tag{6.45}$$

$$\mathbf{P}_k(m+1) = \lambda^{-1}\mathbf{P}_k(m) - \lambda^{-1}\mathbf{g}_k(m+1)\mathbf{u}^H(m+1)\mathbf{P}_k(m). \tag{6.46}$$

The algorithm is initialized with $\mathbf{P}_k(0) = \delta^{-1}\mathbf{I}$, where δ is a small positive number and $\mathbf{w}_k(0) = \mathbf{0}$.

Both of the above two types of adaptive detectors try to exploit the joint statistics of the received signal vector $\mathbf{r}$, the transmitted symbol b_k or $\hat{b}_k$ and the fedback soft symbol estimates $\hat{\mathbf{b}}^{(K/k)}$. In the first iteration of the adaptive SISO PDFD, since there is no fedback information of coded symbols, we only employ a feedforward filter and set the feedback filter coefficients to zeros for each user.

The output of the adaptive SISO PDFD detector in the mth recursion is:

$$x_k^{PDFD}(m) = \mathbf{m}_{fk}^H(m) \cdot \mathbf{r}(m) + \mathbf{m}_{bk}^H(m) \cdot \hat{\mathbf{b}}^{(K/k)}(m). \tag{6.47}$$

By Gaussian assumption for the output in (6.47), we can calculate the soft output for each symbol of each user. For the mth symbol of the kth user, the output $x_k^{PDFD}(m)$ can be written as:

$$x_k^{PDFD}(m) = \mu_k b_k(m) + \eta_k, \tag{6.48}$$

where μ_k is a constant and η_k is a Gaussian random variable with zero mean and variance $\sigma_{\eta_k}^2$.

$$\mu_k = E[b_k^*(m) x_k^{PDFD}(m)] \tag{6.49}$$

$$\sigma_{\eta_k}^2 = E[x_k^{PDFD}(m) - \mu_k b_k(m)]^2 \tag{6.50}$$

Estimates of μ_k and $\sigma_{\eta_k}^2$ can be obtained by the corresponding sample averages in (6.51) and (6.52) respectively, where we replace $b_k(m)$ by $\tilde{b}_k(m)$ in (6.49) and (6.50).

$$\hat{\mu}_k = \frac{1}{N_b} \sum_{m=1}^{N_b} \tilde{b}_k^*(m) x_k^{PDFD}(m) \tag{6.51}$$

$$\hat{\sigma}_{\eta_k}^2 = \frac{1}{N_b} \sum_{m=1}^{N_b} [x_k^{PDFD}(m) - \hat{\mu}_k \tilde{b}_k(m)]^2 \tag{6.52}$$

Therefore, the soft output, i.e. the extrinsic log-likelihood ratio, of each symbol of each user is:

$$\lambda_k^a(m) = \log \frac{P[x_k^{PDFD}(m) | b_k(m) = +1]}{P[x_k^{PDFD}(m) | b_k(m) = -1]} = \frac{2\mu_k x_k^{PDFD}(m)}{\sigma_{\eta_k}^2}. \tag{6.53}$$

6.3.3 Simulation Results

For adaptive detectors, we cannot obtain closed analytic expressions for bit error probabilities of multiple users. Therefore, the bit error rate performance is generally obtained and evaluated by Monte-Carlo simulations. The single-cell DS-CDMA system which we simulate in this subsection has 12 active users. Each user has a randomly selected short spreading code, which is unknown to the receiver. All users employ the same rate

1/2 convolutional codes with constraint length 7 and the following generators [1011011], [1111001]. The spreading code for each coded bit contains 8 chips. Therefore, the spreading factor is 16 chips per information bit. The system load is 12/16 (K/N).

Each information bit frame of each user consists of 200 information bits. After being coded and modulated, each coded symbol frame has 400 coded symbols. There are 200 training symbols inserted at the beginning of each coded symbol frame of each user. Training symbols are randomly selected for each frame of each user.

Iterative SISO single user decoders are based on the log-MAP algorithm in [Hag96]. Different users have different constant block interleavers which are randomly selected. Ten iterations are implemented in the receiver. In the first iteration, since there is no soft inputs of the detector coming from single user decoders, only a feedforward filter is employed by each user. That is, at this time, a linear minimum mean square error filter is used instead. It is initially trained by the training symbols, then is used for the following transmitted coded symbols. In the later iterations, both the feedforward and feedback filters are employed. After the training mode, they are updated by fedback symbol decisions. After each iteration, the filter coefficients are reset as zeros.

For a single-cell synchronous DS-CDMA system over the AWGN channel, an adaptive SISO PDFD based on the NLMS algorithm is employed in the receiver. We use $a = 0.0001$ and step sizes $\tilde{\mu}_f = \tilde{\mu}_b = 0.2$ in the training mode, $\tilde{\mu}_f = \tilde{\mu}_b = 0.05$ in the decision directed mode. We first assume that all users have equal received power. Without loss of generality, the bit error rate performance of the first user is shown in Fig. 6.2 and compared with that of the single user system where the receiver knows this single user's spreading code. We can see that the performance of the adaptive receiver approaches to that of the single user system with the increased number of iterations and increased

signal-to-noise ratios as well.

In order to analyze the convergence property of the NLMS algorithm in the adaptive SISO PDFD, we show the averaged squared errors $e_k^2(m)$ in different iterations of the detector versus the number of updates in the adaptive algorithm in Fig. 6.3. We set the SNR of each user to 5dB. Each curve of the squared error is averaged over 100 independent trials of the experiment. In the first iteration, the feedforward filter is updated only by training symbols. For the later iterations, after the training mode, the feedforward and feedback filters are updated by fedback decisions. In Fig. 6.3, during the decision directed mode the squared error enters into a stable status. Moreover, the squared error in the tenth iteration has a smaller variance than that in the second iteration, which confirms the simulation result in Fig. 6.2.

Now we consider near-far resistance of the adaptive SISO PDFD based on the NLMS algorithm. Here we assume that six users have 3dB more received power than other six users. Other system parameters remain. The bit error rate performances of both higher power users and lower power users are shown in Fig. 6.4. Obviously, higher power users have a little better performance than the users with the lower power. Furthermore, by comparing this figure with Fig. 6.2, we can see that bit error rates of equi-power users lie in between those of higher power users and lower power ones. The reason may be explained as follows. Compared with each lower power user, each higher power user has one more lower power interfering user and one less higher power interfering user. This improves or degrades the convergence performance of the adaptive filters for higher power users or lower power users, respectively. Nevertheless, the bit error rate performances of both higher power users and lower power users approach to that of the single user system with additional iterations when their SNRs are increased. Therefore, our adaptive SISO PDFD has good near-far resistance for both weak users and strong users.

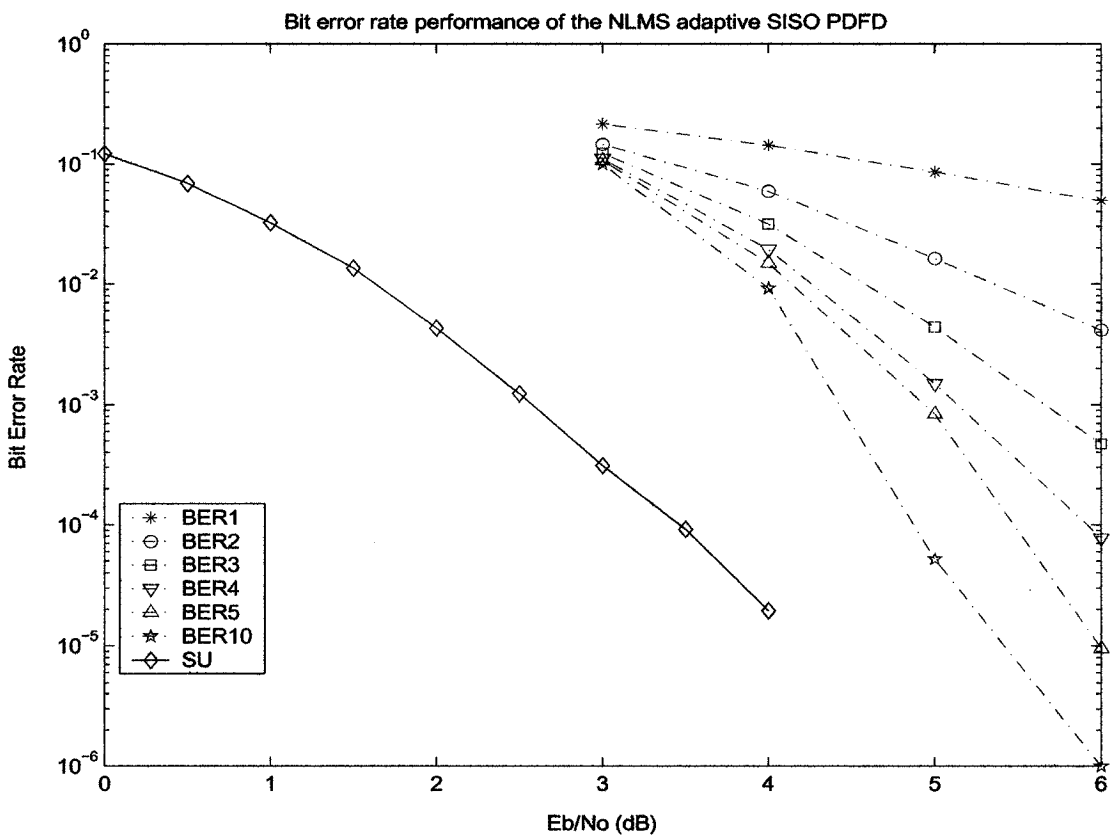

Figure 6.2: Comparison of the bit error rates in the first five iterations (BER1-BER5) as well as the tenth iteration (BER10) of the NLMS adaptive SISO PDFD for the synchronous DS-CDMA system and that of the single user system (SU) over the AWGN channel.

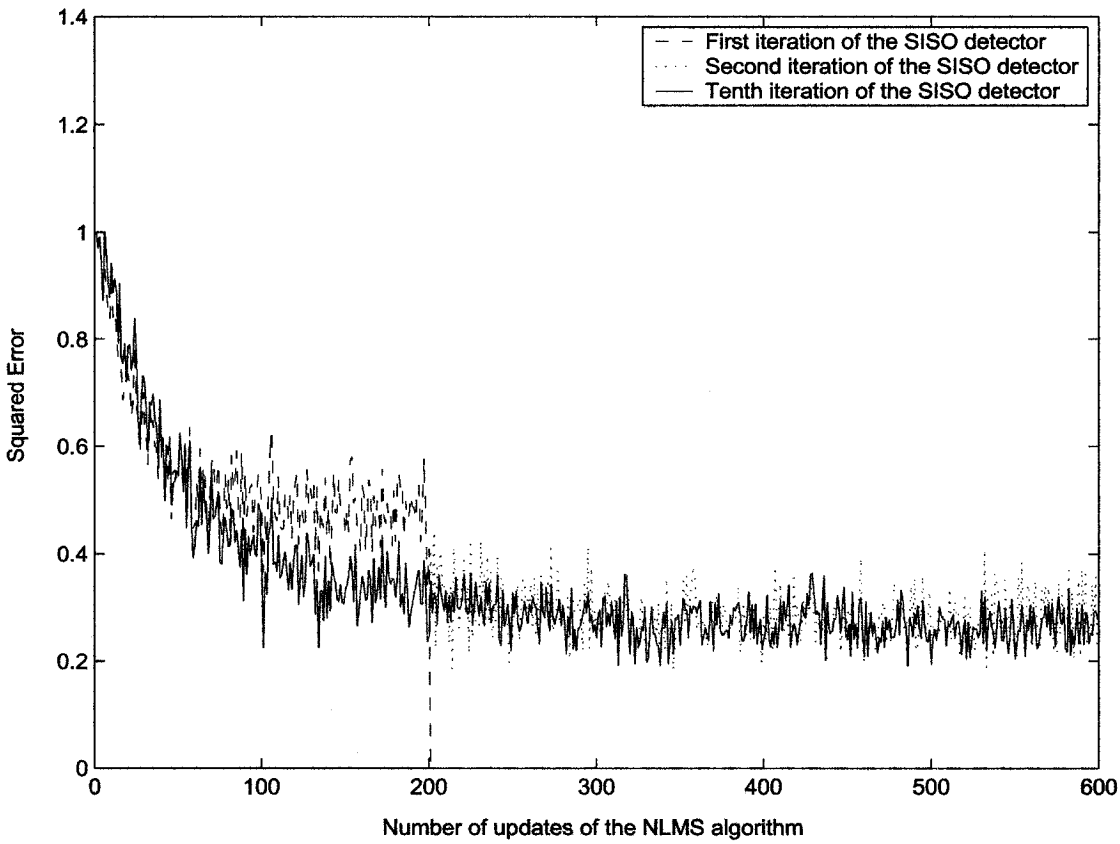

Figure 6.3: Experimental learning curves of the adaptive SISO PDFD based on the NLMS algorithm in the different iterations at SNR=5dB, for the synchronous DS-CDMA system over the AWGN channel.

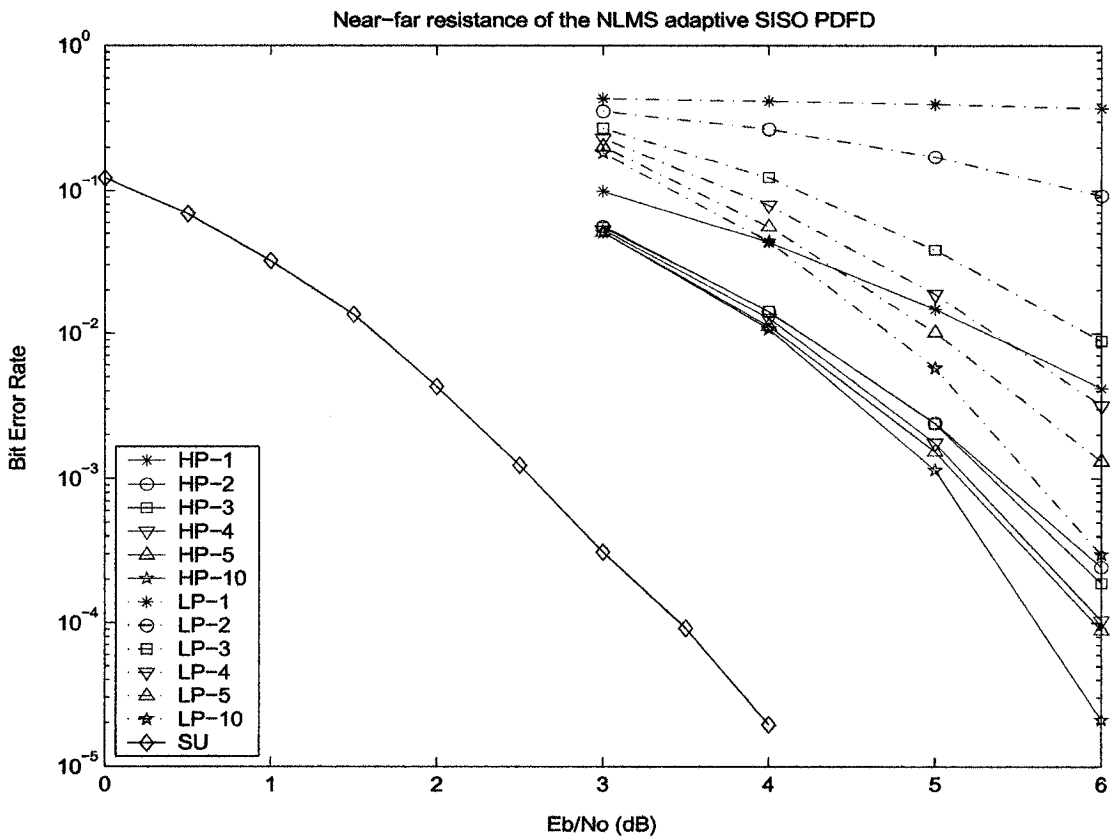

Figure 6.4: The adaptive SISO PDFD based on the NLMS algorithm in a near-far scenario. Comparison of the bit error rates of higher power users in the first five iterations (HP-1 – HP-5), the tenth iteration (HP-10) and those of lower power users (LP-1 – LP-5, LP-10), and that of the single user system (SU). System parameters: six users have 3dB more energy than other six users, synchronous DS-CDMA systems over AWGN channels.

Under the same simulation scenarios as the above (i.e. for the adaptive detector based on the NLMS algorithm), we replace the NLMS algorithm by the RLS algorithm. We employ parameters: $\lambda = 1$ and $\delta = 0.04$. When all users have the same received power, the bit error rates of the first user in the different iterations are shown in Fig. 6.5 and compared with those obtained by the NLMS algorithm in Fig. 6.2. We can see that the bit error rate performance obtained by the adaptive SISO PDFD based on the RLS algorithm is better than that obtained by the adaptive detector based on the NLMS algorithm and converges more quickly to that of the single user system.

The averaged squared errors of the a priori estimation error $\xi^2(m)$ in different iterations of the detector versus the number of updates in the RLS algorithm are shown in Fig. 6.6 and compared in Fig. 6.7 with those of the NLMS algorithm. The SNR of each user is 5dB. These learning curves show that the RLS algorithm has a faster convergence speed than the NLMS algorithm. Furthermore, after about 100 updates, the RLS algorithm has already converged. Therefore, we can reduce the length of the training sequence for each user from 200 symbols to 100 symbols. The bit error rate performance based on the RLS algorithm using 100 training symbols for each user per frame is shown in Fig. 6.8.

The performance of the RLS adaptive SISO PDFD in a near-far scenario is presented in Fig. 6.9. With the increased number of iterations in the receiver, lower power users have a little better bit error rate performance than those of higher power users. Compared with the near-far resistance of the NLMS adaptive detector in Fig. 6.4, this figure shows that the RLS adaptive detector has a little better near-far resistance for weak users.

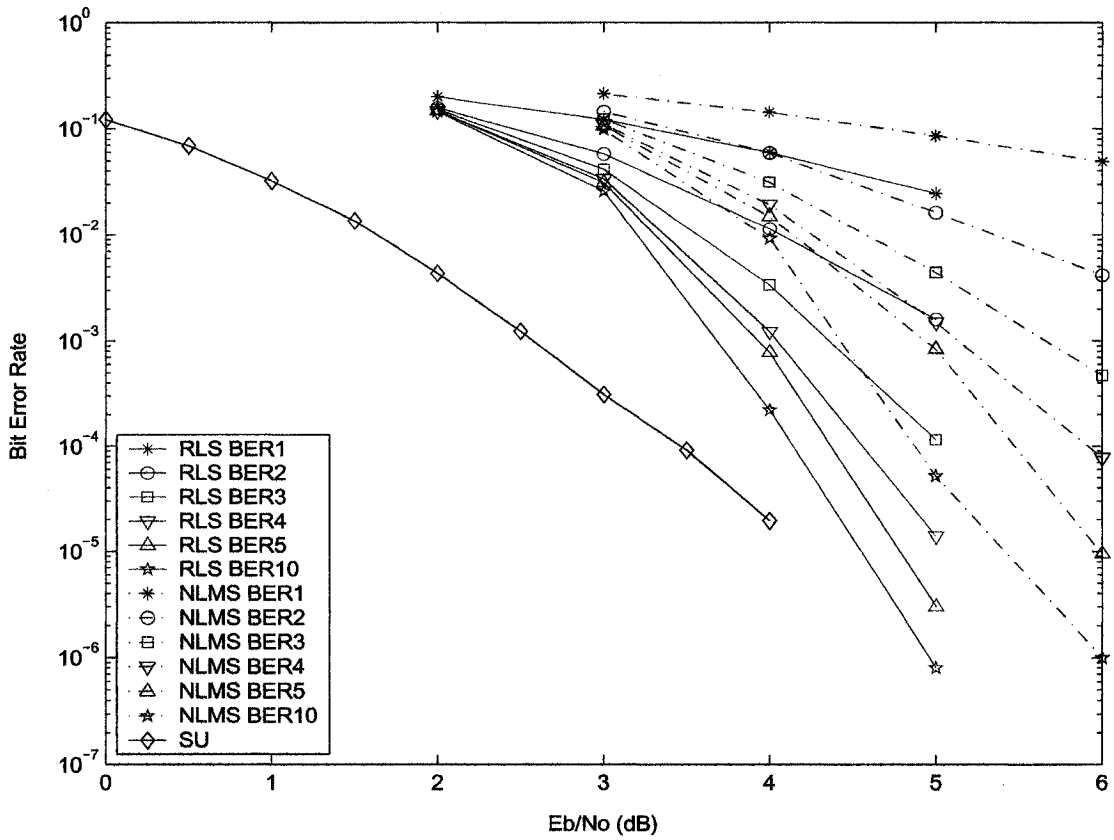

Figure 6.5: Comparison of the bit error rates in the first five iterations (NLMS BER1 - NLMS BER5) as well as the tenth iteration (NLMS BER10) of the normalized LMS adaptive SISO PDFD, those of the RLS adaptive SISO PDFD (RLS BER1 - RLS BER5, RLS BER10) for the synchronous DS-CDMA system and that of the single user system (SU) over the AWGN channel.

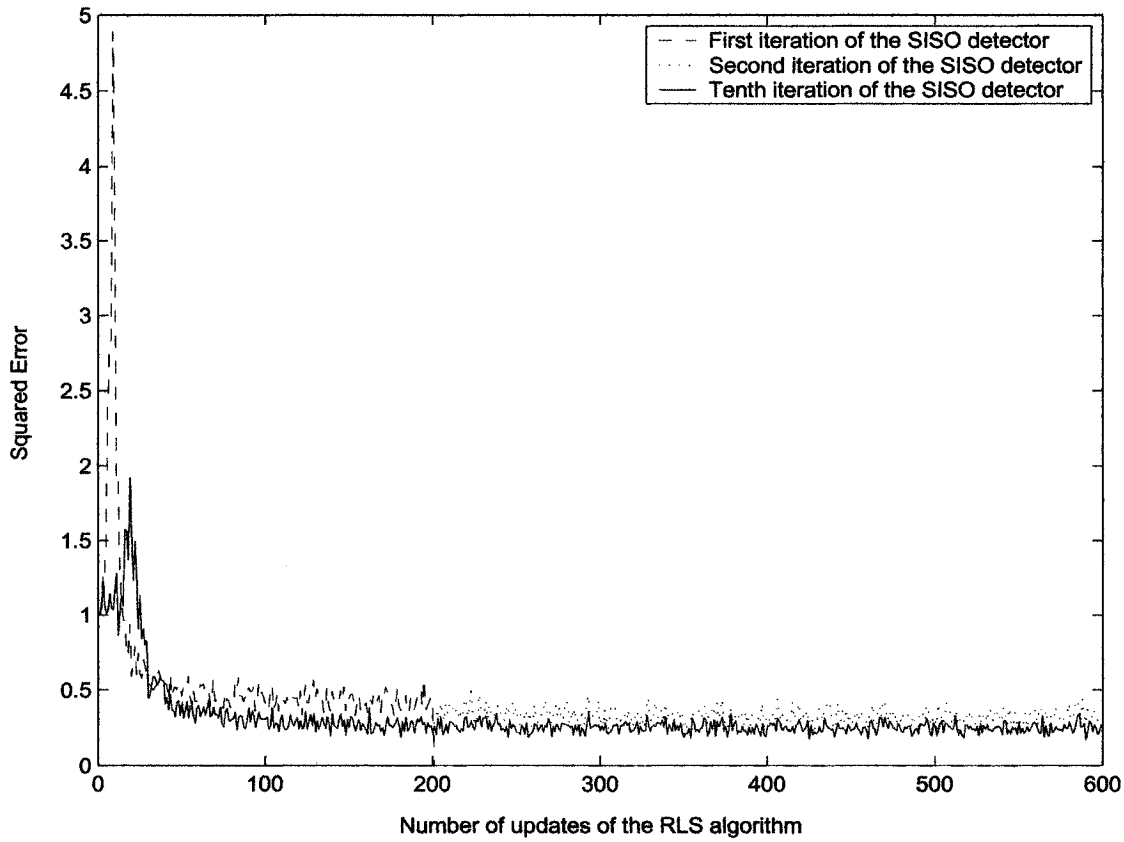

Figure 6.6: Experimental learning curves of the adaptive SISO PDFD based on the RLS algorithm in the different iterations at SNR = 5dB, for the synchronous DS-CDMA system over the AWGN channel.

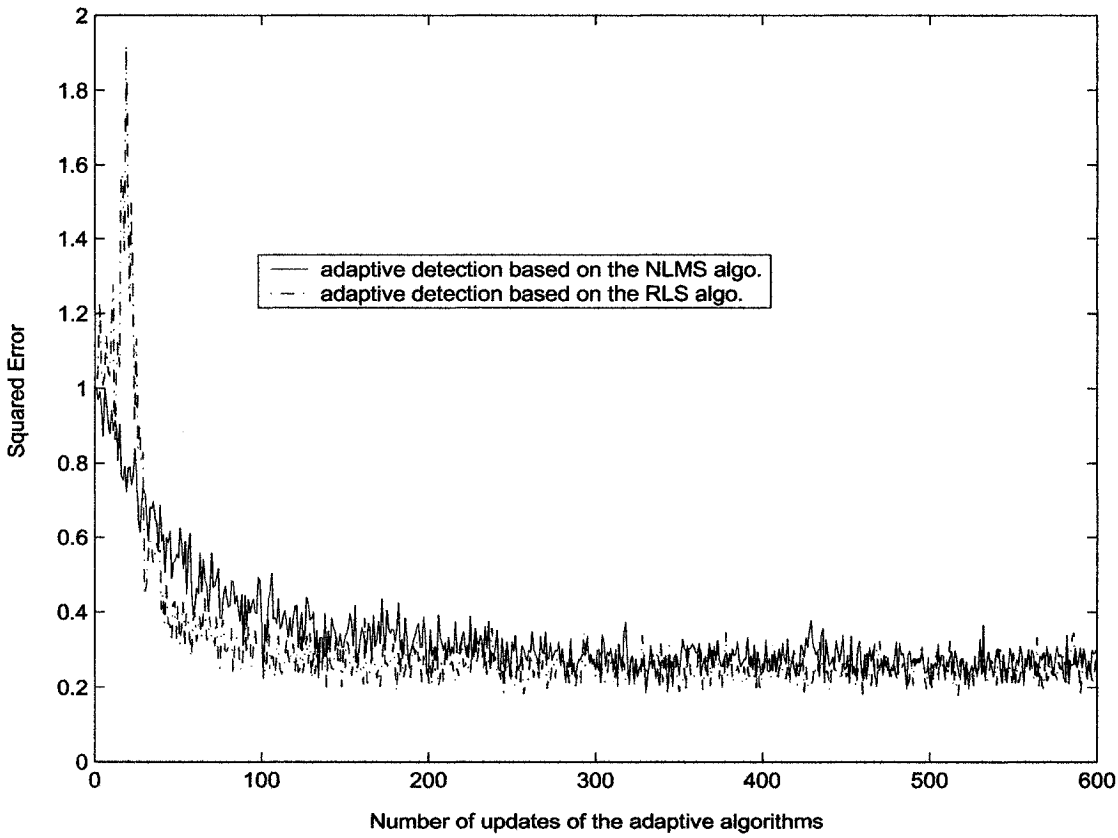

Figure 6.7: Comparison between the experimental learning curve of the adaptive SISO PDFD based on the NLMS algorithm and that of the adaptive detector based on the RLS algorithm in the fifth iteration at SNR = 5dB, for the synchronous DS-CDMA system over the AWGN channel.

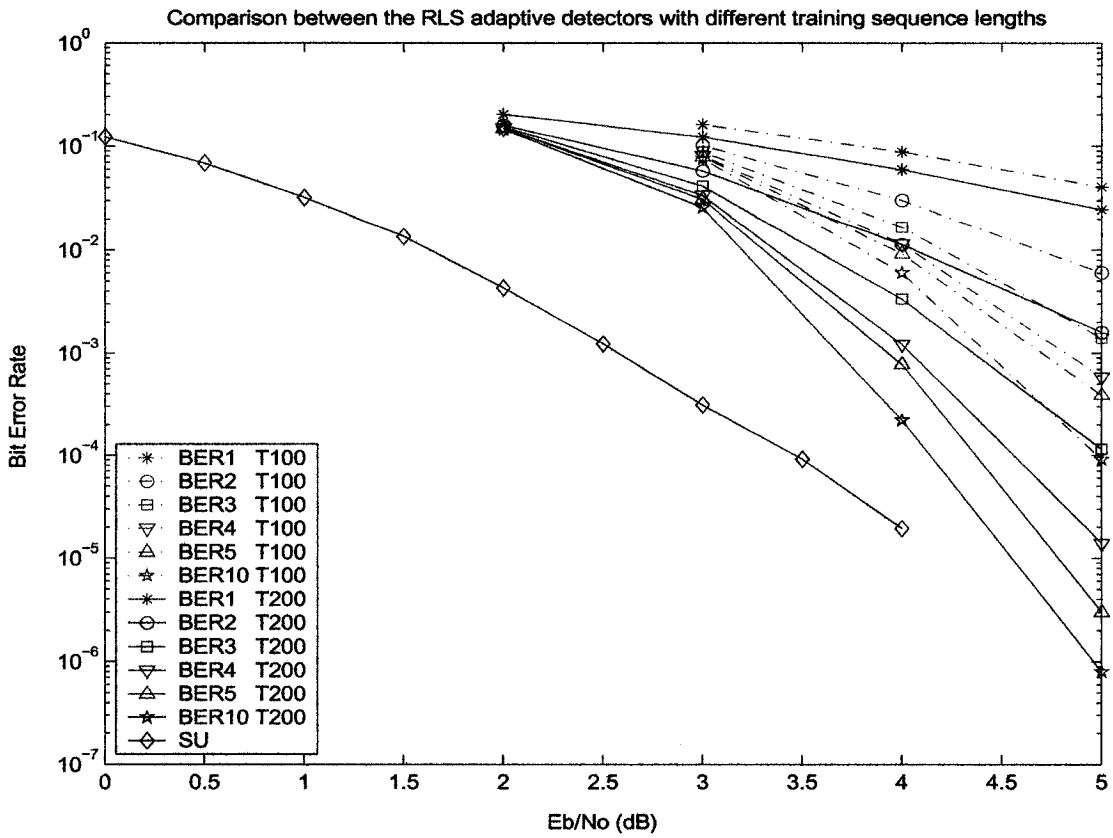

Figure 6.8: Comparison of the bit error rates in the first five iterations as well as the tenth iteration of the adaptive SISO PDFD based on the RLS algorithm with 100 training symbols (BER1 T100 – BER5 T100, BER10 T100), 200 training symbols (BER1 T200 – BER5 T200, BER10 T200) and that of the single user system (SU), for the synchronous DS-CDMA system over the AWGN channel.

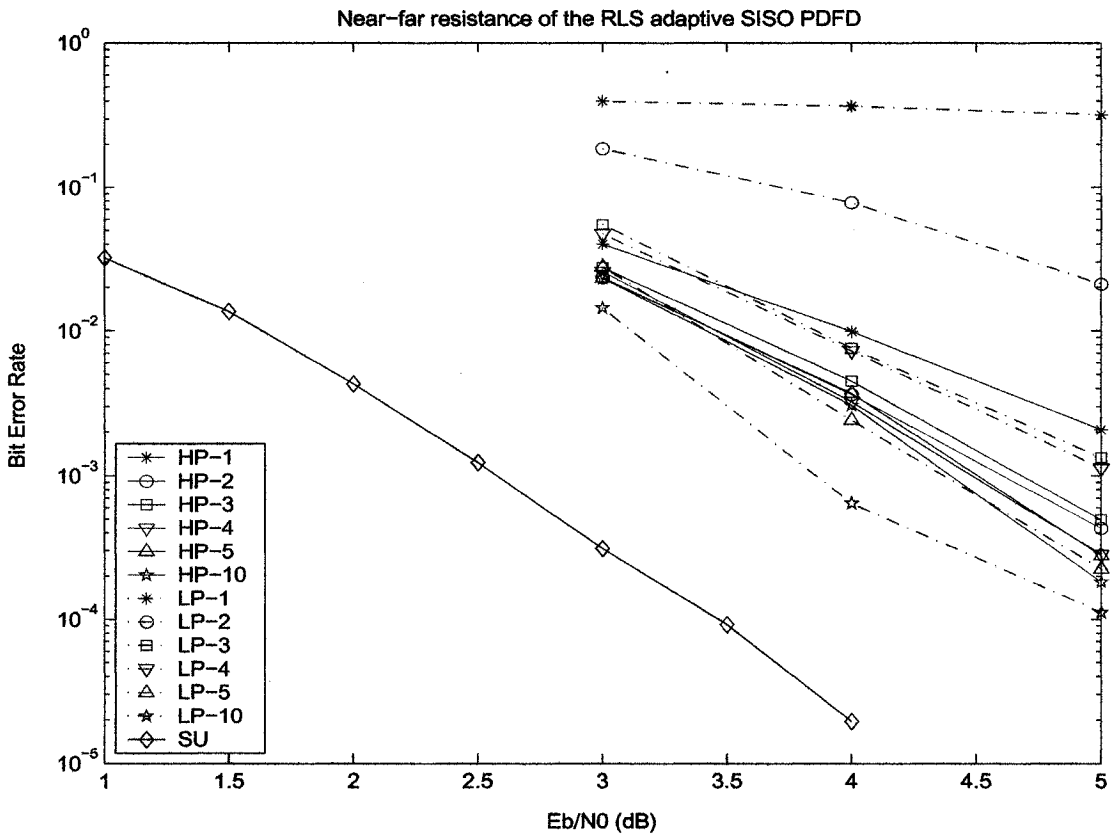

Figure 6.9: The adaptive SISO PDFD based on the RLS algorithm in a near-far scenario. Comparison of the bit error rates of higher power users in the first five iterations (HP-1 – HP-5), the tenth iteration (HP-10), those of lower power users (LP-1 – LP-5, LP-10) and that of the single user system (SU). System parameters: six users have 3dB more energy than other six users, synchronous DS-CDMA systems over AWGN channels.

Based on these simulation results, we can see that the adaptive SISO PDFD based on the RLS algorithm has a better convergence performance than the adaptive detector based on the NLMS algorithm. Therefore, the RLS adaptive detector has a better bit error rate performance than the NLMS adaptive detector and requires fewer training symbols. However, the RLS algorithm has more computational complexity. Denote the length of the adaptive filter as L. The computational complexity of the RLS and the NLMS algorithms are $\sim O(L^2)$ and $\sim O(L)$ per update, respectively. By the simulation results in this subsection, we show that the performance of the adaptive SISO PDFD based on either the NLMS or RLS algorithm approaches to that of the single user system with the increased number of iterations and input SNRs as well. Furthermore, both detectors are near-far resistant.

6.4 SISO PDFDs for Asynchronous DS-CDMA Systems over AWGN Channels

In this section, we first describe an asynchronous DS-CDMA system model and derive the non-adaptive optimum SISO PDFDs in Subsection 6.4.1. Then the adaptive SISO PDFDs in Subsection 6.3.2 are modified for asynchronous DS-CDMA multiuser systems. Here, the focus is on how to select practical finite-length feedforward and feedback filters to obtain good tradeoff between the performance and computational complexity of the receiver. Multiple users' transmitted waveforms and relative delays are unknown to the receiver. We propose three adaptive SISO PDFDs for this case in Subsection 6.4.2, which have the same feedforward filter length and different feedback filter lengths. Based on the Monte-Carlo simulation results shown in Subsection 6.4.3, we will see that the adaptive detector with more feedback filter taps provides us a better bit error rate performance, which approaches to that of the single user system more quickly with additional iteraitons and increased signal-to-noise ratios. However, the detector with more feedback filter taps

has an increased computational complexity.

6.4.1 Non-Adaptive Optimum SISO PDFDs

In general, the optimum SISO PDFD filters for asynchronous DS-CDMA systems have infinite lengths [Hal95]. For implementation purposes, we only consider the finite-length feedforward and feedback filters. Furthermore, these filters are especially suitable for use in adaptive applications, which will be discussed in Subsection 6.4.2.

The equivalent baseband received signal in a single-cell is expressed in (6.1) and the received signal waveform $s_k(t)$ of user k is the same as the transmitted one, i.e. $s_k(t) = f_k(t)$. For simple implementation, we consider a chip-synchronous and symbol-asynchronous DS-CDMA system. All users' delays are uniformly distributed in $[0, T]$ and are multiples of T_c, which is the chip interval. In the receiver, first we employ a chip-matched filter on the received signal $r(t)$ and then sample its output at frequency $1/T_c$. If the system is chip-asynchronous, we can oversample the output of the chip matched filter and design a fractionally spaced feedforward filter instead. Without loss of generality and for simplicity of notation, we assume the delays of multiple users satisfy the following inequality:

$$0 \leq \tau_1 \leq \tau_2 \ldots \leq \tau_K \leq T. \tag{6.54}$$

The symbol vector consisting of the transmitted symbols of all users is denoted as:

$$\boldsymbol{b} = [\mathbf{b}_1^T, \ldots, \mathbf{b}_k^T, \ldots, \mathbf{b}_K^T]^T_{KN_b \times 1}, \tag{6.55}$$

where

$$\mathbf{b}_k = [b_k(1), b_k(2), \ldots, b_k(N_b)]^T. \tag{6.56}$$

The received signal vector $\boldsymbol{r}$ at the output of the chip matched filter during the whole symbol transmission interval can be expressed as follows:

$$\boldsymbol{r} = \boldsymbol{S}\boldsymbol{b} + \boldsymbol{n}, \tag{6.57}$$

where $\boldsymbol{S}$ is the system signature matrix and can be expressed as:

$$\boldsymbol{S} = [\boldsymbol{S}_1, \ldots, \boldsymbol{S}_k, \ldots, \boldsymbol{S}_K]_{N(N_b+1)\times KN_b}. \tag{6.58}$$

The construction of $\boldsymbol{S}_k$ in (6.58) is shown in (6.59).

$$\boldsymbol{S}_k = \begin{pmatrix} \mathbf{0}_{1\times D_l} & (\mathbf{s}_k^T)_{1\times N} & \mathbf{0}_{1\times N} & \cdots & \mathbf{0}_{1\times N} & \mathbf{0}_{1\times D_r} \\ \mathbf{0}_{1\times D_l} & \mathbf{0}_{1\times N} & (\mathbf{s}_k^T)_{1\times N} & \ddots & \mathbf{0}_{1\times N} & \mathbf{0}_{1\times D_r} \\ \vdots & \vdots & \ddots & \ddots & \vdots & \vdots \\ \mathbf{0}_{1\times D_l} & \mathbf{0}_{1\times N} & \cdots & \mathbf{0}_{1\times N} & (\mathbf{s}_k^T)_{1\times N} & \mathbf{0}_{1\times D_r} \end{pmatrix}^T_{N(N_b+1)\times N_b}, \tag{6.59}$$

where N is the number of chips per coded symbol, the kth user's signature vector $\mathbf{s}_k$ is a column vector with size $N \times 1$, and

$$D_l = \tau_k / T_c, \tag{6.60}$$

$$D_r = N - D_l. \tag{6.61}$$

The vector $\boldsymbol{n}$ in (6.57) is an $N(N_b + 1) \times 1$ vector which represents the output noise component of the chip matched filter. It has zero mean and convariance matrix $\sigma_n^2\mathbf{I}$, where σ_n^2 is the variance of the output noise component.

We denote the processing window length in the receiver as N_p which is measured in chips and is much less than $N_b \times N$. In each processing window, the received signal vector is denoted as $\bar{\boldsymbol{r}}_{N_p\times 1}$, which consists of N_p rows of $\boldsymbol{r}$ falling to this processing window. The windowed system signature matrix $\bar{\boldsymbol{S}}_{N_p\times KN_b}$ and noise vector $\bar{\boldsymbol{n}}_{N_p\times 1}$ consist of N_p corresponding rows of $\boldsymbol{S}$ and $\boldsymbol{n}$, respectively. Therefore, we have the following equation:

$$\bar{\boldsymbol{r}} = \bar{\boldsymbol{S}}\boldsymbol{b} + \bar{\boldsymbol{n}}. \tag{6.62}$$

We can write $\boldsymbol{b}$ as the following sum:

$$\boldsymbol{b} = \boldsymbol{b}_U + \boldsymbol{b}_D, \tag{6.63}$$

where $\boldsymbol{b}_U$ consists of the symbols which are not fedback and its other elements are zeros. The non-zero elements of $\boldsymbol{b}_D$ consists of the fedback symbols. They have no common elements. In the same way by which we construct $\boldsymbol{b}_U$ and $\boldsymbol{b}_D$, we extract columns of $\bar{\boldsymbol{S}}$ and construct the corresponding signature matrices $\bar{\boldsymbol{S}}_U$ and $\bar{\boldsymbol{S}}_D$. Therefore, the windowed received signal vector $\bar{\boldsymbol{r}}$ can also be expressed as:

$$\bar{\boldsymbol{r}} = \bar{\boldsymbol{S}}_U \boldsymbol{b}_U + \bar{\boldsymbol{S}}_D \boldsymbol{b}_D + \bar{\boldsymbol{n}}. \tag{6.64}$$

The feedforward filter of user k has N_p taps and is denoted by a column vector $\bar{\boldsymbol{m}}_{fk}$. The feedback filter of user k, $\bar{\boldsymbol{m}}_{bk}$, has the size $KN_b \times 1$, which non-zero elements are corresponding to fedback symbols. That is, its effective number of taps is determined by the number of fedback symbols. The optimum filters satisfy the following minimum mean square error criterion:

$$\min_{\bar{\boldsymbol{m}}_{fk}, \bar{\boldsymbol{m}}_{bk}} E[b_k(i) - \bar{\boldsymbol{m}}_{fk}^H \cdot \bar{\boldsymbol{r}} - \bar{\boldsymbol{m}}_{bk}^H \cdot \hat{\boldsymbol{b}}_D]^2, \tag{6.65}$$

where i is the symbol index. Non-zero elements of $\hat{\mathbf{b}}_D$ are soft symbol estimates of those elements of $\mathbf{b}_D$ (6.13), respectively. Based on the same a priori information of fedback symbols in $\hat{\boldsymbol{b}}_D$ and non-fedback symbols in $\boldsymbol{b}_U$ as that in Subsection 6.3.1, we have the following a priori statistics (6.66) – (6.69) of non-zero elements in $\mathbf{b}_U$ and $\mathbf{b}_D$. For fedback symbols, their mean values are their soft symbol estimates, while non-fedback symbols have zero mean. Note that $b_k(i)$ in (6.65) belongs to non-fedback symbols. Denote u and v as one of non-zero elements of $\mathbf{b}_U$ and $\mathbf{b}_D$, respectively. The soft symbol estimate of v is denoted as $\hat{v}$. Thus, we have:

$$E[u] = 0, \tag{6.66}$$

$$E[u^2] = 1, \tag{6.67}$$

$$E[v] = \hat{v}, \tag{6.68}$$

$$E[v^2] = 1 - (\hat{v})^2. \tag{6.69}$$

We also assume that all users' transmitted symbols are independent of one another and of the background noise vector $\bar{\boldsymbol{n}}$ as well.

Employing the above statistics of the coded symbols, we can get the optimum feedforward and feedback filters of user k which satisfy the MMSE criterion in (6.65):

$$\bar{\boldsymbol{m}}_{fk} = (\bar{\boldsymbol{R}}_U + \bar{\boldsymbol{R}}_D + \sigma_n^2 \mathbf{I})^{-1} \cdot \mathbf{s}_{b_k(i)}, \tag{6.70}$$

$$\bar{\boldsymbol{m}}_{bk} = -\bar{\boldsymbol{S}}_D^H \cdot \bar{\boldsymbol{m}}_{fk}, \tag{6.71}$$

where

$$\bar{\boldsymbol{R}}_U = \bar{\boldsymbol{S}}_U \bar{\boldsymbol{S}}_U^H, \tag{6.72}$$

$$\bar{\boldsymbol{R}}_D = \bar{\boldsymbol{S}}_D[\mathbf{I} - \mathrm{diag}(\hat{\boldsymbol{b}}_D \hat{\boldsymbol{b}}_D^H)]\bar{\boldsymbol{S}}_D^H, \tag{6.73}$$

and $\mathbf{s}_{b_k(i)}$ is one column of $\bar{\boldsymbol{S}}_U$, which column index is the same as the row index of $b_k(i)$ in $\boldsymbol{b}_U$. The feedforward filter in (6.70) is actually a linear MMSE filter which suppresses the interference from non-fedback symbols, as well as the residual interference after canceling the fedback symbols and the background Gaussian noise.

From (6.70) and (6.71), we can see that the optimum finite-length feedforward and feedback filters require the knowledge of all users' signature vectors and delays. In order to avoid the need for this information, we can adaptively implement the SISO PDFD, which will be discussed in the next subsection.

6.4.2 Adaptive SISO PDFDs

In this subsection, we assume that both short spreading codes and relative delays of all users are unknown to the receiver. We design and employ adaptive SISO PDFDs to track these parameters from the received signal directly.

It is well known that the asynchronous system performance can be improved by using detection filters with an increased number of taps. However, increasing the number of taps increases the computational complexity of the detector. Moreover, this will have an adverse effect on the convergence speed. Therefore, we need to select suitable filter lengths to achieve a good tradeoff among the system performance, detector complexity and system overhead.

In the parallel decision feedback detector, the feedforward and feedback filters cooperate to suppress the multiple access interference. Specifically, the feedback filter tries to cancel some interfering symbols, while the feedforward filter suppresses the remaining MAI, as well as the residual interference due to imperfect cancellation by the feedback filter and the background Gaussian noise. Therefore, if the feedback filter effectively cancels most of the interference caused by the interfering symbols, the remaining interference to be suppressed by the feedforward filter is reduced.

In each iteration except for the first one, the SISO PDFD can obtain soft estimates of all symbols of all users from soft inputs. Thus, we have both causal and non-causal soft decisions of interfering symbols for the interested symbol. We may cancel part or all of them by the feedback filter.

In the following, we employ a feedforward filter which covers two symbol duration and consider several options for the feedback filter length. The length of the observation

interval is $2T$, which is the minimum length such that one complete symbol of each user falls in this interval regardless of its relative delay. Fig. 6.10 shows the processing window of the detector in the ith signaling interval. The output vector $\mathbf{r}(i)$ of the chip matched filter in this processing window is:

$$\mathbf{r}(i) = (\mathbf{P}^- \quad \mathbf{P}^0 \quad \mathbf{P}^+) \begin{pmatrix} \mathbf{b}(i-1) \\ \mathbf{b}(i) \\ \mathbf{b}(i+1) \end{pmatrix} + \mathbf{n}(i), \tag{6.74}$$

where $\mathbf{b}(i) = [b_1(i), b_2(i), \ldots, b_K(i)]^T$ and $\mathbf{n}(i)$ is a white Gaussian random vector with zero mean and covariance matrix $\sigma_n^2 \mathbf{I}_{(2N \times 2N)}$. We define the punctured signature vectors of user k as:

$$\mathbf{p}_k^- = \left[(\mathbf{s}_k^r)^H \quad \mathbf{0}^H \right]^H_{(2N \times 1)}, \tag{6.75}$$

$$\mathbf{p}_k^0 = \left[\mathbf{0}^H_{(1 \times N_k^r)} \quad \mathbf{s}_k^H \quad \mathbf{0}^H_{(1 \times N_k^l)} \right]^H_{(2N \times 1)}, \tag{6.76}$$

$$\mathbf{p}_k^+ = \left[\mathbf{0}^H \quad (\mathbf{s}_k^l)^H \right]^H_{(2N \times 1)}, \tag{6.77}$$

where $\mathbf{0}$ is a column vector. $\mathbf{s}_k^l$ and $\mathbf{s}_k^r$ are denoted in Fig. 6.11 and are parts of $\mathbf{s}_k$:

$$\mathbf{s}_k = \left[(\mathbf{s}_k^l)^H (\mathbf{s}_k^r)^H \right]^H. \tag{6.78}$$

The matrices $\mathbf{P}^-$, $\mathbf{P}^0$ and $\mathbf{P}^+$ in (6.74) are constructed as follows:

$$\mathbf{P}^- = [\mathbf{p}_1^- \quad \mathbf{p}_2^- \quad \cdots \quad \mathbf{p}_K^-], \tag{6.79}$$

$$\mathbf{P}^0 = [\mathbf{p}_1^0 \quad \mathbf{p}_2^0 \quad \cdots \quad \mathbf{p}_K^0], \tag{6.80}$$

$$\mathbf{P}^+ = [\mathbf{p}_1^+ \quad \mathbf{p}_2^+ \quad \cdots \quad \mathbf{p}_K^+]. \tag{6.81}$$

Thus, when multiple users' delays are unknown to the receiver, for the symbol of interest $b_k(i)$ of user k, it has at most ($3K$-1) interfering symbols. For implementation of the adaptive SISO multiuser detector in Fig. 6.1, we consider three adaptive SISO PDFDs

with the same feedforward filter length, i.e. $2N$ taps. The feedback filter of the first detector (labeled as Detector1) has $(K-1)$ taps which tries to cancel the current $(K-1)$ interfering symbols for the desired symbol. Detector2 has a feedback filter with $(2K-1)$ taps which tries to cancel the current $(K-1)$ and previous K interfering symbols. The feedback filter of Detector3 has $(3K-1)$ taps and tries to cancel all possible previous, current and future interfering symbols.

After determining the lengths of the feedforward and feedback filters, we apply the normalized LMS and RLS algorithms presented in Subsection 6.3.2 to update and obtain these filters' coefficients. In more detail, the adaptive detector employing the NLMS algorithm updates the feedforward and feedback filters of user k as follows for m=0, 1, 2, ...:

$$\bar{\boldsymbol{m}}_{fk}(m+1) = \bar{\boldsymbol{m}}_{fk}(m) - \frac{\tilde{\mu}_f}{a + \|\bar{\boldsymbol{r}}(m)\|^2} |\tilde{b}_k(m)| e_k^*(m) \bar{\boldsymbol{r}}(m), \tag{6.82}$$

$$\bar{\boldsymbol{m}}_{bk}(m+1) = \bar{\boldsymbol{m}}_{bk}(m) - \frac{\tilde{\mu}_b}{a + \|\tilde{\boldsymbol{b}}_D(m)\|^2} |\tilde{b}_k(m)| e_k^*(m) \tilde{\boldsymbol{b}}_D(m). \tag{6.83}$$

The error signal in the mth recursion is:

$$e_k(m) = \tilde{b}_k(m) - \bar{\boldsymbol{m}}_{fk}^H(m) \cdot \bar{\boldsymbol{r}}(m) - \bar{\boldsymbol{m}}_{bk}^H(m) \cdot \tilde{\boldsymbol{b}}_D(m), \tag{6.84}$$

where $\tilde{b}_k(m) = b_k(m)$ and $\tilde{\boldsymbol{b}}_D(m) = \boldsymbol{b}_D(m)$ in the training mode, and $\tilde{b}_k(m) = \hat{b}_k(m)$ and $\tilde{\boldsymbol{b}}_D(m) = \hat{\boldsymbol{b}}_D(m)$ in the decision directed mode. In the decision directed mode, $|\hat{b}_k(m)|$ is used as the reliability of the error signal $e_k(m)$ in (6.82) and (6.83). Both filters are updated per symbol and their initial states are $\bar{\boldsymbol{m}}_{fk}(0) = \mathbf{0}$ and $\bar{\boldsymbol{m}}_{bk}(0) = \mathbf{0}$.

For the adaptive detector using the RLS algorithm, we denote $\mathbf{w}_k(m) = [\bar{\boldsymbol{m}}_{fk}^H(m)\ \bar{\boldsymbol{m}}_{bk}^H(m)]^H$ and $\mathbf{u}(m) = [\bar{\boldsymbol{r}}^H(m)\ \tilde{\boldsymbol{b}}_D^H(m)]^H$. Then the feedforward and feedback filters of user k are updated as indicated in (6.43) – (6.46).

In summary, the asynchronous system during a two-symbol interval is considered as an equivalent synchronous system with $3K$ users. We use an adaptive SISO PDFD in the receiver with different lengths of the feedback filter. That is, we give different task assignments for the feedforward and feedback filters. Our goal is to achieve a good tradeoff between the detector complexity and system performance.

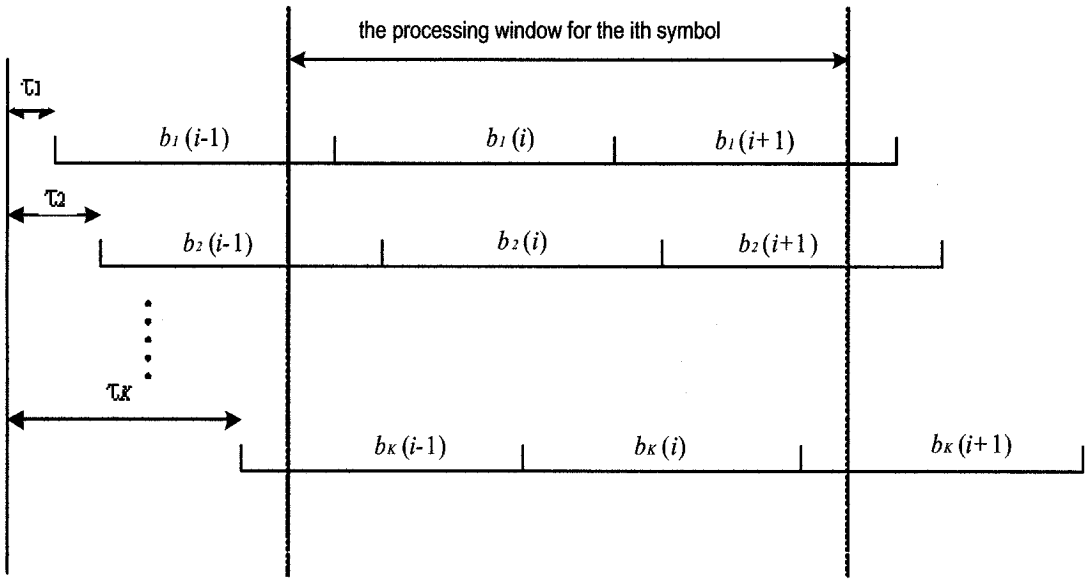

Figure 6.10: A processing window of the detector in the ith symbol duration of an asynchronous DS-CDMA system.

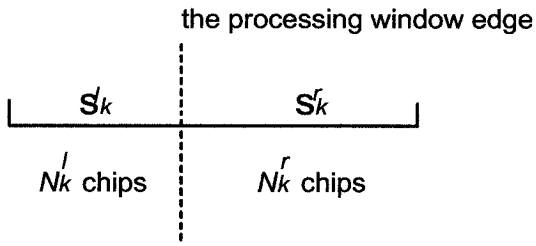

Figure 6.11: Punctured signatures of the kth user in the asynchronous system.

6.4.3 Simulation Results

The multiuser system which we simulate in this subsection has almost the same system parameters as those in Subsection 6.3.3, except that the system here is an asynchronous DS-CDMA system. We assume a chip-synchronous and symbol-asynchronous DS-CDMA system. All users' delays are uniformly distributed in $[0, T]$ and measured by multiples of T_c. These delays are randomly selected and fixed during simulation. Our simulation in this subsection is based on one fixed delay distribution of user 1 – user 12: [2 4 6 8 6 1 4 4 0 3 1 1] (each element is measured in chips). The average bit error rate over all of 12 users is investigated. In the receiver, we assume that all users' short spreading codes and delays are unknown. There are 300 training symbols which are randomly generated and inserted at the beginning of coded symbol frames of each user.

For simple implementation, we set all users' carrier phases as zeros. Only a feedforward filter is employed in the first iteration, while both a feedforward filter and a feedback filter are used in the following iterations. Furthermore, in the first two iterations, the filter coefficients are initialized to zeros before the adaptive algorithm is employed. In each of the following iterations, the filter coefficients are set to the values obtained at the end of the previous iteration.

We consider three adaptive SISO PDFDs with the same feedforward filter length and different feedback filter lengths, which are proposed in Subsection 6.4.2. Fig. 6.12 and Fig. 6.13 show average bit error rates of all users in the first, second, and tenth iterations provided by three adaptive detectors based on the NLMS and RLS algorithms, respectively. The parameters in the NLMS and RLS algorithms are the same as those in Subsection 6.3.3. For comparison, we also show the bit error rate performance of the single user system in these two figures, where the user's spreading code and delay are known to the receiver. In Fig. 6.12 and Fig. 6.13, we observe that at the end of the first

iteration all three detectors have similar performances and their curves appear to overlap. A similar behaviour is observed for the second iteration of Detector1 and Detector2 in Fig. 6.12 and Fig. 6.13.

We can see that with our adaptive SISO detectors, the system performance is improved with the increased number of iterations. Furthermore, Fig. 6.13 shows that the performance provided by the adaptive RLS receiver approaches to the performance of the single user system after a few iterations at high signal-to-noise ratios. Among three adaptive SISO PDFDs proposed in Subsection 6.4.2, Detector3 provides the best performance, while it has the highest computational complexity, since its feedback filter has the maximum number of taps compared with other two detectors.

By comparing average bit error rates of all the users provided by the adaptive detector based on the RLS algorithm in Fig. 6.13 and those obtained by the NLMS algorithm in Fig. 6.12, we can see that the bit error rate performance provided by the adaptive SISO PDFD based on the RLS algorithm is better than the one provided by the detector based on the NLMS algorithm. For example, at a bit error rate 10^{-3}, Detector3 based on the RLS algorithm has about 0.7dB gain with respect to Detector3 based on the NLMS algorithm. This is due to the faster convergence property of the RLS algorithm, which is shown by Fig. 6.14. The averaged squared errors $e_k^2(m)$ and $\xi^2(m)$ after the second iteration of the adaptive Detector3 during the training mode versus the number of updates in the NLMS and RLS algorithms respectively are shown and compared in Fig. 6.14. We set the signal-to-noise ratio of each user to 6dB. Each curve of the squared error is averaged over 200 independent trials of the experiment.

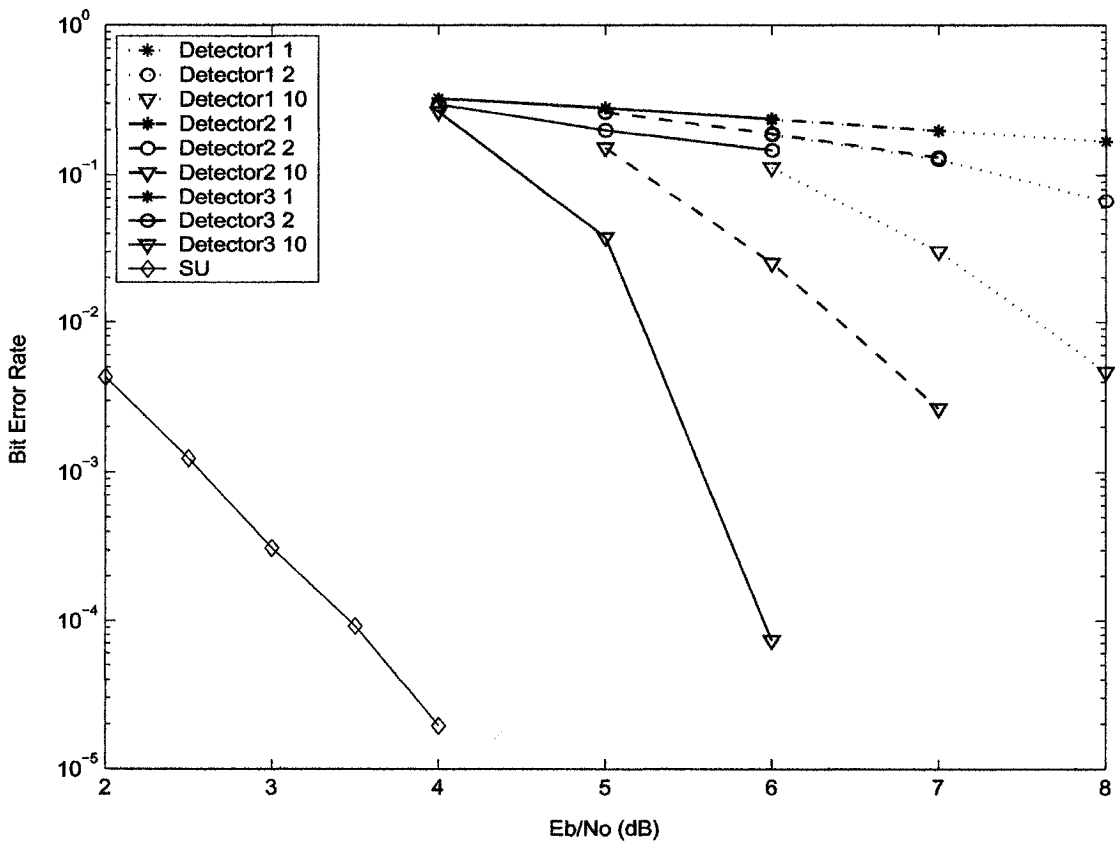

Figure 6.12: Average bit error rate performance provided by three NLMS adaptive SISO PDFDs for the asynchronous DS-CDMA system at the first, second, and tenth iterations, and that of the single user system (SU), for the asynchronous DS-CDMA system over the AWGN channel.

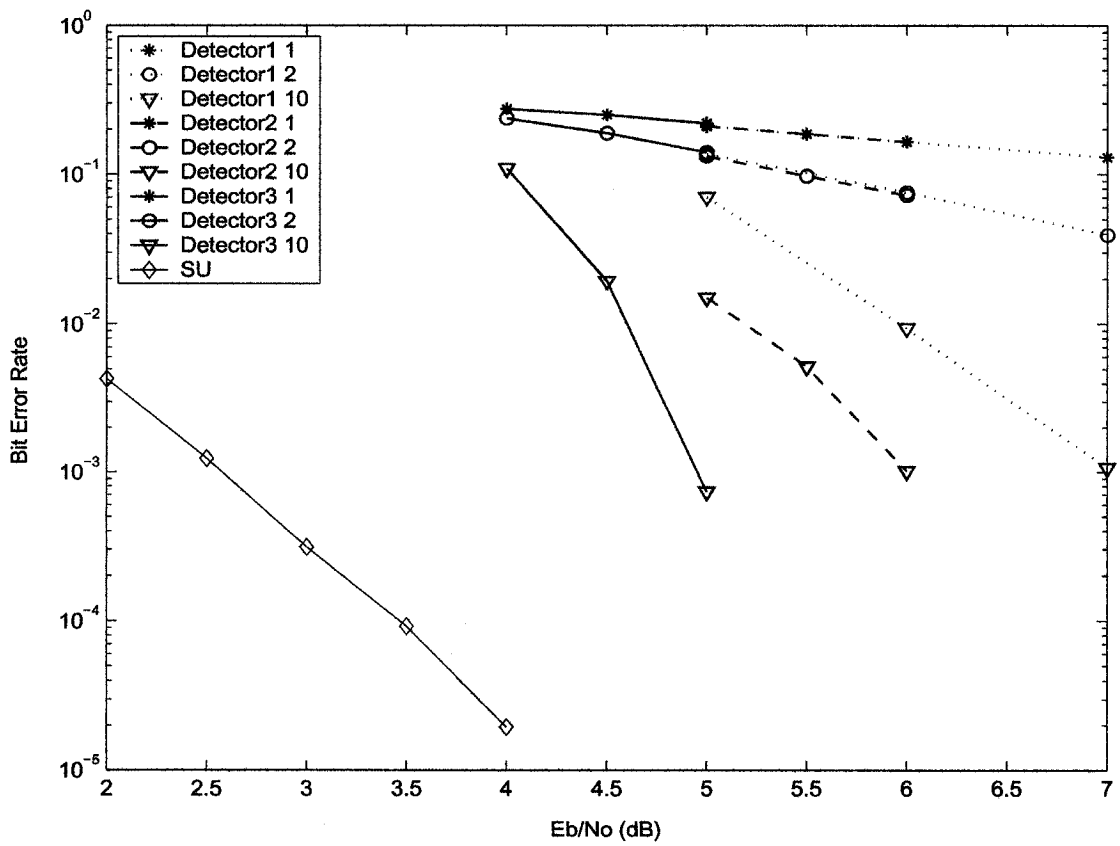

Figure 6.13: Average bit error rate performance provided by three RLS adaptive SISO PDFDs for the asynchronous DS-CDMA system at the first, second, and tenth iterations, and that of the single user system (SU), for the asynchronous DS-CDMA system over the AWGN channel.

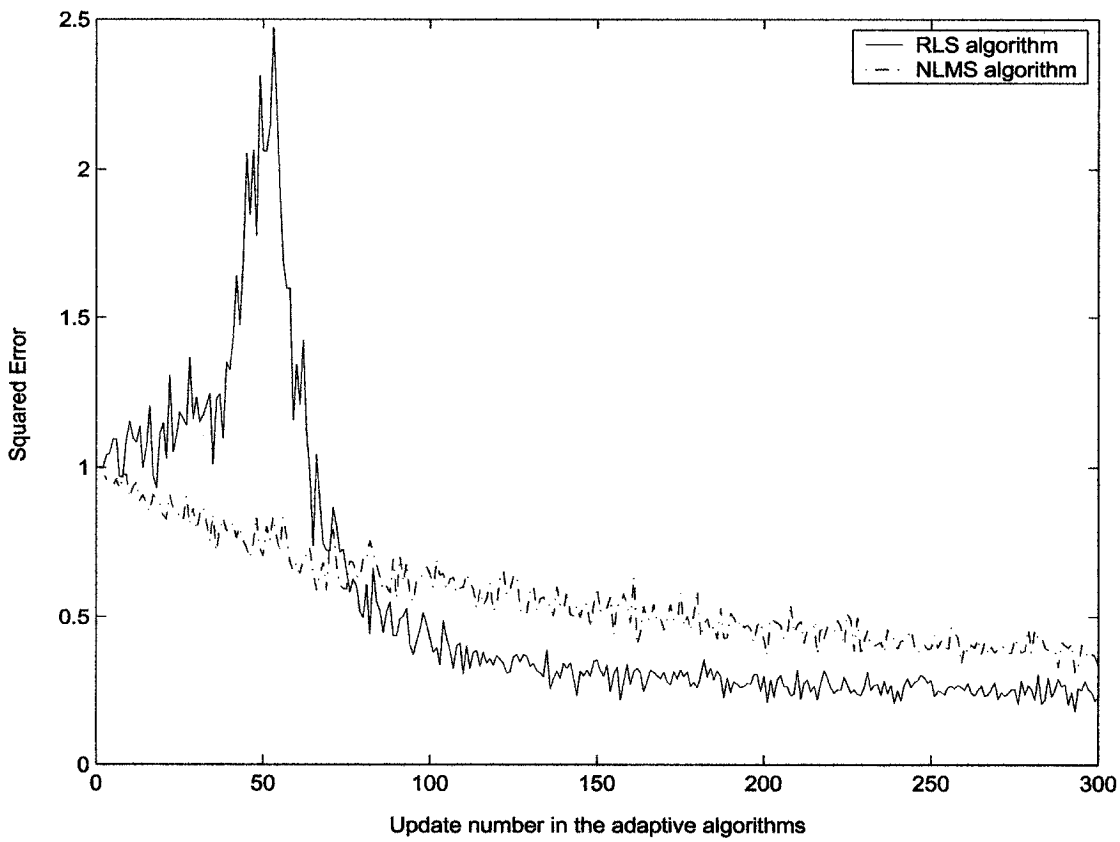

Figure 6.14: Comparison between the experimental learning curves of the adaptive SISO PDFD Detector3 based on the NLMS and RLS algorithms at the second iteration during the training mode at SNR=6dB, for the asynchronous DS-CDMA system over the AWGN channel.

6.5 Adaptive SISO PDFDs for Asynchronous DS-CDMA Systems over Slow Frequency Nonselective Rayleigh Fading Channels

We apply our adaptive SISO PDFDs to asynchronous DS-CDMA systems over slow frequency nonselective Rayleigh fading channels in this section. The channel fading rate is assumed to be slow, such that the Doppler frequency times the transmitted coded symbol interval equals to 0.00025. Asynchronous DS-CDMA systems have the same system parameters as those in Subsection 6.4.3. However, here multiple users pass through their own frequency nonselective Rayleigh fading channels respectively, which are unknown to the receiver. All of 12 users' fading channels have the same statistical property, while they are generated independently. The channel fading rate is assumed to be slow. The channel amplitude of each user is normalized to have unity average energy. For simplicity, we are only interested in slowly time-varying amplitudes of fading channels and assume that the fading channel's phase of each user can be perfectly estimated and compensated in the receiver. Without loss of generality, we assume its phase is zero. If without this assumption, we can apply differential encoding and detection to transmitted symbols to alleviate the task of adaptive detectors, which is to on-line estimate the channel phase as in [Hon97], [Zhu97].

For simplicity, we employ Detector3 based on the RLS algorithm in Subsection 6.4.3 as our detector. The average bit error rates of all users in the first, second, and tenth iterations are shown in Fig. 6.15. Furthermore, the bit error rate performance of the single user system, where the receiver has perfect a priori knowledge of the user's spreading code, delay and the channel impulse response, is also included in that figure. We can see that our adaptive SISO detector can provide a near single user system performance after a few iterations at moderate and high signal-to-noise ratios even under a slowly

varying fading channel. For fast time-varying fading channels, we may need to estimate the channel explicitly.

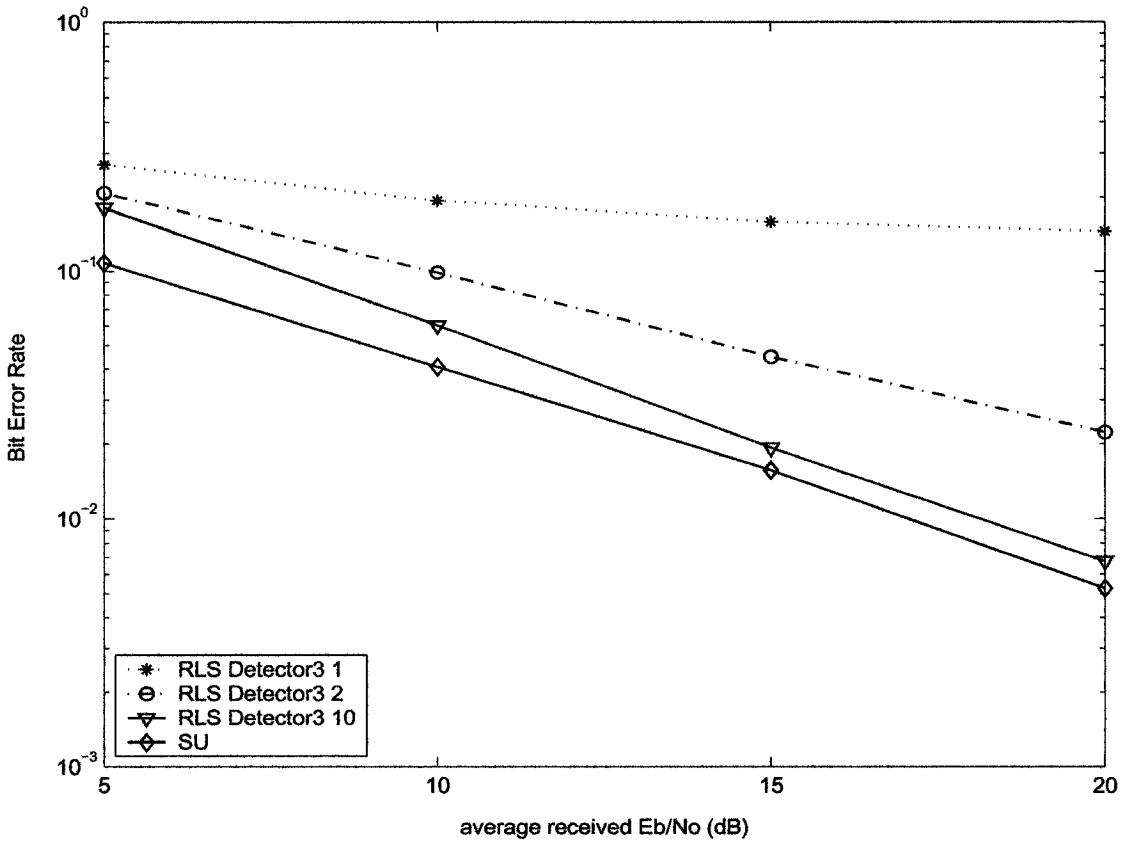

Figure 6.15: Average bit error rate performance provided by Detector3 based on the RLS algorithm for the asynchronous DS-CDMA system under unknown slow frequency nonselective Rayleigh fading channels at the first, second, and tenth iterations, and that of the single user system (SU).

6.6 Summary

In this chapter, we proposed adaptive SISO parallel decision feedback detectors for both synchronous and asynchronous DS-CDMA systems over the AWGN channel. We assumed that all users employ short spreading codes and system parameters, such as multiple users' transmitted waveforms and relative delays, are unknown to the detector. A training sequence is required by each user. We showed that the resulting system performance approaches to that of the single user system with the increased number of iterations and signal-to-noise ratios as well. Moreover, the adaptive detector employing the RLS algorithm provides a better bit error rate performance and requires fewer training symbols than the adaptive detector based on the NLMS algorithm, while at the expense of higher computational complexity. For asynchronous DS-CDMA systems, we further show that the adaptive detector with more feedback filter taps gives a better bit error rate performance, while has a higher computational complexity. Finally, we extended adaptive SISO parallel decision feedback detection to asynchronous DS-CDMA systems over slow frequency nonselective Rayleigh fading channels. Our adaptive SISO PDFDs can work successfully for slowly time-varying Rayleigh fading channels. For fast time-varying channels, we may need to estimate the channel explicitly. Therefore, our adaptive MUD receivers require short codes and could be very sensitive to channel time variations. Furthermore, our adaptive SISO detectors can be extended to multipath channels directly, since the feedback filters cancel intersymbol interference.

In the first iteration, there is no feedback and only a feedforward filter is employed. Therefore, using a larger number of taps in the feedforward filter may improve performance. To limit complexity, the detector reverts to using a $2N$-tap filter as the feedforward filter in the second and subsequent iterations. Some simulations using a feedforward filter with $4N$ taps in the first iteration have been done. However, we did not get a better performance compared with that of the $2N$ tap filter. When we increase the number of

filter taps, its performance is better, however its convergence speed is slower. At the same time, interference falling in the processing window is increased.

For easy reference, Table 6.1 shows performance-versus-complexity of all the adaptive SISO multiuser detectors discussed in this chapter.

Table 6.1: Performance-versus-complexity of adaptive SISO multiuser detectors for DS-CDMA systems. (K - number of users; N - spreading gain)

Adaptive SISO Multiuser Detectors	DS-CDMA Systems ($K = 12$, spreading gain 16)	Performance (required Eb/No(dB) at BER 10^{-3}, at the 10th iteration)	Complexity (number of operations per symbol interval per iteration)
NLMS	synchronous	4.4	$O(N + K - 1)$
RLS	synchronous	3.7	$O(N + K - 1)^2$
NLMS ($K - 1$ feedback filter taps)	asynchronous	8.7	$O(2N + K - 1)$
NLMS ($2K - 1$ feedback filter taps)	asynchronous	7.4	$O(2N + 2K - 1)$
NLMS ($3K - 1$ feedback filter taps)	asynchronous	5.6	$O(2N + 3K - 1)$
RLS ($K - 1$ feedback filter taps)	asynchronous	7.0	$O(2N + K - 1)^2$
RLS ($2K - 1$ feedback filter taps)	asynchronous	6.0	$O(2N + 2K - 1)^2$
RLS ($3K - 1$ feedback filter taps)	asynchronous	4.95	$O(2N + 3K - 1)^2$

Chapter 7

Conclusions

In this thesis, we focused on SISO multiuser detection for coded multiuser systems. First, traditional multiuser detectors, such as decorrelating detectors, linear MMSE detectors and parallel decision feedback detectors, were successfully adapted to be SISO detectors, which can cooperate iteratively with a bank of single user decoders. The system performance converges to that of the single user system after only a few iterations for moderate and high signal-to-noise ratios. The complexity of these SISO detectors is a cubic function of the number of users, making these detectors far less complex than optimum SISO detectors. Performance comparison of these three types of SISO detectors has also been provided in this thesis.

Secondly, we proposed adaptive SISO parallel decision feedback detectors for both synchronous and asynchronous DS-CDMA systems over the AWGN channel. Two adaptive algorithms, NLMS and RLS algorithms, were used. We assumed that all users employed short spreading codes, and multiple users' spreading codes and relative delays were unknown to the receiver. A training sequence is required by each user. We showed that the resulting system performance approaches to that of the single user system where the single user's spreading code and delay are known, after a few iterations at moderate

and high signal-to-noise ratios. Moreover, the adaptive detector employing the RLS algorithm provides a better bit error rate performance than the adaptive detector based on the NLMS algorithm, while at the expense of higher computational complexity. For asynchronous DS-CDMA systems, we further showed that the adaptive detector with more feedback filter taps gives us a better bit error rate performance. Finally, we applied our adaptive SISO parallel decision feedback detectors to asynchronous DS-CDMA systems over slowly fading frequency non-selective Rayleigh channels where the channel coefficients were not available in the receiver. Again, it was shown that our adaptive detectors can provide a near single user system performance after a few iterations at high signal-to-noise ratios. Furthermore, this result means that adaptive SISO detectors have good near-far resistance. For fast varying channels, however, we may need to estimate the channel impulse response explicitly.

There is much work remaining to extend this thesis work, including channel estimation for soft-input soft-output multiuser detection and performance analysis of iterative SISO detectors. Adaptive SISO multiuser detectors proposed in this thesis can work successfully only with unknown slow Rayleigh fading channels. For fast fading channels, it is necessary to estimate channel coefficients explicitly. Efficient channel estimation methods need to be proposed which are suitable in the implementation of iterative multiuser receivers, with respect to their performances and computational complexities. In the iterative receiver for coded multiuser systems, channel estimation can be considered as an independent SISO module that cooperates iteratively with the multiuser detector and single user decoders. How to make these three parts cooperate efficiently and the system performance be improved with the increased number of iterations is a problem. Using analytical and numerical methods, the performances of several parameter estimation techniques can be investigated. For example, the following techniques may be considered: the expectation-maximization (EM) algorithm, pseudo-inverse channel

estimation, pilot symbol assisted modulation, etc.

Since iterative SISO multiuser detectors are non-linear, it is very difficult to theoretically analyze their performances. Usually, we resort to Monte-Carlo simulation techniques to evaluate their bit error rate performances. However, Monte-Carlo simulation has a high complexity. It will be useful to recognize some underlying factors which dominantly influence performances of iterative SISO detectors. By analyzing these factors, we can understand and predict their performance limits and characteristics. The following performance characteristics of iterative SISO multiuser detectors are interesting: threshold phenomenon, asymptotic performance and convergence speed.

Bibliography

[Abd92] M. Abdulrahman and D. Falconer, "Cyclostationary crosstalk suppression by decision feedback equalization on digital subscriber loops," *IEEE J. Selected Areas Commun.*, vol. 10, no. 3, pp.640 – 649, Apr. 1992.

[Abd94] M. Abdulrahman, A. Sheikh and D. Falconer, "Decision feedback equalization for CDMA in indoor wireless communications," *IEEE J. Selected Areas Commun.*, vol. 12, pp.698 – 706, May 1994.

[Abe70] K. Abend and B. D. Fritchman "Statistical detection for communication channels with intersymbol interference," *Proc. IEEE*, vol. 58, pp.779 – 785, May 1970.

[Ale98] P. Alexander, A. Grant, and M. Reed, "Iterative detection in code-division multiple-access with error control coding," *Eur. Trans. Telecommun.*, vol. 9, no.5, pp.419 – 426, Sep. 1998.

[Ale99] P. D. Alexander, M. C. Reed, J. A. Asenstorfer and C. B. Schlegel, "Iterative multiuser interference reduction: Turbo CDMA," *IEEE Trans. Commun.*, vol. 47, no.7, pp.1008 – 1014, Jul. 1999.

[Bah74] L. R. Bahl, J. Cocke, F. Jelinek, and J. Raviv, "Optimal decoding of linear codes for minimizing symbol error rate," *IEEE Trans. Inform. Theory*, vol. IT-20, pp.284 – 287, Mar. 1974.

[Bat79] G. Battail, M. C. Decouvelaere and P. Godlewski, "Replication decoding," *IEEE Trans. Info. Theory*, vol. 25, pp.332 – 345, May, 1979.

[Bat89] G. Battail, "Coding for the Gaussian channel: the promise of weighted output decoding," *Int. J. Sat. Commu.*, vol. 7, pp.183 – 192, 1989.

[Bei02] B. F. Beidas, H. E. Gamal and S. Kay, "Iterative interference cancellation for high spectral efficiency satellite communications," *IEEE Trans. Commun.*, vol. 50, no. 1, pp.31 – 36, Jan. 2002.

[Ben96a] S. Benedetto and G. Montorsi, "Unveiling Turbo codes: some results on parallel concatenated coding schemes," *IEEE Trans. Inform. Theory*, vol. 42, no. 2, pp.409 – 428, Mar. 1996.

[Ben96b] S. Benedetto and G. Montorsi, "Iterative decoding of serially concatenated convolutional codes," *Electronics Letters*, vol. 32, no. 13, pp.1186 – 1188, Jun. 1996.

[Ben96c] S. Benedetto, D. Divsalar, G. Montorsi and F. Pollara, "Soft-output decoding algorithms for continuous decoding of parallel concatenated convolutional codes," *Proc. of IEEE Int. Conf. On Communications (ICC'96)*, vol. 1, pp.112 – 117, Jun. 1996.

[Ben97] S. Benedetto, D. Divsalar, G. Montorsi and F. Pollara, "A soft-input soft-output APP module for iterative decoding of concatenated codes," *IEEE Commun. Letters*, vol. 1, no. 1, pp.22 – 24, Jan. 1997.

[Ben98] S. Benedetto and D. Divsalar, G. Montorsi and F. Pollara, "Serial concatenation of interleaved codes: performance analysis, design, and iterative decoding," *IEEE Trans. Inform. Theory*, vol. 44, no. 3, pp.909 – 926, May 1998.

[Ber93a] C. Berrou, A. Glavieux and P. Thitimajshima, "Near Shannon limit error-correcting coding and decoding: Turbo-codes (1)," *Proc. of IEEE Int. Conf. On Communications (ICC'93)*, pp.1064 – 1070, May 1993.

[Ber93b] C. Berrou, P. Adde, E. Angui and S. Faudeil, "A low complexity soft-output Viterbi decoder architecture," *Proc. of IEEE Int. Conf. On Communications (ICC'93)*, pp.737 – 740, May 1993.

[Ber96] C. Berrou and A. Glavieux, "Near optimum error correcting coding and decoding: Turbo-codes," *IEEE Trans. Commun.*, vol. 44, no. 10, pp.1261 – 1271, Oct. 1996.

[Bor01] D. K. Borah and P. B. Rapajic, "Optimal adaptive multiuser detection in unknown multipath channels," *IEEE J. Selected Areas Commun.*, vol. 19, no. 6, pp.1115 – 1127, Jun. 2001.

[Can00] J. P. Cances, V. Meghdadi, "Turbo soft interference cancellation for coded CDMA," *Proc. of the 2nd Int. Symp. Turbo codes and Related Topics*, pp.435 – 438, Sep. 2000.

[Cha66] R. Chang and J. Hancock, "On receiver structures for channels having memory," *IEEE Trans. Inform. Theory*, vol. 12, pp.463 – 468, Oct. 1966.

[Che94] D. S. Chen and S. Roy, "An adaptive multiuser receiver for CDMA systems," *IEEE J. Selected Areas Commun.*, vol. 12, no. 5, pp.808 – 816, Jun. 1994.

[Chu01] K. Chugg, A. Anastasopoulos and X. Chen, *Iterative Detection: Adaptivity, Complexity Reduction and Applications*, Boston, MA: Kluwer Academic Publishers, 2001.

[Den92] P. Dent, B. Gudmundson and M. Ewerbring, "CDMA-IC: A novel code division multiple access scheme based on interference cancellation," *Proc. of the 3rd*

IEEE Int. Symp. Personal, Indoor and Mobile Radio Commun., pp.98 – 102, Sep. 1992.

[Div95] D. Divsalar, S. Dolinar, R. J. McEliece and F. Pollara, "Transfer function bounds on the performance of turbo codes," TDA Progress Report 42 - 123, Jet Propulsion Lab., pp.44 – 55, Aug. 1995.

[Div98] D. Divsalar, M. Simon and D. Raphaeli, "Improved parallel interference cancellation for CDMA," *IEEE Trans. Commun.*, vol. 46, no. 2, pp.258 – 268, Feb. 1998.

[Due92] A. Duel-Hallen, "Equalizers for multiple input/multiple output channels and PAM systems with cyclostationary input sequences," *IEEE J. Selected Commun.*, vol. 10, no. 3, pp.630 – 649, Apr. 1992.

[Due93] A. Duel-Hallen, "Decorrelating decision feedback multiuser detector for synchronous CDMA," *IEEE Trans. Commun.*, vol. 41, pp.285 – 290, Feb. 1993.

[Due95] A. Duel-Hallen, "A family of multiuser decision-feedback detectors for asynchronous code-division multiple-access channels," *IEEE Trans. Commun.*, vol. 43, pp.421 – 434, Feb./Mar./Apr. 1995.

[Dum98] T. M. Duman and M. Salehi, "New performance bounds for turbo codes," *IEEE Trans. Commun.*, vol. 46, no. 6, pp.717 – 723, Jun. 1998.

[Eld97] H. Elders-Boll, M. Herper and A. Busboom, "Adaptive receivers for mobile DS-CDMA communication systems," *Proc. of the 47th Vehicular Technology Conference*, vol.3, pp.2128 – 2132, May 1997.

[Faw95] U. Fawer and B. Aazhang, "A multiuser receiver for code division multiple access communications over multipath channels," *IEEE Trans. Commun.*, vol. 43, pp.1556 – 1565, Feb. 1995.

[Fos98] M. Fossorier, F. Burkert, S. Lin and J. Hagenauer, "On the equivalence between SOVA and max-log-MAP decodings," *IEEE Commun. Letters*, vol. 2, no. 5, pp.137 – 139, May 1998.

[Fra98] V. Franz and J. B. Anderson, "Concatenated decoding with a reduced-search BCJR algorithm," *IEEE J. Selected Areas Commun.*, vol.16, no.2, pp.186 – 195, Feb. 1998.

[Gam00] H. E. Gamal and E. Geraniotis, "Iterative multiuser detection for coded CDMA signals in AWGN and fading channels," *IEEE J. Selected Areas Commun.*, vol. 18, No. 1, pp.30 – 41, Jan. 2000.

[Gia96a] T. R. Giallorenzi and S. G. Wilson, "Multiuser ML sequence estimator for convolutional coded asynchronous DS-CDMA systems," *IEEE Trans. Commun.*, vol. COM-44, pp.997 – 1008, Aug. 1996.

[Gia96b] T. R. Giallorenzi and S. G. Wilson, "Suboptimum multiuser receivers for convolutionally coded asynchronous DS-CDMA systems," *IEEE Trans. Commun.*, vol. COM-44, no. 9, pp.1183 – 1196, Sep. 1996.

[Gol96] G. H. Golub and G. F. V. Loan, *Matrix Computations*, The Johns Hopkins University Press, 1996.

[Haf96] A. Hafeex and W. E. Stark, "Combined decision-feedback multiuser detection/soft-decision decoding for CDMA channels," *Proc. of IEEE 46th Vehicular Tech. Conf.*, vol. 1, pp.382 – 386, Apr. 1996.

[Hag89] J. Hagenauer and P. Hoeher, "A Viterbi algorithm with soft-decision outputs and its applications," *Proc. of IEEE Globecom. (GLOBECOM'89)*, vol. 3, pp. 1680 – 1689, 1989.

[Hag95] J. Hagenauer, "Source-controlled channel decoding," *IEEE Trans. Commun.*, vol. 43, no. 9, pp.2449 – 2457, Sep. 1995.

[Hag96] J. Hagenauer, E. Offer and L. Papke, "Iterative decoding of binary block and convolutional codes," *IEEE Trans. Inform. Theory*, vol. 42, no. 2, pp.429 – 445, Mar. 1996.

[Hal95] A. Duel-Hallen, "A family of multiuser decision-feedback detectors for asynchronous code-division multiple-access channels," ," *IEEE Trans. Commun.*, vol. 43, no. 2/3/4, pp.421 – 434, Feb./Mar./Apr. 1995.

[Hay96] S. Haykin, *Adaptive Filter Theory*, third edition, Prentice-Hall, Inc. 1996.

[Hol95] J. Holtzman, "DS/CDMA successive interference cancellation," In S. G. Glisic and P. Leppanen, editors, *Code division multiple access communications*, pp.161 – 182, Kluwer Academic, Dordrecht, The Netherlands, 1995.

[Hon95] M. L. Honig, U. Madhow and S. Verdu, "Adaptive blind multi-user detection," *IEEE Trans. Inform. Theory*, vol. 41, no. 4, pp.944 – 960, Jul. 1995.

[Hon97] M. L. Hong, M. J. Shensa, S. L. Miller and L. B. Milstein, "Performancce of adaptive linear interference suppression for DS-CDMA in the presence of flat Rayleigh fading," *Proc. of the 47th Vehicular Technology Conference*, vol.3, pp.2191 – 2195, May 1997.

[Hon98] M. L. Honig and H. V. Poor, "Adaptive interference suppression in wireless communication systems," Chapter 2 in *Wireless Communications: Signal Processing Perspectives*, Prentice Hall, Upper Saddle River, NJ, 1998.

[Hon00] M. L. Honig, G. Woodward and P. D. Alexander, "Adaptive multiuser parallel-decision-feedback with iterative decoding," *Proc. of 2000 IEEE Int. Symp. on Inform. Theory (ISIT'2000)*, pp.335, Jun. 2000.

[Hon01] M. L. Honig and Y. Sun, "Performance of iterative multiuser detection-feedback receivers," *Proc. of 2001 IEEE Inform. Theory Workshop, (ITW'2001)*, pp.30 – 32, Sep. 2001.

[Hue00] S. Huettinger, M. Breiling and J. Huber, "Memory efficient implementation of the BCJR algorithm," *Proc. of the 2nd Int. Symp. Turbo Codes and Related Topics*, pp.479 – 482, Sep. 2000.

[Ket99] K. Kettunen and T. Laakso, "Iterative multiuser receiver utilizing soft decoding information," *Proc. of IEEE Int. Conf. On Communications (ICC'93)*, vol. 2, pp.942 – 946, 1999.

[Koh83] R. Kohno, M. Hatori and H. Imai, "Cancellation techniques of co-channel interference in asynchronous spread spectrum multiple access systems," *Electronics and Communications*, vol. 66-A, pp.20 – 29, 1983.

[Koh90] R. Kohno, H. Imai, M. Hatori and S. Pasupathy, "An adaptive canceller of cochannel interference for spread-spectrum multiple-access communication networks in a power line," *IEEE J. Selected Areas Commun.*, vol. 8, no. 4, pp.691 – 699, Apr. 1990.

[Koh91] R. Kohno, "Pseudo-noise sequences and interference cancellation techniques for spread spectrum systems - spread spectrum theory and techniques in Japan," *IEICE Trans. Commun. Japan*, vol. E.74, pp.1083 – 1092, May 1991.

[Kua03] E. Kuan and L. Hanzo, "Burst-by-burst adaptive multiuser detection CDMA: a framework for existing and future wireless standards", *Proceedings of the IEEE*, vol. 91, no. 2, pp.278 – 302, Feb. 2003.

[Kub92] S. Kubota, S. Kato and K. Feher, "Inter-channel interference cancellation technique for CDMA mobile/personal communication systems," *Proc. of the 2nd*

IEEE Int. Symp. on Spread Spectrum Techniques and Applications, pp.112 – 117, 1992.

[Lam99] A. Lampe and J. B. Huber, "On improved multiuser detection with iterated soft decision interference cancellation," *Proc. of Communication Theory Mini-Conference*, pp.172 – 176, 6-10 Jun. 1999.

[Lee96] K. B. Lee, "Orthogonalization based adaptive interference suppression for direct-sequence code-division multiple-access systems", *IEEE Trans. Commun.*, vol. 44, no. 9, pp.1082 – 1085, Sep. 1996.

[Lup86] R. Lupas-Golaszewski and S. Verdu, "Asymptotic efficiency of linear multiuser detectors," *Proc. of the 25th IEEE Conf. on Decision and Control*, pp.2094 – 2100, Dec. 1986.

[Lup88] R. Lupas and S. Verdu, "Optimum near-far resistance of linear detectors for code-division multiple-access channels," *Proc. of IEEE Int. Symp. Inform. Theory 1988*, pp.14, Jun. 1988.

[Lup89] R. Lupas and S. Verdu, "Linear multiuser detectors for synchronous code-division multiple-access channels," *IEEE Trans. Inform. Theory*, vol. 35, pp.123 – 136, Jan. 1989.

[Lup90] R. Lupas and S. Verdu, "Near-far resistance of multiuser detectors in asynchronous channels," *IEEE Trans. Commun.*, vol. 38, pp.496 – 508, Apr. 1990.

[Mad94] U. Madhow and M. L. Honig, "MMSE interference suppressing for direct-sequence spread-spectrum CDMA", *IEEE Trans. Commun.*, vol. 42, no. 12, pp.3178 – 3188, Dec. 1994.

[Moh93] M. Moher, "Decoding via cross-entropy minimization," *Proc. of IEEE Globecom. (GLOBECOM'93)*, pp.809 – 813, Nov. 1993.

[Moh97a] M. Moher, "Cross-entropy and iterative detection," Ph.D. dissertation, Carleton Univ., Ottawa, Ont., Canada, May 1997.

[Moh97b] M. Moher, "Turbo-based multiuser detection," *Proc. of 1997 IEEE Int. Symp. on Inform. Theory (ISIT'97)*, pp.195, Jun. 1997.

[Moh98a] M. Moher,"An iterative multiuser decoder for near-capacity communications", *IEEE Trans. Commun.*, vol. 46, pp.870 – 880, Jul. 1998.

[Moh98b] M. Moher and P. Guinand, "An iterative algorithm for asynchronous coded multiuser detection," *IEEE Commun. Letters*,vol. 2, no. 8, pp.229 – 231, Aug. 1998.

[Moh98c] M. Moher, "An iterative multiuser decoder for asynchronous BPSK users," *Proc. of 1998 IEEE Int. Symp. on Inform. Theory (ISIT'98)*, pp.423, Aug. 1998.

[Moh01] M. Moher, "Methods and limits of iterative multiuser decoding", *Proc. of IEEE Info. Theory Workshop*, pp.45 – 47, Sep. 2001.

[Nag99] S. Nagaraj, S. Gollamudi and Y. Huang, "A fast converging adaptive multiuser detection scheme with reduced complexity for CDMA systems," *Proc. of Thirty-Third Asilomar Conf. on Signals, Systems and Computers*, vol. 1, pp.649 – 653, 1999.

[Nor63] D. North, "Analysis of the factors which determine signal/noise discrimination in pulsed carrier system," *Proc. IEEE*, vol. 51, pp.1016 – 1027, Jul. 1963.

[Pap96] L. Papke and P. Robertson, "Improved decoding with the SOVA in a parallel concatenated (Turbo-code) scheme," *Proc. of IEEE Int. Conf. On Communications (ICC'96)*, vol. 1, pp.102 – 106, 1996.

[Pat93] P. Patel and J. Holtzman, "Analysis of a DS/CDMA successive interference cancellation scheme using correlations," *Proc. of IEEE Global Commun. Conf. (GLOBECOM'93)*, pp.76 – 80, Nov. 1993.

[Pat94] P. Patel and J. Holtzman, "Analysis of a simple successive interference cancellation scheme in DS/CDMA system," *IEEE. J. Selected Areas Commun.*, vol. 12, pp.796 – 807, Jun. 1994.

[Ped96] K. Pedersen, T. Kolding, I. Seskar and J. Holtzman, "Practical implementation of successive interference cancellation in DS/CDMA systems," *Proc. of Int. Conf. on Universal Personal Communications*, pp.321 – 325, Sep. 1996.

[Pet94] B. Petersen and D. Falconer, "Suppression of adjacent-channel, cochannel, and intersymbol interference by equalizers and linear combiners," *IEEE Trans. Commun.*, vol. 42, pp.3109 – 3118, Dec. 1994.

[Pin03] L. Ping, L. Liu and W. K. Leung, "A simple approach to near-optimal multiuser detection: interleave-division multiple-access," *IEEE Wireless Commun. and Networking, (WCNC'2003)*, vol. 1, pp.391 – 396, 2003.

[Poo95] H. V. Poor, "Adaptivity in multiple-access communications," *Proc. of the 34th conference on Decision & Control*, pp.835 – 840, New Orleans, LA, Dec. 1995.

[Poo97] H. V. Poor and S. Verdu, "Probability of error in MMSE multiuser detection," *IEEE Trans. Inform. Theory*, vol. IT-43, pp.858 – 871, May 1997.

[Qin00a] Z. Qin, K. C. Teh and E. Gunawan, "Reduced state turbo multiuser detection for convolutionally coded asynchronous CDMA," *Proc. of the 2nd Int. Symp. Turbo Codes and Related Topics*, pp.283 – 286, Sep. 2000.

[Qin00b] Z. Qin and K. C. Teh, "Iterative multiuser detection with Gauss-Seidel soft detector as first stage for asynchronous coded CDMA," *Electronics Letters*, vol. 36, no. 23, pp.1939 – 1940, Nov. 2000.

[Qin01] Z. Qin, K. C. Teh and E. Gunawan, "Iterative multiuser detection for asynchronous CDMA with concatenated convolutional coding," *IEEE. J. Selected Areas Commun.*, vol. 19, no. 9, pp.1784 – 1792, Sep. 2001.

[Rap94] P. B. Rapajic and B. S. Vucetic, "Adaptive receiver structures for asynchronous CDMA systems," *IEEE J. Selected Areas Commun.*, vol. 12, no. 4, pp.685 – 697, May 1994.

[Rap99a] P. B. Rapajic and D. K. Borah, "Adaptive MMSE maximum likelihood CDMA multiuser detection," *IEEE J. Selected Areas Commun.*, vol. 17, no. 12, pp.2110 – 2122, Dec. 1999.

[Rap99b] P. B. Rapajic, M. L. Honig and G. Woodward, "Multiuser Decision-feedback detection: performance bounds and adaptive algorithms," *Proc. of 1999 IEEE Int. Symp. on Inform. Theory (ISIT'1999)*, pp.34, Aug. 1999.

[Ree98] M. C. Reed, C. B. Schlegel, P. D. Alexander, and J. A. Asenstorfer, "Iterative multiuser detection for CDMA with FEC: Near single user performance," *IEEE Trans. Commun.*, vol.46, pp.1693 – 1699, Dec. 1998.

[Rob95] P. Robertson, E. Villebrun and P. Hoeher, "A comparison of optimal and sub-optimal MAP decoding algorithms operating in the log domain," *Proc. of IEEE Int. Conf. On Communications (ICC'95)*, pp.1009 – 1013, Seattle, WA, 1995.

[Sas98] I. Sason and S. Shamai(shitz), "Improved upper bounds on the performance of parallel and serial concatenated turbo codes," *Proc. of 1998 IEEE Int. Symp. on Inform. Theory (ISIT'1998)*, p.30, Aug. 1998.

[Sch97] C. Schlegel, *Trellis Coding*, The Institute of Electrical and Electronics Engineers, Inc., New York, 1997.

[Ses98] I. Seskar, K. Pedersen, T. Kolding and J. Holtzman, "Implementation aspects of successive interference cancellation in DS/CDMA systems," *Wireless Networks*, vol. 4, pp.447 – 452, 1998.

[Shi01] Z. Shi and C. Schlegel, "Joint iterative decoding of serially concatenated error control coded CDMA", *IEEE J. Selected Areas Commun.*, vol. 19, no. 8, pp.1646 – 1653, Aug. 2001.

[Sim94] M. Simon, J. Omura, R. Scholtz and B. Levitt, *Spread spectrum communication handbook*, McGraw-Hill, New York, 1994.

[Sin99] R. Singh and L. B. Milstein, "Interference suppression for DS/CDMA", *IEEE Trans. Commun.*, vol. 47, no. 3, pp.446 – 453, Mar. 1999.

[Skl97] B. Sklar, "A primer on Turbo code concepts," *IEEE Commun. Magazine*, pp.94 – 102, Dec. 1997.

[Str94] E. G. Strom and S. L. Miller, "Optimum complexity reduction of minimum mean square error DS-CDMA receivers", *Proc. of IEEE 44th Vehicular Technology Conference*, pp.568 – 572, Jun. 1994.

[Tid95] C. Tidestav, A. Ahlen and M. Sternad, "Narrowband and broad-band multiuser detection using a multivariable DFE," *Proc. of IEEE Int. Symp. on Personal, Indoor and Mobile Radio Commun.*, vol. 2, pp.732 – 736, Sep. 1995.

[Var88] M. Varanasi and B. Aazhang, "Near-optimum demodulation for coherent communications in asynchronous Gaussian CDMA channels," *Proc. of the 22nd Conf. on Information Sciences and Systems*, pp.832 – 839, Mar. 1988.

[Var90] M. Varanasi and B. Aazhang, "Multistage detection in asynchronous code-division multiple-access communications," *IEEE Trans. Commun.*, vol. 38, pp.509 – 519, Apr. 1990.

[Var91] M. Varanasi and B. Aazhang, "Near-optimum detection in synchronous code-division multiple-access systems," *IEEE Trans. Commun.*, vol. 39, no. 5, pp.725 – 735, May 1991.

[Var99] M. Varanasi, "Decision feedback multiuser detection: A systematic approach," *IEEE Trans. Inform. Theory*, vol. 45, no. 1, pp.219 – 240, Jan. 1999.

[Ver83a] S. Verdu, "Optimum sequence detection of asynchronous multiple-access communications," *Proc. of 1983 IEEE Int. Symp. on Information Theory*, pp.80, Sep. 1983.

[Ver83b] S. Verdu, "Minimum probability of error for asynchronous multiple access communication systems," *Proc. of 1983 IEEE Military Communications Conf.*, vol. 1, pp.213 – 219, Nov. 1983.

[Ver86] S. Verdu, "Minimum probability of error for asynchronous Gaussian multiple-access channels," *IEEE Trans. Inform. Theory*, vol. 32, pp.85 – 96, Jan. 1986.

[Ver87] S. Verdu and H. V. Poor, "Abstract dynamic programming models under commutativity conditions," *SIAM J. Control and Optimization*, vol. 24, pp.990 – 1006, Jul. 1987.

[Ver98] S. Verdu, *Multiuser detection*, Cambridge University Press, Cambridge, U.K., 1998.

[Vit98a] A. J. Viterbi, "An intuitive justification and a simplified implementation of the MAP decoder for convolutional codes", *IEEE J. Selected Areas Commun.*, vol. 16, no. 2, pp.260 – 264, Feb. 1998.

[Vit98b] A. M. Viterbi and A. J. Viterbi, "Improved union bound on linear codes for the input-binary AWGN channel with applications to turbo-codes," *Proc. of 1998 IEEE Int. Symp. on Inform. Theory (ISIT'1998)*, p.29, Aug. 1998.

[Wan98] X. Wang and H. V. Poor, "Blind multiuser detection: a subspace approach," *IEEE Trans. Inform. Theory*, vol. 44, no. 2, pp.677 – 690, Mar. 1998.

[Wan99] X. Wang and H. V. Poor, "Iterative (turbo) soft interference cancellation and decoding for coded CDMA," *IEEE Trans. Commun.*, vol. 47, no. 7, pp.1046 – 1061, Jul. 1999.

[Wei94] L. Wei and C. Schlegel, "Synchronous DS-SSMA system with improved decorrelating decision-feedback multiuser detection," *IEEE Trans. Vehicular Tech.*, vol. 43, no. 3, pp.767 – 772, Aug. 1994.

[Woo98] G. Woodward and B. S. Vucetic, "Adaptive detection for DS-CDMA", *Proceedings of the IEEE*, vol. 86, no. 7, pp.1413 – 1434, Jul. 1998.

[Woo99] G. Woodward, R. R. Ratasuk and M. L. Honig, "Multistage multiuser decision feedback detection for DS-CDMA," *Proc. of IEEE Int. Conf. On Communications (ICC'99)*, vol. 1, pp.68 – 72, Jun. 1999.

[Woo02] G. Woodward, R. Ratasuk, M. L. Honig and P. B. Rapajic, "Minimum mean-squared error multiuser decision-feedback detectors for DS-CDMA," *IEEE Trans. on Comm.*, vol. 50, no. 12, pp.2104 – 2112, Dec. 2002.

[Wu94] H. Wu and A. Duel-Hallen, "Performance of multiuser decision-feedback detectors for flat fading synchronous CDMA channels," *Proc. of Conf. on Inform. Sciences and Systems*, pp.133 – 138, Mar. 1994.

[Xie90] Z. Xie, R. Short and C. Rushforth, "A family of suboptimum detectors for coherent multiuser communications," *IEEE J. Selected Areas Commun.*, vol. 8, pp.683 – 690, May 1990.

[Xue99] G. Xue, J. Weng, T. Le-Ngoc and S. Tahar, "Adaptive multistage parallel interference cancellation for CDMA," *IEEE. J. Selected Areas Commun.*, vol. 17, no. 10, pp.1815 – 1827, Oct. 1999.

[Yan94] J. Yang and S. Roy, "Joint transmitter/receiver optimization for multi-input multi-output systems with decision feedback," *IEEE Trans. Inform. Theory*, vol. 40, pp.1334 – 1347, Sep. 1994.

[Yoo93a] Y. Yoon, R. Kohno and H. Imai, "Cascaded co-channel interference cancelling and diversity combining for spread-spectrum multi-access over multipath fading channels," *IEICE Trans. Commun.*, vol. E76-B, no. 2, pp.163 – 168, Feb. 1993.

[Yoo93b] Y. Yoon, R. Kohno and H. Imai, "A spread-spectrum multi-access system with co-channel interference cancellation over multipath fading channels," *IEEE J. Selected Areas Commun.*, vol. 11, no. 7, pp.1067 – 1075, Sep. 1993.

[Zha03] W. Zhang, C. D'Amours, "Iterative multiuser detection and decoding for highly correlated narrowband systems and heavily loaded CDMA systems", *Proc. of IEEE Can. Conf. Elect. Comp. Eng. (CCECE 2003)*, pp.1637 – 1640 , May 2003.

[Zhe00] Y. Zheng and Y. T. Su, "A new real-time MAP decoding algorithm," *Proc. of the 2nd Int. Symp. Turbo Codes and Related Topics*, pp.507 – 510, Sep. 2000.

[Zhu97] L. J. Zhu and U. Madhow, "Adaptive interference suppression for direct sequence CDMA over severely time-varying channels," *Proc. of IEEE Global Commun. Conf. (GLOBECOM'97)*, vol. 2, pp.917 – 922, Nov. 1997.

Appendix A

Analysis of Noise Variances at the Output of the SISO Decorrelating Detector

In this appendix, we show the simulation results based on which we give the relationship between $\sigma_{uk}^2, k \in [1, K]$ and intermediate values of $\{\xi_i \in [0,1], 1 \leq i \leq K\}$ in Section 5.2.2.

In a multiuser system where all users have the same received signal amplitude, they will have almost the same performance. Therefore, we can assume that at each iteration we have the same $\{\xi_i, 1 \leq i \leq K\}$. That is, denote:

$$\xi = \xi_i, \quad 1 \leq i \leq K. \tag{A.1}$$

Thus, the noise variances $\{\sigma_{uk}^2\}$ of different user k $(1 \leq k \leq K)$ are also the same. Denote

$$\sigma_u^2 = \sigma_{uk}^2, \quad 1 \leq k \leq K. \tag{A.2}$$

In this case, noise variance σ_u^2 has only one argument ξ. For the K-symmetric multiuser systems simulated in Section 5.2.3 (i.e. the number of users $K = 5$ or 10, the cross

correlation between any two users $\rho = 0.3$, 0.5, 0.7 or 0.9), we can obtain relationships between the normalized noise variance σ_u^2/σ^2 (σ^2 is the double-sided power spectral density of the background Gaussian noise) and ξ, which are shown in Fig. A.1. Based on this figure, we can see that in general σ_u^2 is a mono-increasing function of ξ for moderate and large ξ. While for small ξ, it remains small and changes slowly.

When the multiuser system is in a near-far scenario, that is the received signal amplitudes of all users are different, σ_{uk}^2 is a function with multiple arguments $\{\xi_i, 1 \leq i \leq K\}$. We still consider the K-symmetric multiuser systems in Secion 5.2.3. In this case, we investigate the relationship between σ_{uk}^2 and one $\xi_j, j \in [1, K]$ for all possible (K-1)-dimensional vectors $[\xi_1, \ldots, \xi_{j-1}, \xi_{j+1}, \xi_K]$, where $\xi_i \in [0, 1]$ and $i \neq j$. By simulation, we found that the relationship between σ_{uk}^2 and ξ_j is almost the same as those shown in Fig. A.1. That is, for small ξ_j, σ_{uk}^2 is a mono-decreasing function and has slowly changed small values, while for moderate and large ξ_j, it is a mono-increasing function. The slope of the function curve depends on the value of $[\xi_1, \ldots, \xi_{j-1}, \xi_{j+1}, \xi_K]$, thus depends on the near-far scenario.

For example, Fig. A.2 shows the relationships between the normaized noise variances $\{\sigma_{uk}^2/\sigma^2, 1 \leq k \leq K\}$ and ξ_1 when the multiuser system has $K = 5, \rho = 0.5$ and $[\xi_2, \xi_3, \xi_4, \xi_5] = [0.1, 0.2, 0.3, 0.4]$. Fig. A.3 shows the relationships when $[\xi_2, \xi_3, \xi_4, \xi_5] = [0.5, 0.6, 0.7, 0.8]$. By simulation, we can obtain the relationship between any one noise variance $\sigma_{uk}^2, k \in [1, K]$ and any one argument $\xi_j, j \in [1, K]$.

In summary, generally σ_{uk}^2 is an increasing function of $\{\xi_i, 1 \leq i \leq K\}$ respectively, for moderate and large $\{\xi_i\}$. While for small $\{\xi_i\}$, it remains small and changes slowly.

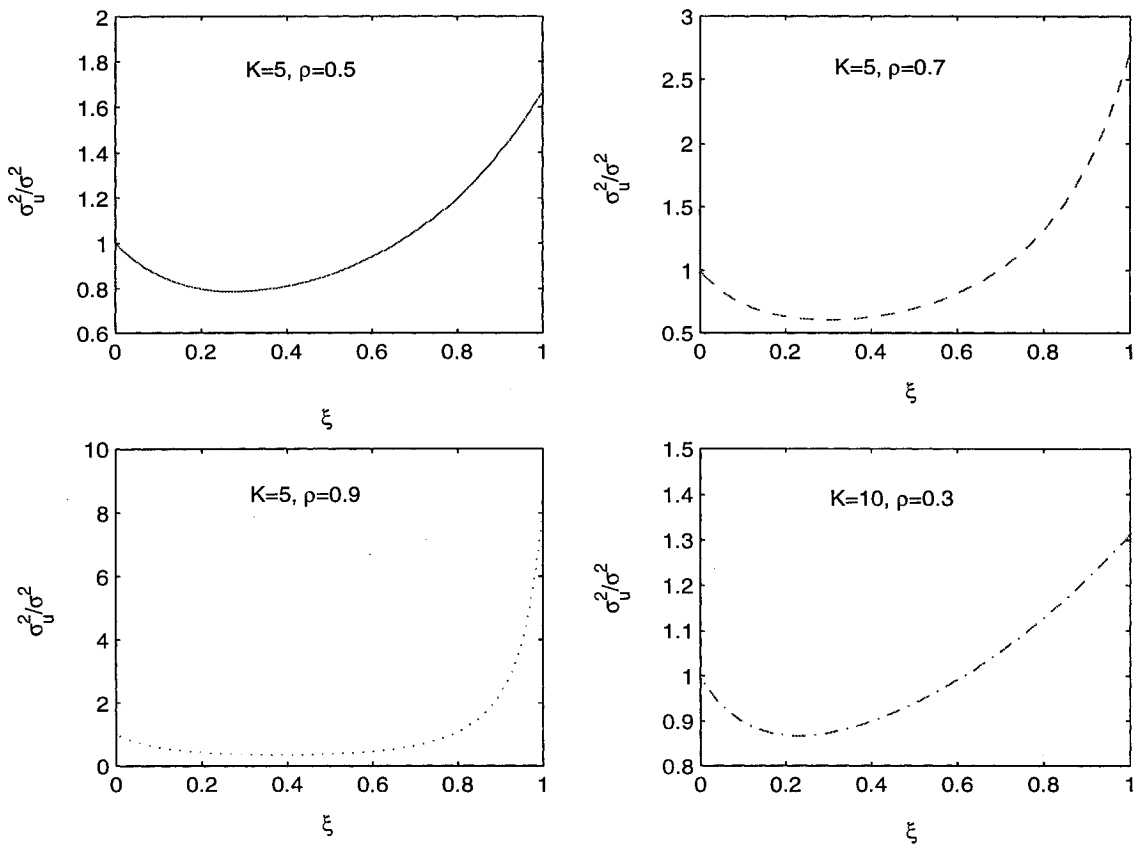

Figure A.1: Relationships between σ_u^2/σ^2 and ξ for four K-symmetric multiuser systems when the received signal amplitudes of all users are the same.

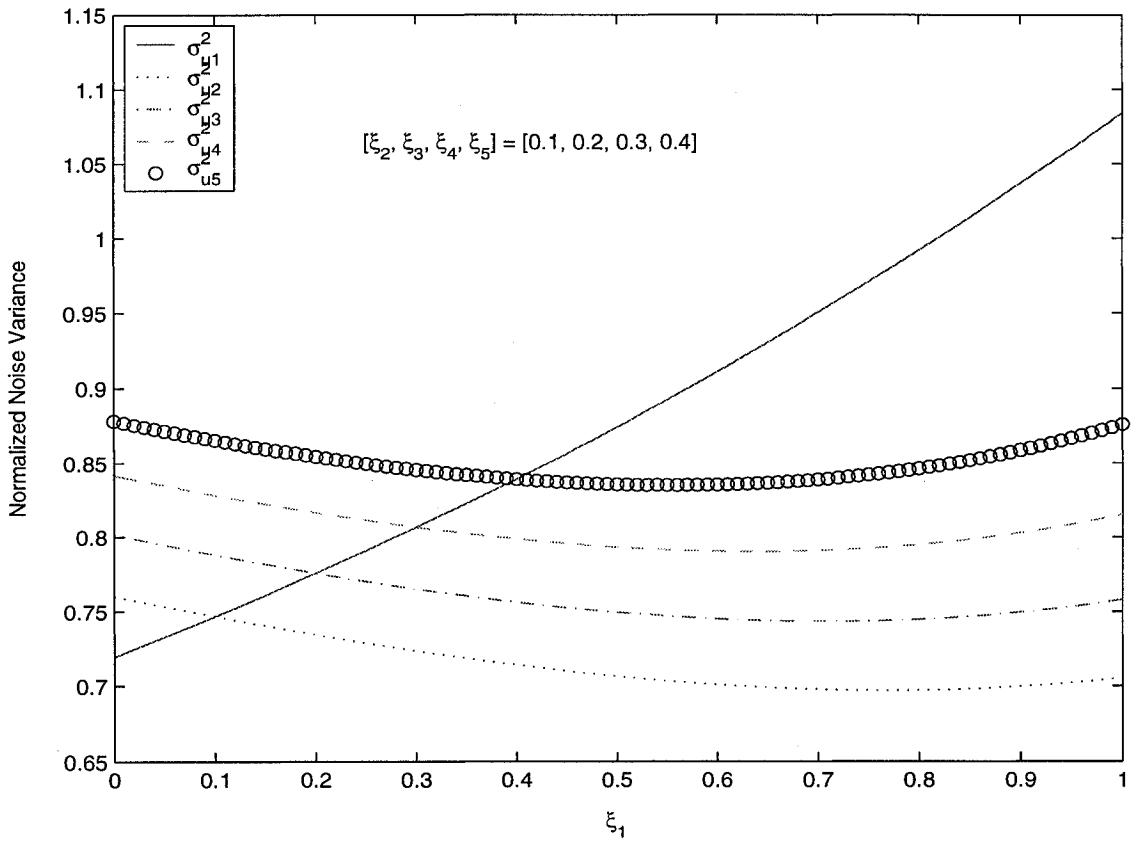

Figure A.2: Relationships between $\{\sigma_{uk}^2/\sigma^2, 1 \leq k \leq 5\}$ and ξ_1 for the multiuser system with $K = 5, \rho = 0.5$, and $[\xi_2, \xi_3, \xi_4, \xi_5] = [0.1, 0.2, 0.3, 0.4]$.

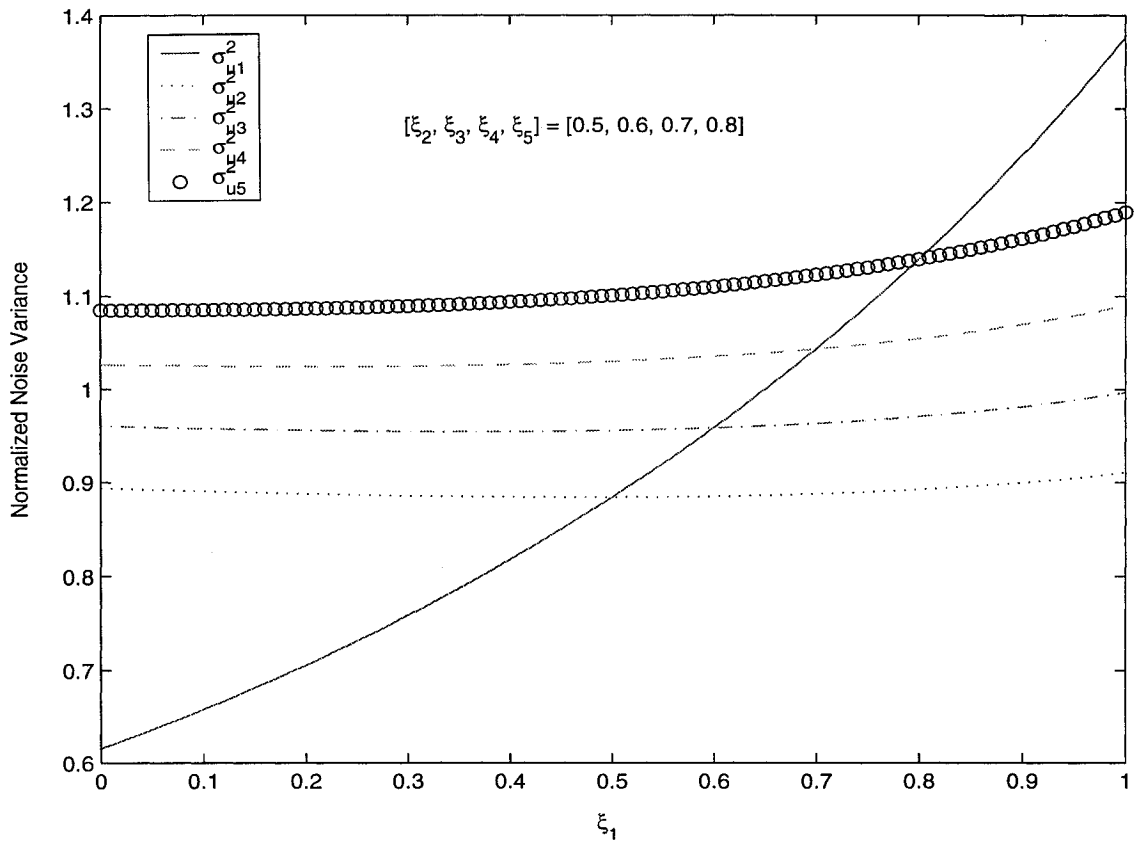

Figure A.3: Relationships between $\{\sigma_{uk}^2/\sigma^2, 1 \leq k \leq 5\}$ and ξ_1 for the multiuser system with $K = 5, \rho = 0.5$, and $[\xi_2, \xi_3, \xi_4, \xi_5] = [0.5, 0.6, 0.7, 0.8]$.

Appendix B

Computational Complexity of the SISO Decorrelator

In this appendix, Table B.1 shows the number of operations required in each step of the SISO decorrelator, proposed in Section 5.2.

Table B.1: Computational complexity of the SISO Decorrelator

Processing	Number of Operations
1. soft interference cancellation in (5.5)	$K^2 + 2K$
2. Constructing $\hat{\mathbf{R}}_u$ as in (5.16)	K^2
3. Calculating the matrix inverse $\hat{\mathbf{R}}_u^{-1}$ as in (5.28)	$2K^3$
4. Calculating the output vector $\mathbf{x}^{DEC}$ of the SISO decorrelator in (5.20)	K^2
5. Calculating the noise variances which are diagonal elements in (5.21)	$K^3 + K^2 + K$
6. Obtaining the soft output $\lambda_o^{DEC}[b_k]$ in (5.22) for $1 \leq k \leq K$	$3K$
Total	$3K^3 + 4K^2 + 6K$

Appendix C

Computational Complexity of the Linear SISO MMSE Detector

In this appendix, we analyze the computational complexity of the linear SISO MMSE detector, proposed in Section 5.3.

Substitute (5.46) into (5.47), we have:

$$\begin{aligned} x_k^{MMSE} &= \mathbf{m}_k^T \cdot (\mathbf{y} - E[\mathbf{y}]_k) \\ &= \left(A_{kk}\mathbf{R}^{-1}(\mathbf{A}\boldsymbol{\Lambda}_k\mathbf{A} + \sigma^2\mathbf{R}^{-1})^{-1}\mathbf{e}_k\right)^T \cdot [\mathbf{y} - E(\mathbf{y})_k] \\ &= A_{kk}\mathbf{e}_k^T(\mathbf{A}\boldsymbol{\Lambda}_k\mathbf{A} + \sigma^2\mathbf{R}^{-1})^{-1}\mathbf{R}^{-1}[\mathbf{y} - E(\mathbf{y})_k]. \end{aligned} \tag{C.1}$$

We need to calculate the following matrix inverse $\boldsymbol{\Phi}^{(k)}$ for each user k in (C.1):

$$\begin{aligned} \boldsymbol{\Phi}^{(k)} &= (\mathbf{A}\boldsymbol{\Lambda}_k\mathbf{A} + \sigma^2\mathbf{R}^{-1})^{-1} \\ &= \Big(\sum_{j\neq k} A_{jj}^2[1 - \hat{b}_j^2]\mathbf{e}_j\mathbf{e}_j^T + A_{kk}^2\mathbf{e}_k\mathbf{e}_k^T + \sigma^2\mathbf{R}^{-1}\Big)^{-1}. \end{aligned} \tag{C.2}$$

In order to calculate (C.2), we can first recursively compute the following matrix inverse using the matrix inverse lemma [Gol96]:

$$\boldsymbol{\Psi}^{(K)} = \Big(\sum_{j=1}^{K} A_{jj}^2[1 - \hat{b}_j^2]\mathbf{e}_j\mathbf{e}_j^T + \sigma^2\mathbf{R}\Big)^{-1}. \tag{C.3}$$

Table C.1: Computational complexity of the SISO MMSE Detector

Processing	Number of Operations
1. Recursively calculating $\mathbf{\Psi}^{(K)}$ in (C.3)	$2K^3 + K^2$
2. Calculating the matrix inverse $\mathbf{\Phi}_k(i)$ in (C.4) for $1 \leq k \leq K$	$2K^3$
3. Calculating the output of the SISO MMSE detector x_k^{MMSE} in (C.1) for $1 \leq k \leq K$	$4K^2$
4. Obtaining the soft output $\lambda_o^{MMSE}[b_k]$ in (5.51) for $1 \leq k \leq K$	$3K$
Total	$4K^3 + 5K^2 + 3K$

Then $\mathbf{\Phi}^{(k)}$ can be obtained by:

$$\begin{aligned}\mathbf{\Phi}^{(k)} &= \left((\mathbf{\Psi}^{(K)})^{-1} + A_{kk}^2 \hat{b}_k^2 \mathbf{e}_k \mathbf{e}_k^T\right)^{-1}, \\ &= \mathbf{\Psi}^{(K)} - \frac{1}{(A_{kk}\hat{b}_k)^{-2} + (\mathbf{\Psi}^{(K)})_{kk}} [\mathbf{\Psi}^{(K)}\mathbf{e}_k][\mathbf{\Psi}^{(K)}\mathbf{e}_k]^T. \end{aligned} \tag{C.4}$$

Table C.1 shows the number of operations required in each step of the linear SISO MMSE detector.

Appendix D

Related Publications

D.1 Papers Appearing in or Submitted to Referred Journals

- W. Zhang, C. D'Amours, and A. Yongaçoğlu, "Adaptive iterative soft-input soft-output parallel decision feedback detectors for asynchronous coded DS-CDMA systems", accepted for publication by *EURASIP Journal on Wireless Communications And Networking*, special issue on Advanced Signal Processing Algorithms for Wireless Communications, Nov. 2004.

- W. Zhang, C. D'Amours, and A. Yongaçoğlu, "Soft-input soft-output decorrelating detectors for coded multiuser systems", accepted for publication by *IEEE Trans. Sig. Proc.*, Apr. 2004.

- W. Zhang, C. D'Amours, "Iterative multiuser detection and decoding for highly correlated narrowband systems and heavily loaded CDMA systems", *Can. Journal of Elect. Comp. Eng.*, vol. 28, no. 2, pp.75 - 80, Apr. 2003.

D.2 Papers Appearing in Conference Proceedings or Submitted for Presentation at Conference

- W. Zhang, C. D'Amours, and A. Yongaçoğlu, "Adaptive soft-input soft-output parallel decision feedback detectors for asynchronous coded DS-CDMA systems", accepted for publication by *IEEE Wireless Communications and Networking Conference*, New Orleans, USA, Mar. 2005.

- W. Zhang, C. D'Amours, and A. Yongaçoğlu, "Adaptive soft-input soft-output parallel decision feedback multiuser detectors for coded DS/CDMA systems," *Proc. of Global Mobile Congress (GMC2004)*, pp.395 – 401, Shanghai, China, Oct. 2004.

- W. Zhang, C. D'Amours, and A. Yongaçoğlu, "Performance comparison of three soft-input soft-output multiuser detectors for coded multiuser systems", *Proc. of the 22nd Biennial Symp. On Commun.*, pp.328 - 330, Kingston, ON, Jun. 2004.

- W. Zhang, C. D'Amours, and A. Yongaçoğlu, "Adaptive soft-input soft-output multiuser detection for coded CDMA systems", *Proc. of IEEE Canadian Conf. Elect. Comp. Eng.*, pp.1203 - 1206, Niagara Falls, ON, May 2004.

- W. Zhang, C. D'Amours, "Iterative multiuser detection and decoding for highly correlated narrowband systems and heavily loaded CDMA systems", *Proc. of IEEE Can. Conf. Elect. Comp. Eng. (CCECE 2003)*, pp.1637 - 1640, Montreal, QC, May 2003. (***received an award for outstanding student paper for this submission.***)

- W. Zhang, C. D'Amours, and A. Yongaçoğlu, "Linear soft-input soft-output multiuser detection for coded multiuser systems", *Proc. of IEEE Int. Symp. Pers. Indoor Mobile Radio Commun. (PIMRC 2003)*, pp.2928 - 2932, Beijing, China, Sep. 2003.